



universität
wien

DIPLOMARBEIT

Titel der Diplomarbeit

Characterization of a novel inhibitor of fatty acid
synthase in malignant, immortalized and normal ovarian
surface epithelial cells

verfasst von

Daniel Veigel

angestrebter akademischer Grad

Magister der Naturwissenschaften (Mag.rer.nat.)

Wien, 2013

Studienkennzahl lt. Studienblatt:

A 441

Studienrichtung lt. Studienblatt:

Diplomstudium Genetik - Mikrobiologie

Betreut von:

Univ.-Prof. Dr. Thomas Decker

Danksagung

Mein Dank gilt all jenen Personen, die mein Studium ermöglicht und mich bei dieser Arbeit unterstützt haben.

Ein großes Dankeschön richte ich an Herrn Univ.-Prof. Mag. Dr. Thomas W. Grunt für die Themenstellung und die Finanzierung dieser Arbeit, sowie für die tolle Unterstützung, Ratschläge, Ideen und Gespräche.

Besonders bedanken möchte ich mich bei Frau Renate Wagner, die durch ihre Hilfsbereitschaft und ihre Erklärungen dafür gesorgt hat, dass die Arbeit im Labor große Freude bereitet.

Ich danke außerdem Herrn Univ.-Prof. Dr. Thomas Decker für die offizielle Betreuung dieser Arbeit.

Mein innigster Dank gilt meiner Freundin Evelyn für ihr Interesse ihre Geduld und ihre Ratschläge, aus denen ich stets Kraft und Motivation schöpfe, sowie im Besonderen meinen Eltern Margarita und Walter, ohne deren unglaubliche Unterstützung mein Studium nicht möglich gewesen wäre.

Herzlichen Dank!

Table of Contents:

Abstract	7
Zusammenfassung	9
1 Introduction	11
1.1 Ovarian cancer	11
1.1.1 Epidemiology	11
1.1.2 Etiology	11
1.1.3 Risk factors	12
1.1.4 Therapy	13
1.2 Cancer metabolism	14
1.3 Fatty acid synthesis and cancer	16
1.3.1 FASN as target for anti-cancer therapy	19
2 Materials and Methods	20
2.1 Cell lines and cell culture	20
2.2 Drugs	21
2.2.1 C75	21
2.2.2 G28UCM	22
2.2.3 Palmitic acid	22
2.2.4 Oleic acid	23
2.3 Cell growth assay	23
2.3.1 Treatment with C75 or G28UCM	24
2.3.2 Combination treatment with palmitic acid and C75 or G28UCM	24
2.3.3 Combination treatment with oleic acid and C75 or G28UCM	25
2.3.4 Measurement and analysis	25
2.4 Western Blotting	25
2.4.1 Culture and treatment of cells	25
2.4.2 Preparation of protein samples	26
2.4.3 Separation and transfer of proteins	27

2.4.4 Immunostaining and detection of specific proteins	28
2.5 Flow Cytometry	30
2.5.1 Culture, treatment and harvesting of cells	30
2.5.2 Active caspase 3 assay	30
2.5.3 Cell cycle analysis	31
2.6 Statistics	31
3 Results.....	32
3.1 Expression of FASN in malignant and non-malignant cells	32
3.2 Targeting FASN inhibits cell growth	34
3.3 Effects of exogenously delivered palmitic acid or oleic acid on growth in cells treated with FASN-inhibitors.....	38
3.4 Effects of FASN-blockade by C75 and G28UCM on major intracellular signaling pathways	40
3.5 Induction of apoptosis by C75 or G28UCM	46
3.6 Induction of autophagy by C75 or G28UCM.....	52
3.7 Inhibition of FASN can interfere with cell cycle distribution	53
3.8 HSP70 but not HSP90 is induced by FASN-inhibition via C75.....	65
3.9 Protein ubiquitination occurs in C75-treated cells.....	68
4 Discussion	70
4.1 Malignant and non-malignant ovarian surface epithelial cells express FASN and are sensitive to FASN-blockade by C75 and G28UCM.....	70
4.2 Oleic acid but not palmitic acid can ameliorate growth-inhibitory/cytocidal effects of FASN blockade.....	71
4.3 C75 and G28UCM decrease signaling through MAPK and PI3K/Akt pathways in malignant and non-malignant ovarian surface epithelial cells.....	72
4.4 Mechanisms implicated in the anti-proliferative effects of C75 and G28UCM include apoptosis, autophagy, protein degradation and cell cycle arrest.....	74
4.5 HSP70 is upregulated by C75 and may ameliorate cytotoxic effects of FASN-inhibition	76

4.6 Conclusion.....	77
5 References	78
Curriculum vitae.....	91

Abstract

Ovarian cancer is the most fatal gynecological disease with about 140.000 deaths worldwide in the year 2008. Many patients are diagnosed at an advanced stage, due to missing screening options and late appearance of symptoms. Standard therapeutic interventions include surgery (salpingo-oophorectomy) and platinum/taxane based chemotherapy. Unfortunately, after a period of regression, relapse of tumor growth and chemo-resistance are a common phenomenon. Recent progressions in the understanding of ovarian cancer etiology allow for better predictions of the efficacy of a certain therapeutic approach, including modern antibody- or small molecule- based treatments. Although clinical trials using targeted therapies were able to document increases in progression-free survival, overall survival rates remain poor. Therefore, novel approaches targeting certain characteristics of malignant cells are urgently needed.

Metabolic reprogramming is a distinctive feature of tumor cells. Certain alterations in the metabolism of malignant cells were already recognized in the 1920s by Otto Warburg, who found that cancer cells show a high rate of aerobic glycolysis (the Warburg effect). With the availability of modern analytical and genomic tools, more and more characteristics of malignant metabolic reprogramming were discovered. In recent years, there is increasing scientific interest in the research of metabolic targets for cancer therapy. One potentially targetable and thus druggable feature of many cancers, including ovarian cancer – which is in the focus of this study - is the increased rate of de novo synthesis of fatty acids.

Fatty acid synthase (FASN), the key enzyme responsible for the production of long-chain saturated fatty acids (predominantly palmitic acid) was found to be frequently upregulated in tumors. Several small molecule inhibitors of FASN have shown efficacy in reducing tumor cell growth in preclinical trials. In this project, C75 – a well characterized inhibitor of FASN – as well as the novel compound G28UCM have been used to study and compare the effects of blockade of fatty acid synthesis on malignant, immortalized and non-malignant ovarian surface epithelial (OSE) cells. A major advantage of G28UCM is that, unlike C75, it does not modulate the protein carnitine palmitoyltransferase 1 (CPT1) which is involved in the oxidation of fatty acids and causes severe side effects in vivo.

Using cell growth assays, Western blot technique and flow cytometry, we could prove that both inhibitors of FASN are able to reduce cell growth of malignant, but also of immortalized and of non-malignant OSE cells via induction of apoptosis, autophagy, protein degradation (only C75) and cell cycle arrest, respectively. Concomitantly, both FASN-inhibitors elicited a decrease in cellular signaling – predominantly through the phosphoinositide-3 kinase/Akt pathway – which may be responsible for some of the observed cytotoxic effects. Decreased cellular proliferation established by either C75 or G28UCM could be – at least partially – restored by the addition of exogenous oleic acid, highlighting the importance of lipids in cancer cell metabolism and the specificity of the inhibitory drugs. Interestingly, we observed a very divergent expression pattern for heat-shock protein 70 (HSP70) after treatment with C75 and G28UCM, respectively. While C75-treated cells experienced a remarkable increase in expression of HSP70, no such effect was obtained with G28UCM. Given the (protective) role of HSP70 in cellular stress response, this may explain the better efficacy of G28UCM in reducing cell growth and may be important in the development of new FASN-inhibiting agents. A major improvement of G28UCM over C75 is that it does not induce protein ubiquitination and causes less cytotoxicity, especially in non-malignant cells.

Zusammenfassung

Das Ovarialkarzinom gilt mit ungefähr 140.000 weltweiten Todesfällen im Jahr 2008 als die schwerwiegendste gynäkologische Erkrankung. Wegen fehlender Screening-Möglichkeiten und dem späten Auftreten von Symptomen werden viele Patientinnen erst diagnostiziert, wenn sich die Krankheit bereits in einem fortgeschrittenen Stadium befindet. Die Standardtherapie umfasst die chirurgische Entfernung der Eierstöcke und von Teilen der Eileiter (Salpingo-Oophorektomie), sowie auf Platin/Taxanen basierende Chemotherapien. Unglücklicherweise folgt auf eine initiale Regression häufig rezidives Wachstum des Tumors bei gleichzeitigem Auftreten einer Resistenz gegenüber Chemotherapeutika. Neue Erkenntnisse über die Ätiologie von Eierstockkrebs erlauben eine bessere Vorhersage der Wirksamkeit bestimmter therapeutischer Ansätze, wie zum Beispiel moderner Antikörper-basierender oder niedermolekularer Behandlungen. Obwohl zielgerichtete Therapien in klinischen Studien bereits einen Anstieg des progressionsfreien Überlebens erbracht haben, konnte damit im Bereich der Gesamtüberlebensrate von Ovarialkarzinom-Patientinnen noch kein deutlicher Fortschritt erzielt werden. Es herrscht daher dringender Bedarf an neuen Behandlungsmöglichkeiten, die auf bestimmte Charakteristika maligner Zellen abgestimmt sind.

Die Reprogrammierung metabolischer Eigenschaften ist ein typisches Merkmal von Tumorzellen. Bestimmte Veränderungen im Metabolismus maligner Zellen wurden bereits 1920 von Otto Warburg entdeckt, als er feststellte, dass Krebszellen eine gesteigerte aerobe Glykolyse aufweisen (der Warburg Effekt). Moderne analytische und genetische Werkzeuge haben zur Entdeckung zahlreicher weiterer Merkmale im Metabolismus maligner Zellen verholfen. Das führte in den letzten Jahren zu einem gesteigerten Interesse an der Erforschung von Tumortherapien, die auf metabolische Eigenschaften zielen. Eine dieser metabolischen Besonderheiten von Krebszellen (u.a. auch Ovarialkrebszellen), die gesteigerte Syntheserate von Fettsäuren, ist Gegenstand dieser Arbeit.

Fettsäure-Synthase (engl.: fatty acid synthase) (FASN) ist das Schlüsselenzym in der Synthese von langkettigen, gesättigten Fettsäuren (vor allem Palmitinsäure) und ist in Tumoren häufig überexprimiert. Präklinische Studien beschreiben die Effektivität in der Reduktion von Tumorzellwachstum einiger niedermolekularer Inhibitoren der FASN. Dieses Projekt bedient sich der gut beschriebenen, FASN-inhibierenden

Wirksubstanz C75, sowie des neuen niedermolekularen FASN-Inhibitors G28UCM. Damit sollten die Effekte der Blockade der Fettsäuresynthese auf maligne, immortalisierte und normale ovariale Oberflächenepithelzellen (OSE) studiert und verglichen werden. Dabei hat G28UCM gegenüber C75 den Vorteil, dass dieser Wirkstoff keine unspezifische Bindung an das Enzym Carnitin-Palmityltransferase (CPT1) – welches an der Oxidation von Fettsäuren beteiligt ist – aufweist. Die bekannte Modulation von CPT1 durch C75 wird in vivo mit schweren Nebenwirkungen in Verbindung gebracht.

Mittels Wachstumsassays, Western Blot und Durchflusszytometrie konnte festgestellt werden, dass beide FASN-Inhibitoren das Wachstum von malignen, aber auch immortalisierten und normalen Oberflächenepithelzellen des Ovars reduzieren. Als dafür verantwortliche zelluläre Prozesse konnten Apoptose, Autophagie, Proteindegradation (nur bei C75) und Zellzyklusarretierung identifiziert werden. Damit einhergehend wurde für beide Inhibitoren eine Beeinträchtigung intrazellulärer Signaltransduktionskaskaden – allen voran des Phosphatidylinositol-3 Kinase/Akt Signaltransduktionsweges – nachgewiesen, die für einen Teil der beobachteten zytotoxischen Effekte verantwortlich sein könnten. Exogene Bereitstellung von Oleinsäure konnte die von beiden FASN-Inhibitoren hervorgerufene Reduktion der Zellproliferation zumindest partiell aufheben. Dadurch wurde die Wichtigkeit von Lipiden für den Metabolismus von Tumorzellen, sowie die Spezifität beider Inhibitoren hervorgehoben. Interessanterweise konnte nach Behandlung mit C75, bzw. G28UCM eine äußerst divergente Expression des Hitzeschockproteins (engl.: heat-shock protein) HSP70 gezeigt werden. Behandlung mit C75 führte im Gegensatz zu einer Behandlung mit G28UCM zu einem beträchtlichen Anstieg der Proteinmenge von HSP70. Im Hinblick auf die (protektive) Rolle dieses Proteins bei der Verarbeitung zellulären Stresses, könnte dies erklären warum G28UCM das Zellwachstum effektiver reduziert. Diese Eigenschaft könnte auch bei der Entwicklung neuer Fettsäure-Synthase-Inhibitoren wichtig sein. Zudem weisen die Ergebnisse dieser Arbeit darauf hin, dass G28UCM im Gegensatz zu C75 keine Ubiquitinierung von Proteinen verursacht und (speziell in nicht-malignen Zellen) der weniger zytotoxische Wirkstoff ist.

1 Introduction

1.1 Ovarian cancer

1.1.1 Epidemiology

Ovarian cancer (OC) is a highly divergent group of neoplasms of the ovary. With an estimated number of 225.500 new cases and 140.200 deaths in the year 2008, it is the 8th most common type of cancer and the 7th most cause of cancer-related death among females worldwide. The incidences vary between more developed (9.4 per 100.000) and less developed countries (5.0 per 100.000) (Jemal et al. 2011, Lowe et al. 2013). Ovarian cancer is the most fatal gynecologic disease in developed countries and the second most fatal gynecologic disease in less developed countries. The high mortality is contributed by the fact that most patients are asymptomatic until the cancer has metastasized and therefore two thirds of the cases are diagnosed at late stages (Holschneider and Berek, 2000).

1.1.2 Etiology

The etiology of ovarian cancer is a matter of scientific debate, as the exact tissue of origin is not quite clear. Basically, epithelial ovarian tumors can be divided into two main groups according to their histologic, clinicopathologic and molecular genetic properties. Type I tumors comprise endometrioid (10%), clear cell (10%), low-grade serous (<5%) and mucinous carcinomas (<3%). Prototypic type II tumors are high-grade serous carcinomas and they make up for 70-75% of all epithelial ovarian carcinomas (EOC) (Shih and Kurman 2004, 2011, Prat 2012). Type I neoplasms often are confined to the ovary and present as indolent, large masses with good prognosis. They likely arise in a series of steps from well-recognized precursor lesions which themselves originate from ovarian surface epithelium, epithelial inclusion cysts, endometriosis or endometriomas. They are further characterized by a low proliferation rate, they frequently have mutations in BRAF, KRAS or PTEN (in case of endometrioid OC) genes and they respond poorly to chemotherapeutics (Singer et al. 2002, Shih and Kurman 2011, Landen et al. 2008, Obata et al. 1998). On the contrary, no definitive precursor lesions are known in the genesis of most type II ovarian epithelial carcinomas. This may be due to the rapid transition of these aggressive tumors from microcarcinomas to clinical detectable neoplasms. In favor of this hypothesis is the finding that high-grade serous carcinomas have a significantly

higher Ki-67 nuclear labeling (proliferation) index than low-grade serous carcinomas (Garzetti et al. 1995, Shih and Kurman 2004). Furthermore, type II EOCs typically show mutations in TP53 (>95%) (Ahmed et al. 2010) as well as mutations or inhibition of expression of BRCA (40-50%) (Senturk et al. 2010) and amplification of Her2/neu is present in up to 66% of type II carcinomas (Ross et al. 1999). Additionally, they usually have no mutations found in type I tumors (Kurman and Shih 2011). The lack of clearly characterized precursor lesions makes it very difficult to identify the tissue of origin of type II neoplasms of the ovary. Although it was proposed, that they likely arise from ovarian surface epithelium or postovulatory inclusion cysts (Bell and Scully 1994, Auersperg et al. 2001), this paradigm slowly starts to shift as more and more evidence points to distal oviductal fimbriae as the tissue of origin from which primary neoplastic cells secondarily involve the ovary (Lee et al. 2007, Vang et al. 2013, Auersperg 2013).

1.1.3 Risk factors

Family history is the most significant risk factor for ovarian cancer, depending on the number of affected first- and second-degree relatives. Mutations in two types of genes – BRCA1, BRCA2 and the mismatch repair genes associated with Hereditary Nonpolyposis Colorectal Cancer (HNPCC) - have been linked to susceptibility to ovarian cancer. Approximately 10% of ovarian cancer are hereditary, the majority (90%) of which are caused by mutations in BRCA1 or BRCA2 (Holschneider and Berek 2000, Daniilidis and Karagiannis 2007). U.S. population based studies suggest that the lifetime risk for ovarian cancer for individuals with mutations in BRCA1 or BRCA2 is around 27.8% and 27%, respectively (Whittemore et al. 1997, Ford et al. 1998). Mutations in the mismatch repair genes associated with HNPCC confer a lifetime risk for malignant ovarian disease of 5-13% (Lynch et al. 1998, Farrell et al. 2006).

There is evidence that reproductive factors such as increasing parity and breast feeding reduce the risk of developing ovarian cancer. Compared to nulliparas, multiparas have a risk reduction of up to 60% (Hankinson et al. 1995, Holschneider and Berek 2000). On the other hand, infertility is linked to an elevated risk of ovarian cancer, whereby it is presumed that the biological parameters that cause infertility also increase ovarian cancer susceptibility (Ness et al. 2002). Furthermore, the use

of oral contraceptives has a strong protective effect on the risk for ovarian cancer including familial ovarian cancer (Gross and Schlesselman 1994, Walker et al. 2002).

As mentioned above, a certain amount of ovarian cancers seem to originate from the fallopian tube. Interestingly, a recent study has addressed the question whether risk factors of ovarian cancer vary with the tissue of origin. This study reported that reproductive factors like tubal ligation, parity, endometriosis and age were more strongly associated with tumors that are more likely of ovarian origin and less likely of fallopian tube origin (Kotsopoulos et al. 2013).

1.1.4 Therapy

The evolving new paradigm of ovarian carcinogenesis ultimately has to result in individualized treatment options. Type I ovarian neoplasms are often diagnosed when they are still at a low stage and therefore salpingo-oophorectomy may be sufficient. However, when these tumors are diagnosed at a later stage and thus are not confined to the ovary, additional therapies are needed. Unfortunately late-stage type I ovarian tumors do not respond well to standard chemotherapeutics (platinum, taxane), probably due to their relatively slow proliferation rate. Deregulated signaling through the MAPK pathway via mutations of KRAS or BRAF is a common event in the progression of those cancers. Therefore, approaches targeting aberrant signaling could provide distinct advantages in treatment of advanced-stage type I tumors. Unfortunately, phase II clinical trials using monoclonal antibodies targeting EGFR family receptors (e.g. erlotinib, pertuzumab) against recurrent ovarian cancer showed only modest efficacy (Gordon et al. 2005, Makhija et al. 2010, Itamochi and Kigawa 2012).

Regarding type II ovarian neoplasms, early detection is very important. Therefore, sensitive and specific biomarkers are needed. High-grade serous carcinomas as the prototypic type II tumors often show a response to chemotherapy using platinum or taxane components, but regularly experience recurrence accompanied by resistance (Gilks and Prat 2009, Hankaer et al. 2012). Since these tumors are often characterized by a loss of DNA repair mechanisms (e.g. BRCA1/2 mutation/hypermethylation), therapies targeting other mechanisms involved in the repair of DNA damage are promising approaches (Kurman and Shih, 2011). Efficacy of this strategy has already been observed in studies using small molecule inhibitors of poly ADP-ribose

polymerase (PARP) such as olaparib or rucaparib (Chen et al. 2013, Audeh et al. 2010, Drew et al. 2011).

Targeting angiogenesis is another promising approach in treatment of ovarian cancer. Angiogenesis is critical for tumor growth, invasion and metastasis. The family of vascular endothelial growth factors (VEGF) and its receptors (VEGFR) are critical components in the process of neovascularization. Overexpression of VEGF was observed in ovarian cancer (Fujimoto et al. 1998, Li et al. 2004) and is therefore considered as a potential target. Bevacizumab, a monoclonal antibody targeted at VEGF-A represents the most intensive studied targeted therapy in ovarian cancer. Several phase II and phase III trials have shown that bevacizumab in combination with chemotherapy can significantly increase progression-free survival. However, beneficial effects on overall survival have not been reported (Itamochi and Kigawa 2012).

1.2 Cancer metabolism

First insights into tumor metabolism were gained by the work of Otto Warburg in the 1920s. He found that tumors show increased glucose uptake compared to normal tissue and that tumors metabolize glucose via aerobic glycolysis rather than oxidative phosphorylation – a phenomenon also known as the Warburg effect (Warburg et al. 1927, Vander Heiden et al. 2009), even though aerobic glycolysis is inefficient in terms of ATP production. Aerobic glycolysis generates only 2 ATP molecules per molecule of glucose, while complete oxidation of one molecule of glucose by oxidative phosphorylation generates up to 36 ATP molecules. The reason, why cancer cells show high rates of aerobic glycolysis lies in their high proliferation rate. The generation of a daughter cell requires the replication of all cellular contents, including DNA, RNA, proteins and lipids. The precursors for these macromolecules are provided by upregulated glycolysis (Lunt and Vander Heiden 2011). Therefore, altered metabolism is crucial for supporting rapid proliferation, evasion of growth inhibitory signals, cell migration and metastasis via the production of macromolecules like nucleotides, proteins, complex sugars and lipids. In the past decade, the availability of advanced analytical and genomic tools as well as bioinformatics has provided the means to identify many pathways and enzymes that are involved in metabolic reprogramming of cancer cells (Jones and Schulze 2012, Schulze and Harris 2012).

One way by which tumor cells exhibit altered metabolic activity is through oncogenic signaling. The phosphatidylinositol-3 kinase (PI3K)/Akt pathway – one of the most commonly altered pathways in cancer – has been shown to increase glycolytic flux by upregulation of glucose transporter expression and activation of glycolytic enzymatic activity (Robey and Hey 2009, Elstrom et al. 2004, Majewski et al. 2004). Furthermore, PI3K/Akt signaling promotes the synthesis of fatty acids (Porstmann et al. 2005). Overexpression of Myc is also involved in alteration of glycolytic processes via induction of the pyruvate kinase gene PKM2. PKM2 can shift from a tetrameric, high-activity isoform to a dimeric isoform with low activity, thereby causing the accumulation of glycolytic intermediates for biosynthetic processes (David et al. 2010, Schulze and Harris 2012). Moreover, oncogenic expression of Myc drives glutaminolysis, which provides building blocks for amino acids and lipids. The tumor micro-environment is often associated with low oxygen availability. Hypoxia-inducible factor (HIF) is the main transcription factor responsible for adaptation to hypoxic conditions. HIF induces glycolytic enzymes like glucose transporter 1 and 3 and prevents the entry of pyruvate into the mitochondrial tricarboxylic acid (TCA) cycle by induction of pyruvate dehydrogenase kinase 1 (PDHK1). Again, this causes the accumulation of intermediary glycolytic metabolites that can be used in the biosynthesis of macromolecules (Jones and Schulze 2012, Schulze and Harris 2012, Soga 2013).

Altered metabolism in tumor cells could also be driven by mutations in metabolic enzymes, rendering them as tumor suppressors. For example, inherited mutations in the genes encoding succinate dehydrogenase (SDHB, SDHC, SDHD) or fumarate hydratase (FH) are associated with familial cancer syndromes (Schulze and Harris 2012).

Altered metabolic activity in tumor cells is recognized as an important platform offering a multitude of possibilities for cancer treatment. Many potential drugs targeting cancer metabolism are currently being developed, most of them are interfering with glycolytic processes. However, the majority of these agents is still in early development and in preclinical trials, or lacks clinical efficacy (Jones and Schulze 2012, Schulze and Harris 2012).

This study focuses on the de novo synthesis of fatty acids as a potentially targetable pathway in ovarian cancer.

1.3 Fatty acid synthesis and cancer

Fatty acids are essential constituents of cellular membranes. They are important as substrates in energy metabolism and posttranslational protein modification, and they act as second messengers in cellular signaling pathways. Humans and other mammals can utilize two sources of fatty acids – exogenous dietary lipids or endogenous synthesis of fatty acids. De novo synthesis of fatty acids involves the lipogenic enzymes ATP citrate lyase (ACL), acetyl-CoA carboxylase (ACC) and fatty acid synthase (FASN) (Figure 1). When excess amounts of citrate are available, it can enter the cytosol where it is cleaved into oxaloacetate and acetyl-CoA by ACL. ACC carboxylates acetyl-CoA to form malonyl-CoA. FASN synthesizes long chain fatty acids (predominantly palmitate) by using acetyl-CoA as a primer and malonyl-CoA as a two-carbon donor. NADPH acts as a reducing equivalent in this series of condensing reactions (Menendez and Lupu 2007, Flavin et al. 2010, Abramson 2011).

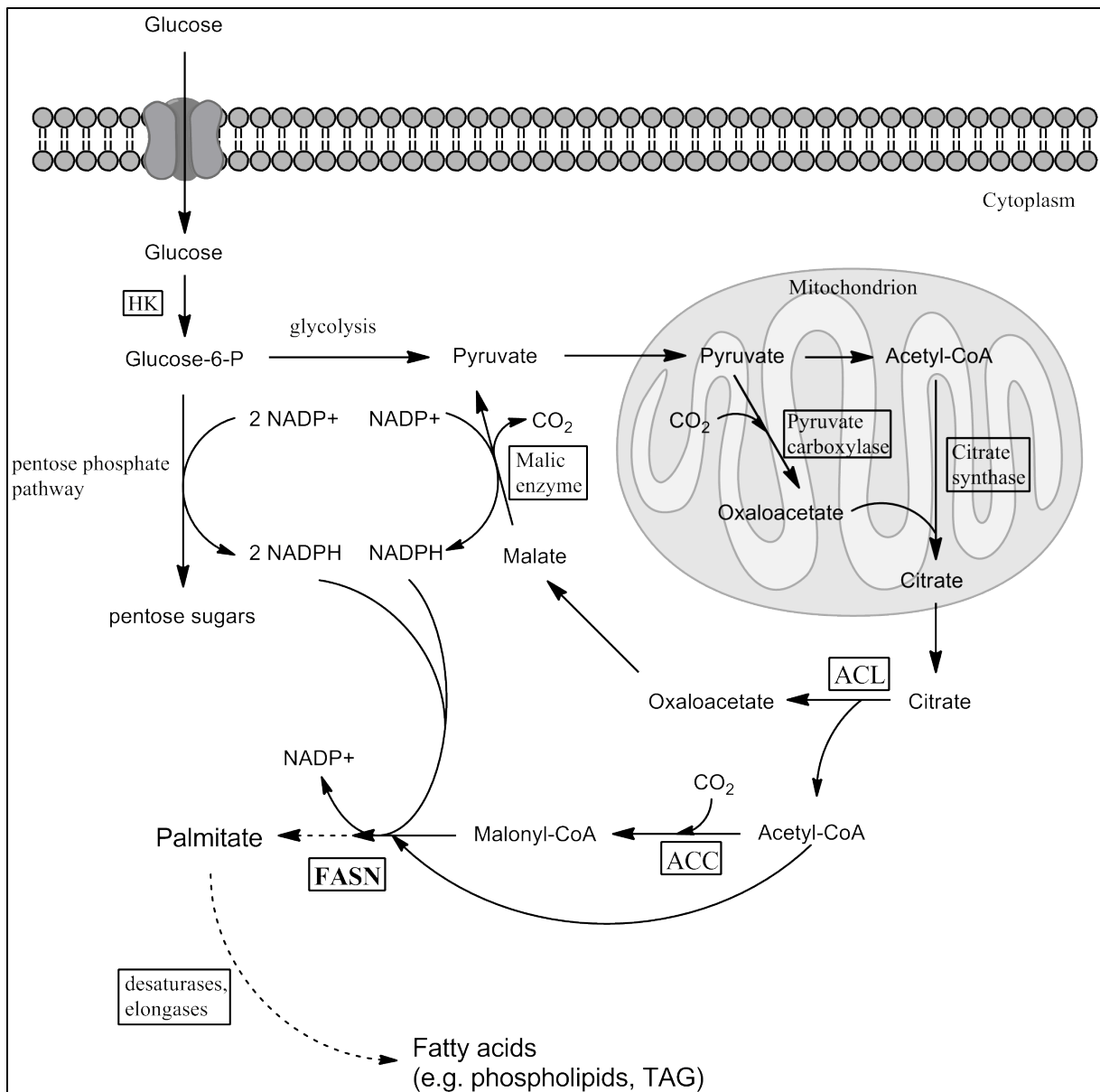


Figure 1 | De novo synthesis of fatty acids; glucose is taken up from the environment and phosphorylated by hexokinases (HK); now it is available for glycolysis in order to gain energy or is directed to the pentose phosphate pathway to generate building blocks for nucleotides; pyruvate, the end product of glycolysis gets transported into the mitochondria, where it is either decarboxylated (pyruvate dehydrogenase, not shown) to form acetyl-CoA or carboxylated (pyruvate carboxylase) to form oxaloacetate; citrate synthase catalyses the condensation of oxaloacetate and acetyl-CoA to yield citrate; when citrate concentrations are high, it gets transported into the cytosol where ATP citrate lyase (ACL) splits citrate again into oxaloacetate and acetyl-CoA; acetyl-CoA can get carboxylated by acetyl-CoA carboxylase (ACC) to form malonyl-CoA; the synthesis of fatty acids is a cyclic sequence of different reactions, involving fatty acid synthase (FASN) as the catalytic enzyme, one molecule of acetyl-CoA (at the start of the reaction) and 7 molecules of malonyl-CoA; during each cycle, the fatty acid chain gets elongated by two carbon atoms; the predominant end-product palmitate is further elongated by special elongases and/or desaturated (introduction of C-C double bonds) to

generate phospholipids (needed for membrane maintenance and growth), triacylglycerides (TAGs, as storage fat) and other products.

In most human tissues, the cells preferentially satisfy their need for lipids by utilizing dietary fatty acids. However, during embryogenesis, in the fetal lung, in adult adipose- and liver-tissue as well as in hormone-sensitive tissues, cells are capable of de novo synthesis of fatty acids (Wagle et al. 1999, Kusakabe et al. 2000). Most importantly, it was found that many tumors and pre-neoplastic lesions exhibit increased endogenous production of fatty acids, to be able to maintain their high proliferation profile. Elevated fatty acid synthesis is marked by overexpression of lipogenic enzymes – first and foremost FASN. Immunohistochemical studies revealed high levels of FASN in many epithelial cancers including breast, colon, prostate and ovary (Menendez and Lupu 2007). Increased synthesis of fatty acids is accompanied by an elevated need for carbon donors and reducing equivalents. In cancer cells the high rate of aerobic glycolysis leads to accumulation of pyruvate (Costello and Franklin 2005), which can ultimately function as a carbon donor in the synthesis of fatty acids (see Figure 1). NADPH, the reducing equivalent used in fatty acid synthesis is provided either by the action of malic enzyme or via the pentose phosphate pathway (see Figure 1), another pathway of major importance in cancer cells (Menendez and Lupu 2007). Thus, de novo lipogenesis is tightly integrated in the altered metabolic phenotype of tumor cells.

Unlike in normal cells, the regulation of lipogenesis in malignant cells seems to be insensitive to external nutritional signals (Menendez and Lupu 2007). Although the exact molecular mechanisms leading to enhanced lipogenesis in cancer cells are still not fully understood, reports suggest a strong association with increased signaling via the PI3K/AKT and mitogen activated protein kinase (MAPK) pathways. These signaling cascades induce expression and/or maturation of the transcription factor sterol regulatory element binding protein-1c (SREBP1c) via action of mammalian target of rapamycin complex 1 (mTORC1). SREBP1c binds to promoters of various lipogenic enzymes including FASN and enhances their transcription (Swinnen et al. 2000, Yang et al. 2002, Van de Sande 2002). Furthermore, steroid hormones in conjunction with their receptors can contribute to elevated production of fatty acids (Swinnen et al. 1997). FASN expression in cancer cells may also be enhanced by

post-translational stabilization of the enzyme. A ubiquitin-specific protease (USP2a) was found to remove ubiquitin and thereby stabilizes FASN in prostate cancer cells (Graner et al. 2005).

The high expression of FASN in tumors compared to most normal tissues renders it a promising target for anti-cancer therapy.

1.3.1 FASN as target for anti-cancer therapy

FASN is a homodimeric, cytosolic protein of approximately 270kDa and – as mentioned above – a key enzyme in the generation of the 16 carbon saturated fatty acid palmitate. Each subunit has an acyl carrier protein and six different catalytic domains (starting from C-terminus: thioesterase (TE), acetyl carrier protein (ACP), β -keto reductase (KR), enoyl reductase (ER), dehydratase (DH), malonyl/acetyl transferase (MAT) and β -ketoacyl synthase (KS)). Together, these domains facilitate the reactions in the iterative process of fatty acid synthesis. Some of these domains – most importantly the KS and the TE domain – are binding sites for natural and synthetic small molecule inhibitors of FASN (Menendez and Lupu 2007, Flavin et al. 2010). Blockade of FASN can reduce cancer cell growth and induces apoptosis. There are several proposed mechanisms that could explain these cytotoxic effects, including end-product starvation, disturbance of lipid membrane integrity, cell cycle arrest, accumulation of malonyl-CoA and inhibition of anti-apoptotic proteins, respectively (Lupu and Menendez 2006, Huang et al. 2009).

In this study, two synthetic compounds – the well characterized substance C75 and a novel derivative of the natural occurring substance epigallocatechin-3-gallate (EGCG) named G28UCM - were used to inhibit FASN in malignant, immortalized and normal ovarian surface epithelial cells. C75 covalently binds to the KS domain of FASN, thus preventing the condensation reaction of the elongating fatty acid chain and successive acetyl or malonyl residues (Menendez and Lupu 2007). Previous studies have shown the effectiveness of C75 in reducing cancer cell growth (including colon, mammary, lung, liver and ovarian cancer cells) in vitro and of breast and lung cancer xenografts (Pizer et al. 2000, Li et al. 2001, Gao et al. 2006, Grunt et al. 2009, Relat et al. 2012). Unfortunately it was reported that C75 modulates food intake and energy expenditure via modulation of carnitine palmitoyltransferase 1 (CPT1), thereby causing weight loss and loss of adipose mass. Therefore C75 is only regarded as a laboratory tool (Loftus et al. 2000, Thupari et al. 2002). G28UCM is a synthetic

compound derived from the green tea ingredient EGCG and similar to C75 binds to FASN at the KS domain. It has been reported that G28UCM is capable to reduce growth of breast cancer cells in vivo and in vitro. One advantage over C75 is that G28UCM does not induce weight loss by modulation of CPT1 (Puig et al. 2009, Oliveras et al. 2010).

2 Materials and Methods

2.1 Cell lines and cell culture

All cell lines were incubated in polystyrene tissue flasks (Falcon) at 37°C, 95% humidity, 5% CO₂. Malignant cell lines and CRL2522 foreskin fibroblasts were cultured in respective media (Table 1) containing 10% heat inactivated fetal calf serum (HI-FCS) (Gibco, #10270106), 100 IU/ml penicillin/ 100 µg/ml streptomycin (Gibco, #15140-148), 2mM L-Glutamine (Gibco, #25030-032). IOSE80,-364,-386 cells were cultured in IOSE-medium (Table 1) containing 5% HI-FCS, 100 IU/ml penicillin/ 100 µg/ml streptomycin. OSE cells were cultured in OSE-medium (Innoprot, #P60132) containing 1% ovarian epithelial cell growth supplement (OEpiCGS, Innoprot) and 100 IU(µg)/ml penicillin/streptomycin (Innoprot). Tissue flasks and dishes assigned for the culture of OSE cells were coated with 2µg/cm² poly-L-lysine (Innoprot) at 37°C for a minimum of 1h before use to provide a positively charged surface to which OSE cells could adhere.

Cell line	Source	Cancer / Cell type	Medium	Split ratio	Split interval
A2774	M. Krainer, Medical University of Vienna, Austria	ovarian adenocarcinoma	α-MEM	1:10	3-4d
A2780	M. Krainer, Medical University of Vienna, Austria	ovarian adenocarcinoma	RPMI1640	1:15	3-4d
A2780ADR	M. Krainer, Medical University of Vienna, Austria	ovarian adenocarcinoma	RPMI1640	1:15	3-4d
CAOV3	ATCC (Manassas, VA, USA)	ovarian adenocarcinoma	α-MEM	1:15	7d
CRL2522	ATCC (Manassas, VA, USA)	foreskin fibroblast	α-MEM	1:2 - 1:3	7d
H134	H.J. Broxterman, Free University Hospital, Amsterdam, The Netherlands	ovarian adenocarcinoma	α-MEM	1:12	7d

HEY	R.N. Buick, University of Toronto, Toronto, Canada	ovarian adenocarcinoma	D-MEM	1:20	3-4d
HOC7	R.N. Buick, University of Toronto, Toronto, Canada	ovarian adenocarcinoma	α -MEM	1:20	3-4d
IOSE80	COTB*, British Columbia Cancer Research Centre, Canada	primary ovarian surface epithelial cells (immortalized**)	IOSE-medium	1:12	3-7d
IOSE364	COTB*, British Columbia Cancer Research Centre, Canada	primary ovarian surface epithelial cells (immortalized**)	IOSE-medium	1:12	3-7d
IOSE386	COTB*, British Columbia Cancer Research Centre, Canada	primary ovarian surface epithelial cells (immortalized**)	IOSE-medium	1:12	3-7d
OSE	Innoprot, Derio, Spain (#P10982)	primary ovarian surface epithelial cells	OSE-medium	1:3	7d
OVCAR3	ATCC (Manassas, VA, USA)	ovarian adenocarcinoma	α -MEM	1:10	7d
PA1	ATCC (Manassas, VA, USA)	ovarian teratocarcinoma	α -MEM	?	?
SKOV3	ATCC (Manassas, VA, USA)	ovarian adenocarcinoma	α -MEM	1:15	7d
TR170	B.T. Hill, Imperial Cancer Research Fund, London, UK	ovarian adenocarcinoma	α -MEM	1:2 - 1:3	7d

Table 1 | Specifications of malignant and non-malignant cell lines. α -MEM (Gibco, #22571-020), D-MEM (Gibco, #41965-039), IOSE-medium (1:1 Medium 199, Sigma, #M5017, MCDB105, Sigma #M6395), OSE-medium (Innoprot, #P60132). *...Canadian Ovarian Tissue Bank; **...immortalized by transfection of Simian Virus 40 T/t antigen

2.2 Drugs

2.2.1 C75

The FASN-inhibitor C75 (Sigma, #C5490) was dissolved in dimethyl sulfoxide (DMSO) (Sigma, #D2650) at a stock concentration of 39,320541mM. Aliquots of 50 μ l were stored at -80°C.

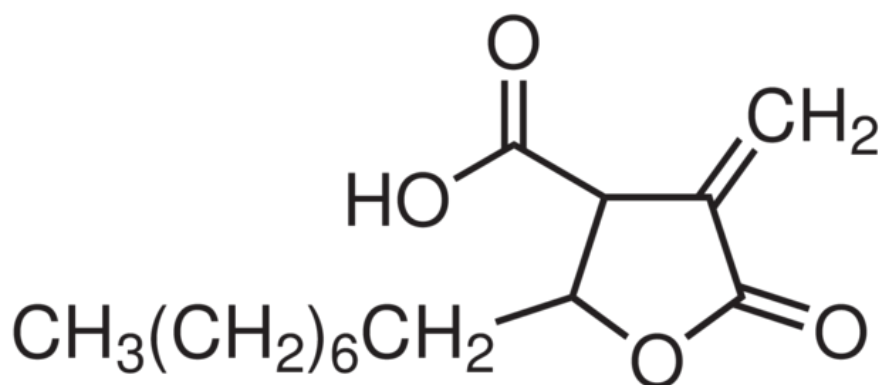


Figure 2 | Chemical structure of the FASN-inhibitor C75. Source: <http://www.sigmaaldrich.com/catalog/product/sigma/c5490?lang=de®ion=AT> as of February 24th, 2013

2.2.2 G28UCM

G28UCM (kind gift from the University of Madrid, Spain) was dissolved in DMSO at a stock concentration of 41,460229mM. Aliquots of 100µl were stored at -80°C.

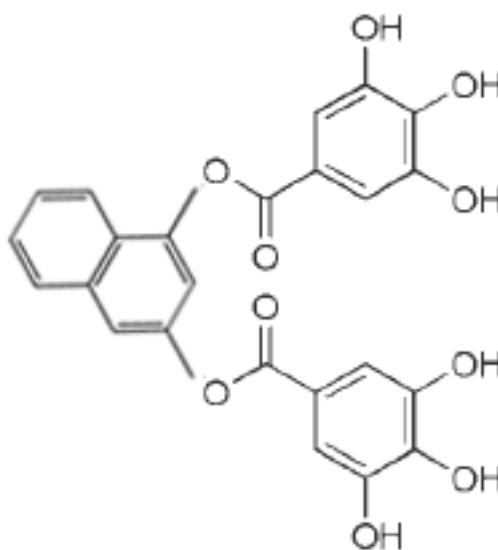


Figure 3 | Chemical structure of the FASN-inhibitor G28UCM. Source: adapted from Puig T et al. 2009

2.2.3 Palmitic acid

Palmitic acid (not dissolved) was obtained from Sigma (#P0500) and stored at room temperature (RT).

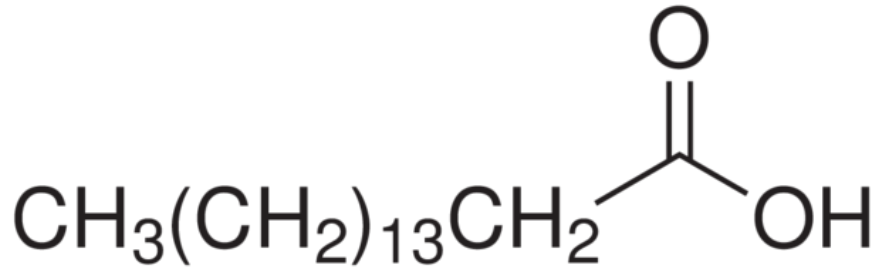


Figure 4 | Palmitic acid chemical structure. Source: <http://www.sigmaaldrich.com/catalog/product/sigma/p0500?lang=de®ion=AT> as of February 24th, 2013

2.2.4 Oleic acid

Oleic acid (OA) complexed to bovine serum albumin (BSA) at a 2:1 molar ratio (2mol OA/1mol BSA) dissolved in Dulbecco's phosphate buffered saline (DPBS) was obtained from Sigma (#O3008). The stock concentration of OA was 3,3279mM and was stored at 4°C.

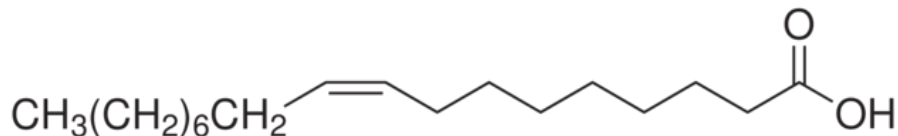


Figure 5 | Oleic acid chemical structure: <http://www.sigmaaldrich.com/catalog/product/sial/o1008?lang=de®ion=AT> as of February 24th, 2013

2.3 Cell growth assay

Cells were grown in cell culture flasks until they reached a confluence of 85 – 100%. After removal of the culture medium and washing of the cells with DPBS at room temperature, detaching of the cells was accomplished by adding trypsin-EDTA solution (GIBCO, #15400-054, #25300-054, concentration: 0,5% - 0,05%) and incubation for 5-10 minutes at 37°C. Detached cells were transferred into 50ml tubes (Falcon) and centrifuged to remove excess trypsin-EDTA solution. Cells were resuspended in respective growth medium, counted using a hemocytometer and further diluted in growth medium to a final concentration of $0,5 \times 10^4$ – $3,0 \times 10^4$ cells/ml (according to the requirements of the experiment; see Results section). 100µl of this

cell suspension were pipetted into wells of a 96 well plate (TPP, #Z707902) using a handdispenser (Multipette plus, Eppendorf) and incubated at 37°C for 18-24 hours, so that the cells could attach to the surface of the bottom of the wells. Wells used for blank measurement were filled with 100µl of medium without cells. Treatment of the cells was highly dependent on the individual experiments and was carried out as follows:

2.3.1 Treatment with C75 or G28UCM

As C75 and G28UCM are potentially light sensitive substances, all steps of the procedure were executed with minimal lighting. Serial dilutions of each compound were made in respective growth medium without FCS. 100µl containing twice the final concentration of the compound were pipetted into the designated wells in triplicates using a handdispenser. 100µl of growth medium without FCS were pipetted into wells for blank measurement. Vehicle control wells received 100µl of growth medium without FCS containing twice the final concentration of DMSO as was present in wells treated with FASN-inhibitors.

2.3.2 Combination treatment with palmitic acid and C75 or G28UCM

Dilutions of C75 and G28UCM in respective growth medium were made as described above. 50µl of each 4x-solution were pipetted into the designated wells. Vehicle control wells received 50µl of growth medium without FCS containing an equal concentration of DMSO like wells treated with C75 or G28UCM. 20mg of palmitic acid (PA) were dissolved in 1ml 100% ethanol by shaking it for 1h at 37°C, which resulted in a stock solution of PA with a concentration of 77,991µM. This stock solution was further diluted to a concentration of 10 and 40µM respectively in growth medium containing fatty acid free BSA (Serva, #11945). The final ratio of PA:BSA was 10:1 (Lee et al. 2001). The formation of PA-BSA complexes is necessary for a sustained solvation of PA in aqueous solutions. Both, the PA stock solution as well as the PA-BSA solutions were prepared freshly for each experiment. 50µl of respective PA-BSA solution were pipetted into the designated wells of the 96-well plate. Vehicle control wells received 50µl of growth medium without FCS containing the same concentration of DMSO as wells treated with FASN-inhibitors and 50µl of growth medium without FCS containing the same amount of ethanol as wells treated with palmitic acid.

2.3.3 Combination treatment with oleic acid and C75 or G28UCM

Again, dilutions of C75 and G28UCM in respective growth medium were made as described above. 50µl of each 4x-solution were pipetted into designated wells. Oleic acid stock solution was diluted to a concentration of 70µM in growth medium without FCS immediately before use. 50µl of this OA solution were pipetted into designated wells of the 96-well plate. Vehicle control wells received 100µl of growth medium without FCS containing equal amounts of DMSO like wells treated with C75 or G28UCM.

Wells for blank measurement received 100µl of respective growth medium without FCS. For each experiment, the final volume in each well was 200µl and the concentration of FCS was 5% (OSE-medium contained 1% OEpiCGS instead of 5% FCS, see chapter 2.1). After adding all agents, the cells were incubated in the dark for 72h at 37°C, 5% CO₂ before measurement.

2.3.4 Measurement and analysis

To measure the amount of cells in each well, a colorimetric assay (EZ4U, Biomedica, #BI-5000) was performed, where the yellowish tetrazolium salt MTT (3-(4,5-Dimethylthiazol-2-yl)-2,5-diphenyltetrazolium bromide) is reduced by cellular oxidoreductases to yield formazan, giving the solution a red to purple color.

In the described experiments, 20µl of MTT solution were added to the wells after 72h of treatment followed by another incubation period in the dark for 2,5h at 37°C, 5% CO₂. Plates were shaken gently immediately before measurement to homogeneously dispense the formazan in the wells. Analysis was performed by measuring the absorbance at 490nm using a microplate reader (Bio Rad). Absorbance at 650nm was used as reference. Resulting values were analyzed using Microsoft Excel software and vehicle control samples were set to 100%.

2.4 Western Blotting

2.4.1 Culture and treatment of cells

6x10⁶ cells suspended in 7ml of the respective growth medium containing 5% FCS (OSE-medium contained 1% OEpiCGS instead of 5% FCS, see chapter 2.1) were

seeded into 60mm culture dishes (Corning?). For adherence to the bottom surface of the culture dishes, the cells were incubated for 18-24h at 37°C, 5% CO₂. For treatment with the FASN-inhibitors C75 and G28UCM, these compounds were diluted to the designated concentrations in DMSO and pipetted into the culture dishes. Dishes were shaken gently to homogeneously dispense the treatment agents in the culture medium. Vehicle control samples were treated with the same amount of DMSO as samples treated with FASN-inhibitors. The cells were incubated for 48 to 72 hours at 37°C, 5% CO₂.

2.4.2 Preparation of protein samples

Medium was removed from culture dishes and cells were washed twice using DPBS (4°C). RIPA⁺ (radioimmunoprecipitation assay) buffer was freshly prepared by adding to 1,9ml RIPA buffer, 80µl Complete (Roche Diagnostics, #11697498001) and 20µl 200mM sodium orthovanadate solution. 100µl RIPA⁺ buffer were pipetted onto the cells and evenly distributed over the cells by gently swiveling the dishes. Dishes were kept on ice for 15-20 minutes before cells were scraped off and pipetted into precooled (4°C) 1,5ml reaction tubes, where they were vortexed several times during incubation on ice for 10 minutes. Crude samples were centrifuged for 30min at 4°C, 12500rpm and the supernatant of each sample containing proteins was transferred to another 1,5ml reaction tube. The protein concentration was measured using a protein assay from Bio Rad. BSA (Bio Rad, #500-0007) (0,156µg/µl – 10,0µg/µl) dissolved in RIPA⁺ was used to provide a standard curve. 5µl RIPA⁺ (blank measurement) or 5µl BSA standard solution or 5µl protein sample solution were pipetted in triplicates into designated wells of a 96-well plate. 20µl of reagent A' and 200µl of reagent B (Bio Rad, #500-0114) were added to the wells and incubated in the dark for 20 minutes at RT. Reagent A' was provided by mixing 1ml of reagent A (Bio Rad, #500-0113) and 20µl reagent S (Bio Rad, #500-0115) immediately before use. Absorbance of samples was measured using a microplate reader (Bio Rad) at a wavelength of 655nm and a reference wavelength of 450nm. Protein samples were adjusted to a concentration of 1,33µg/µl by adding RIPA⁺ and subsequently diluted with 4x sample buffer to achieve a final concentration of 1µg/µl. Samples were kept on ice during the whole procedure and stored at -80°C. Buffers used for protein preparation are shown in Table 2 and Table 3.

RIPA buffer			
Reagent	Stock concentration	Volume	Final concentration
NaCl	5M	3ml	150mM
Tris pH 7,4	1M	5ml	50mM
DOC (Sodium deoxycholate)	10%	5ml	0,5%
EGTA	50mM	4ml	2mM
EDTA pH 7,4	50mM	10ml	5mM
NaF	500mM	6ml	30mM
β -Glycerophosphate pH 7,2	400mM	10ml	40mM
Tetrasodium pyrophosphate	100mM	10ml	10mM
Benzamidine	30mM	10ml	3mM
Igepal Ca-630	pure	1ml	1%

4x sample buffer			
Reagent	Stock concentration	Volume	Final concentration
Glycerol	pure	5ml	50%
Tris-HCl pH 6,8	1M	1,25ml	125mM
SDS	20%	2ml	4%
Bromophenol blue	1%	1,25ml	0,125%
β -mercaptoethanol *	pure	0,5ml	5%

Table 2 and 3 | Buffers used for the preparation of protein samples. *...add immediately before use

2.4.3 Separation and transfer of proteins

Protein samples were denatured before separation by heating them for 10 minutes to 95°C. Depending on the experiment, 20 μ g – 25 μ g of protein were applied to an SDS-polyacrylamide gel (4% stacking gel; 7,5% - 12% running gel) and electrophoresed for approximately 2h at a constant voltage of 100V. For molecular weight estimation, 2 μ l protein marker (MagicMark XP, Invitrogen, #LC5602) was applied to the SDS-polyacrylamide gel prior to separation. Electrotransfer of proteins onto a polyvinylidene fluoride (PVDF) membrane was performed at a constant current of 290mA at 4°C over night. Buffers used for transfer are shown in Table 4.

1x transfer buffer	
Reagent	Mass/Volume
Glycine	16,8g
ddH ₂ O	1117,5ml
1M Tris pH 8,3	75ml
10% SDS	7,5ml
Methanol	300ml
total volume	1500ml

Table 4 | Buffers used for transfer of proteins from an SDS-polyacrylamide gel to a PVDF membrane.

2.4.4 Immunostaining and detection of specific proteins

PVDF membranes (Perkin Elmer, #NEF1000) were incubated in blocking solution (Tris buffered saline (TBS) with 1% Tween-20 (TBS-T) and 4% BSA) for 1h at RT to prevent antibodies from binding to nonspecific proteins. Membranes were then washed 3x5min in TBS-T at RT. Thereafter, membranes were incubated in a solution containing the designated first antibody at 4°C over night. Again, membranes were washed 2x5min and 2x10min in TBS-T. A solution containing the second (horseradish peroxidase – conjugated) antibody was applied onto the membranes and kept for 1h at RT. Membranes were washed for 2x5min and 2x10min in TBS-T followed by 2x5min and 2x10min in TBS. Enhanced chemiluminescence (ECL) reaction was initiated by pipetting 5ml of a 1:1 mixture of detection solution 1 and 2 (peroxide buffer, luminol/enhancer solution, Pierce, #32106) onto the membrane and incubating in the dark for 5min on a shaker. Protein bands were visualized by exposing photographic film (Amersham, #28906837) to the PVDF membranes. Stated in the tables below are buffers and solutions for immunostaining as well as the first and secondary antibodies used.

4% blocking solution

Reagent	Mass/Volume
1x TBS-T	100ml
BSA	4g

4,21% blocking solution

Reagent	Mass/Volume
1x TBS-T	100ml
BSA	4,21g

1x TBS-T

Reagent	Volume
10x TBS	100ml
ddH ₂ O	950ml
Tween20	1ml

1,053x TBS-T

Reagent	Volume
10x TBS	100ml
ddH ₂ O	850ml
Tween20	1ml

first antibody-solution		secondary antibody-solution	
Reagent	Volume	Reagent	Volume
4,21% blocking solution	4,75ml	4% blocking solution	5ml
1,053x TBS-T	14,25ml	1x TBS-T	15ml
1% sodium azide solution	1ml	total volume	20ml
total volume	20ml		

Table 5 | Buffers and solutions for immunostaining of proteins on a PVDF membrane.

Protein recognized	Phosphoryl-lated AA	MW (kDa)	Manufacturer	Prod. #	Working dilution	Species	Clonality
FASN		265	BD Biosciences	610963	1:500	mouse	monoclonal
AKT		60	Cell Signaling	9272	1:1000	rabbit	polyclonal
pAKT	Ser 374	60	Cell Signaling	9271	1:500	rabbit	polyclonal
ERK1/2		42/44	Cell Signaling	9102	1:1000	rabbit	polyclonal
pERK1/2	Thr 202 / Tyr 204	42/44	Cell Signaling	9101	1:1000	rabbit	polyclonal
S6		32	Cell Signaling	2217	1:1000	rabbit	monoclonal
pS6	Ser 240 / 244	32	Cell Signaling	2215	1:2000	rabbit	polyclonal
PARP1 / cleaved PARP1		116 / 89 / 24	Cell Signaling	9542	1:500	rabbit	polyclonal
LC3B I / LC3B II		18 / 16	Gene Tex Inc.	GTX82986	1:2000	rabbit	polyclonal
HSP70		70	Cell Signaling	4872	1:1000	rabbit	polyclonal
HSP90		90	Cell Signaling	4875	1:1000	rabbit	polyclonal
p16INK4A/CDKN2A		17	Abcam	ab81278	1:2000	rabbit	monoclonal
p21/WAF1		21	Cell Signaling	2947S	1:1000	rabbit	monoclonal
Ubiquitin			Cell Signaling	3936	1:1000	mouse	monoclonal
β -Actin		43	Santa Cruz	sc1616	1:1000	goat	polyclonal
α/β -Tubulin		55	Cell Signaling	2148	1:1000	rabbit	polyclonal

Table 6 | Primary antibodies used in Western blot experiments.

Protein recognized	Manufacturer	Prod. #	Working dilution	Species	Clonality
mouse IgG1	Santa Cruz	sc2954	1:10000	chicken	unknown
rabbit IgG1	Promega	V795A	1:15000	donkey	unknown
goat IgG1	Santa Cruz	sc2020	1:15000	donkey	polyclonal

Table 7 | Secondary antibodies used in Western blot experiments. All secondary antibodies are conjugated to horseradish peroxidase.

2.5 Flow Cytometry

2.5.1 Culture, treatment and harvesting of cells

For each sample, 6×10^5 cells suspended in respective growth medium containing 5% FCS (OSE-medium contained 1% OEpiCGS instead of FCS, see chapter 2.1) were seeded into tissue culture flasks and incubated for 18-24h at 37°C, 5% CO₂ to let cells adhere. Designated dilutions of FASN-inhibitors C75 and G28UCM were prepared in DMSO immediately before use and pipetted into respective tissue flasks. Flasks for vehicle control received the same amount of DMSO as treated samples. To dispense the treatment substances throughout the culture medium, flasks were shaken gently. Cells were treated for 6, 18, 24 and 48 hours respectively, while they were incubated in the dark at 37°C, 5%CO₂. After the treatment period, cells were detached from the surface of the tissue flasks by using trypsin-EDTA solution. Cells from each treatment sample were transferred into 50ml tubes, centrifuged for 5min at 1000rpm, resuspended in DPBS and counted. 2×10^5 cells from each sample were then transferred into FACS-tubes and 1ml of DPBS was added to each tube. From this point on, procedures for the assays conducted differ from each other and will be explained separately.

2.5.2 Active caspase 3 assay

Cells were centrifuged for 5min at 1000rpm and the supernatant was removed carefully by using a Pasteur pipette (also used in consecutive steps). 500µl of formaldehyde solution (2%) was added to the cells and incubated for 15min at RT to fixate cells. Again, cells were centrifuged for 5min at 1000rpm and supernatant was removed. To permeabilize the cell membranes, 500µl methanol (pure, -20°C) were added while tubes were vortexed gently. Tubes were kept at -20°C over night in pure methanol. After centrifugation for 5min at 1000rpm, the supernatant was removed and 2ml PBS containing 0,1% BSA were added to the cells. Following another centrifugation step, 100µl DPBS containing 0,1% BSA and 3% phycoerythrin (PE) – labeled anti-caspase 3 antibody (BD Pharmingen, #561011) were added to the samples and incubated in the dark for 30min at RT. 2ml DPBS containing 0,1% BSA were added and samples were centrifuged. Supernatant was removed and 250µl DPBS were added. Samples were now ready for acquisition of flow cytometric data (BD FACScan). Analysis of the obtained data was done using “Flowing Software 2” (Terho P, Turku Centre for Biotechnology, Finland) software. Vehicle-treated ($\leq 0,2\%$

DMSO) cells were used as negative control (without anti-active caspase 3 antibody). Vehicle-treated ($\leq 0,2\%$ DMSO) cells (labeled with anti-active caspase 3 antibody) were used as no treatment control (0h). Regions H1 (viable population) and H2 (apoptotic population) were manually set in histograms of the negative control samples, whereby the base of the right slope of the population marks the boundary between H1 and H2. These constraints were retained unchanged for all subsequent samples of the respective experiment.

2.5.3 Cell cycle analysis

Cells were centrifuged for 5min at 1000rpm and supernatant was removed using a Pasteur pipette (also used in consecutive steps). 1ml 80% ethanol (-20°C) was added to the samples and kept at -20°C over night. Ethanol was removed after centrifugation and 1ml of DPBS was added. Again, samples were centrifuged and the supernatant was removed. 250 μl of propidium iodide (PI) solution (Table 8) was added and samples were incubated at RT for 20min. Samples were kept on ice and in the dark until acquisition of flow cytometric data (BD FACScan). Data was analyzed using “Mod Fit” (Verity Software House) software. Vehicle-treated ($\leq 0,2\%$ DMSO) cells were used as control.

Propidium iodide (PI) solution			
Reagent	Stock concentration	Volume	Final concentration
Triton X-100	1%	2,0ml	0,10%
EDTA-disodium	10mM	0,2ml	0,1mM
RNAse A	10mg/ml	0,1ml	50 $\mu\text{g}/\text{ml}$
PI	1mg/ml	1,0ml	50 $\mu\text{g}/\text{ml}$
DPBS		16,7ml	
total volume		20,0ml	

Table 7 | Propidium iodide solution used for staining of DNA in cell cycle experiments.

2.6 Statistics

Statistical analysis was performed using Sigma Plot 12 software. Tests included One-Way-ANOVA, Student’s t-test and Mann-Whitney Rank Sum Test. The latter was used in substitution for Student’s t-test in cases of a failing normality test (Shapiro-Wilk), which is a prerequisite for Student’s t-Test. p-Values below 0,05 were considered statistically significant. Correlation analysis was performed using Microsoft Excel software.

3 Results

3.1 Expression of FASN in malignant and non-malignant cells

Upregulated expression of FASN is now known to be a common feature in many tumors, including ovarian cancer (Smith Sehdev et al. 2010). In non-malignant tissues, however, expression of FASN seems to be restricted only to cells with high lipid metabolism (e.g. adipocytes) and hormone-sensitive tissue (e.g. cycling endometrium) (Kusakabe et al. 2000). To get an idea about the extent and variability of expression of FASN in vitro, protein samples from 10 ovarian cancer cell lines as well as from immortalized (IOSE) and normal ovarian surface epithelial cells (OSE) and normal CRL2522 foreskin fibroblasts were obtained (see Materials and Methods section). Two independent samples were analyzed for SKOV3 and OSE (18 days and 22 days in culture). Most malignant cell lines showed minor variances in FASN expression (Figure 6 and 7). In contrast, OVCAR3 has a remarkably elevated expression of FASN (Figure 6A). FASN levels in immortalized ovarian surface epithelial cells were in the range of most malignant cell lines. Both samples obtained from SKOV3 cells exhibited almost equal expression levels, whereas OSE cells displayed a distinct variability between day 18 and day 22 (Figure 6B). CRL2522 foreskin fibroblasts were found to have a very low expression level of FASN (Figure 6C).

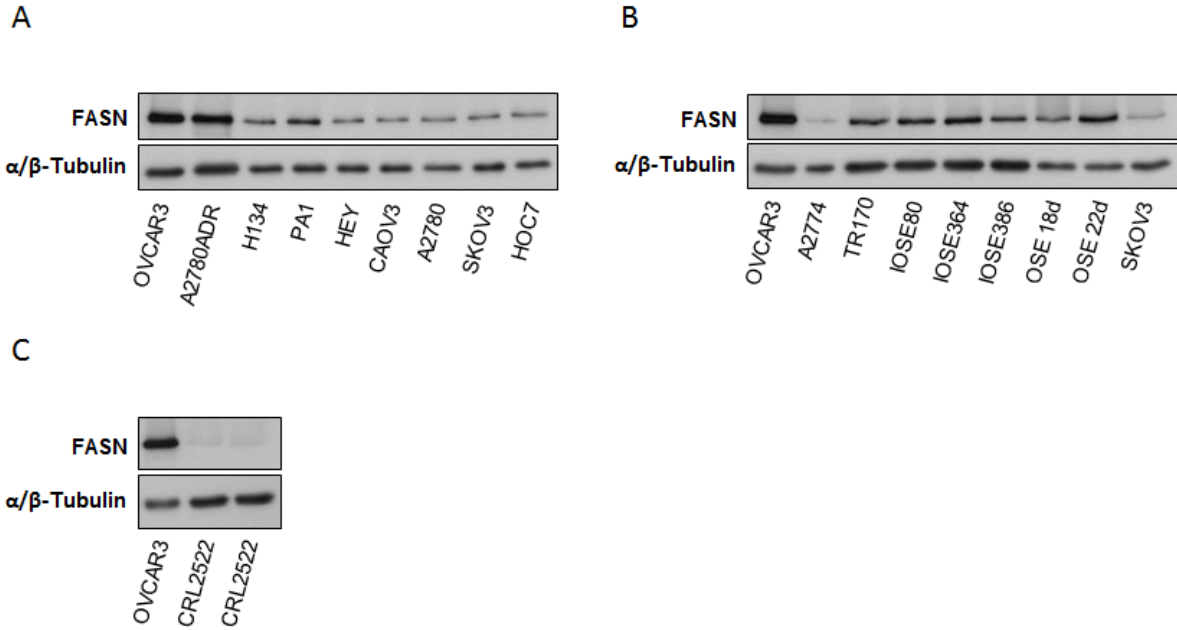


Figure 6 | Expression of FASN in malignant and non-malignant ovarian cells as well as in CRL2522 foreskin fibroblasts. Cells were grown in 60mm dishes for 72h at 37°C, 5% CO₂, 5% FCS in respective media before harvesting. OVCAR3 protein sample was used as a standard in all three blots depicted. α/β -Tubulin was used as a loading control.

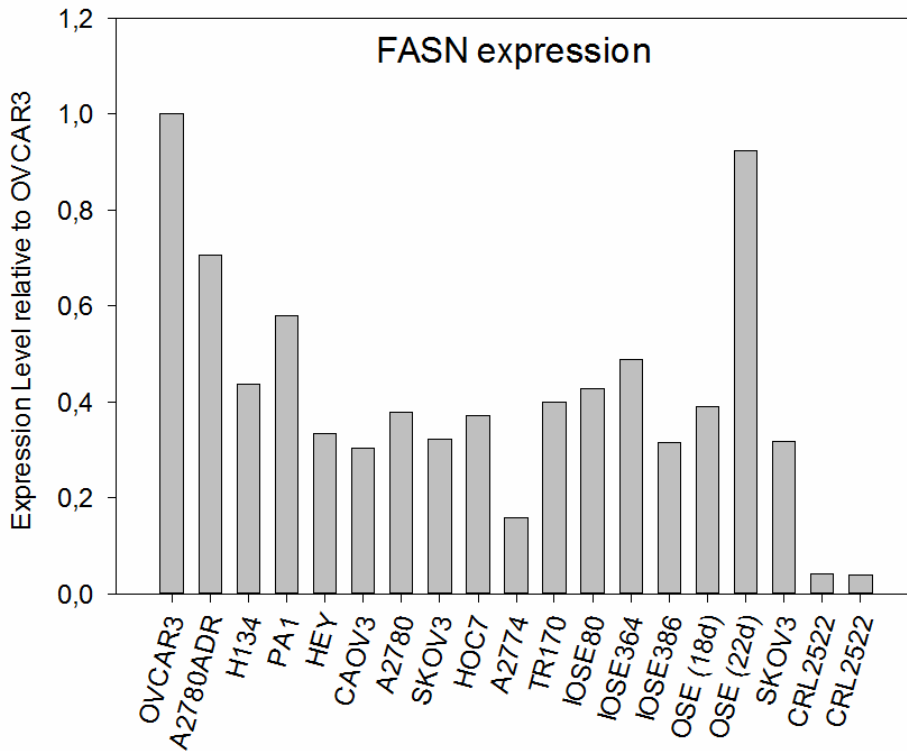
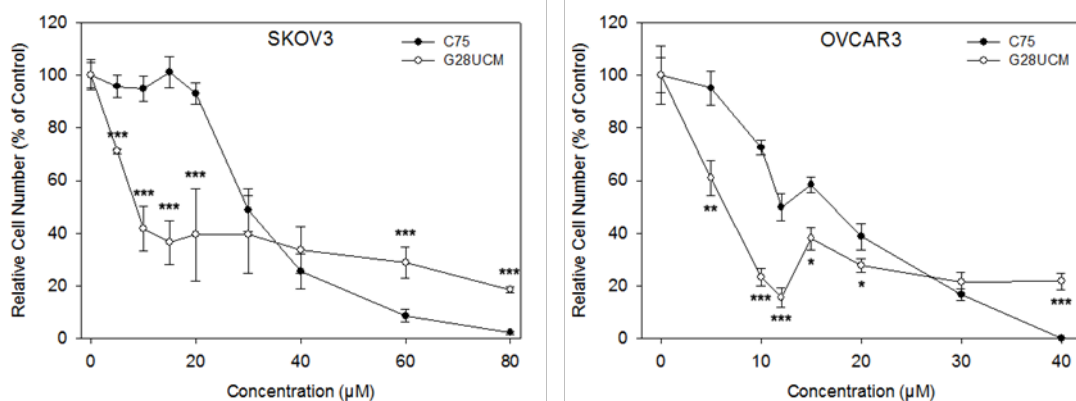


Figure 7 | Relative expression levels of FASN in ovarian cells and in CRL2522 foreskin fibroblasts. FASN expression was related to α/β -Tubulin and normalized to expression in OVCAR3 which was

arbitrarily set at 1.0. Densitometry data from protein bands in Figure 6.

3.2 Targeting FASN inhibits cell growth

Previous studies have shown that FASN-blockade by small molecule inhibitors like C75 is cytotoxic to ovarian cancer cells in vitro (Grunt et al. 2009). The novel FASN-targeting compound G28UCM has been proven to reduce cell growth of breast cancer cells in vitro and in vivo (Puig et al. 2011). However, there is currently no data available regarding its effects on cells of ovarian epithelial origin. To demonstrate possible effects on cell growth, dose response to treatment with the FASN-inhibitors C75 and G28UCM was examined in cell proliferation assays (see Materials and Methods). Figure 8 shows corresponding dose response relationships. All cell lines tested responded to inhibition of FASN by C75 as well as by G28UCM with reduced proliferation and exhibited cytotoxic/cytocidal effects. While the malignant cell lines SKOV3, OVCAR3, HOC7 and the immortalized cell line IOSE80 were more susceptible to G28UCM than to C75, OSE cells showed the opposite result, with G28UCM being the less potent anti-proliferative compound. Interestingly, C75 was generally found to be capable to completely abolish cell proliferation, when high doses were applied, whereas high doses of G28UCM were not able to induce a total cell loss in these experiments.



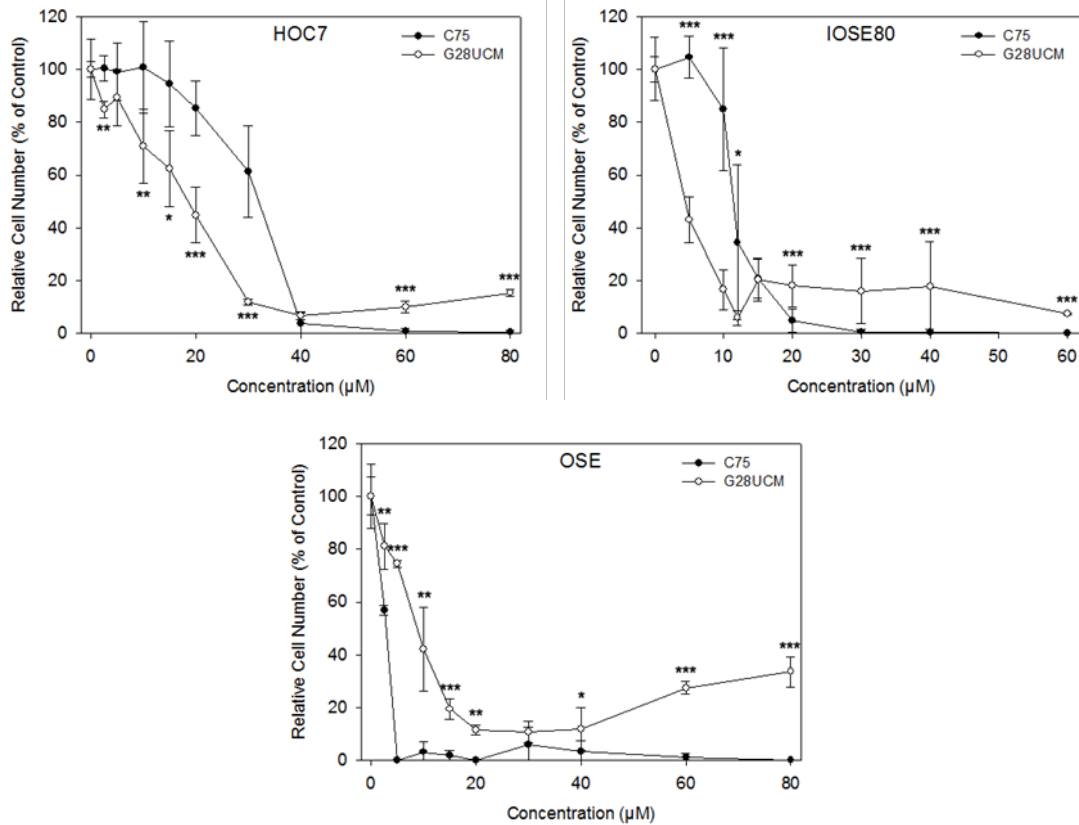


Figure 8 | Cell proliferation assays of malignant (SKOV3, OVCAR3, HOC7) and non-malignant (IOSE80, OSE) cell lines after FASN blockade by C75 or G28UCM. $1,5 \times 10^3$ – $3,0 \times 10^3$ cells were seeded into wells of a 96 well plate and treated for 72h at 37°C, 5% CO₂, 5% FCS. Means ± SD; n ≥ 3; Student's t-test or Mann-Whitney Rank Sum Test; C75 vs. G28UCM; * p<0,05; ** p<0,01; *** p<0,001

The main difference between C75 and G28UCM observed in cell proliferation experiments was that the IC₅₀ values for G28UCM were significantly lower in all of the malignant and non-malignant cell lines with the exception of OSE cells (Figure 9). Normal ovarian surface epithelial cells showed a significantly higher IC₅₀ value for G28UCM than for C75. Immortalized ovarian surface epithelial cells displayed comparable IC₅₀ values for both C75 and G28UCM. Unexpectedly, all non-malignant ovarian cell lines exhibit lower IC₅₀ values than most cancerous cell lines. CRL2522 foreskin fibroblasts have relatively high IC₅₀ values, as could be expected due to their low expression level of FASN.

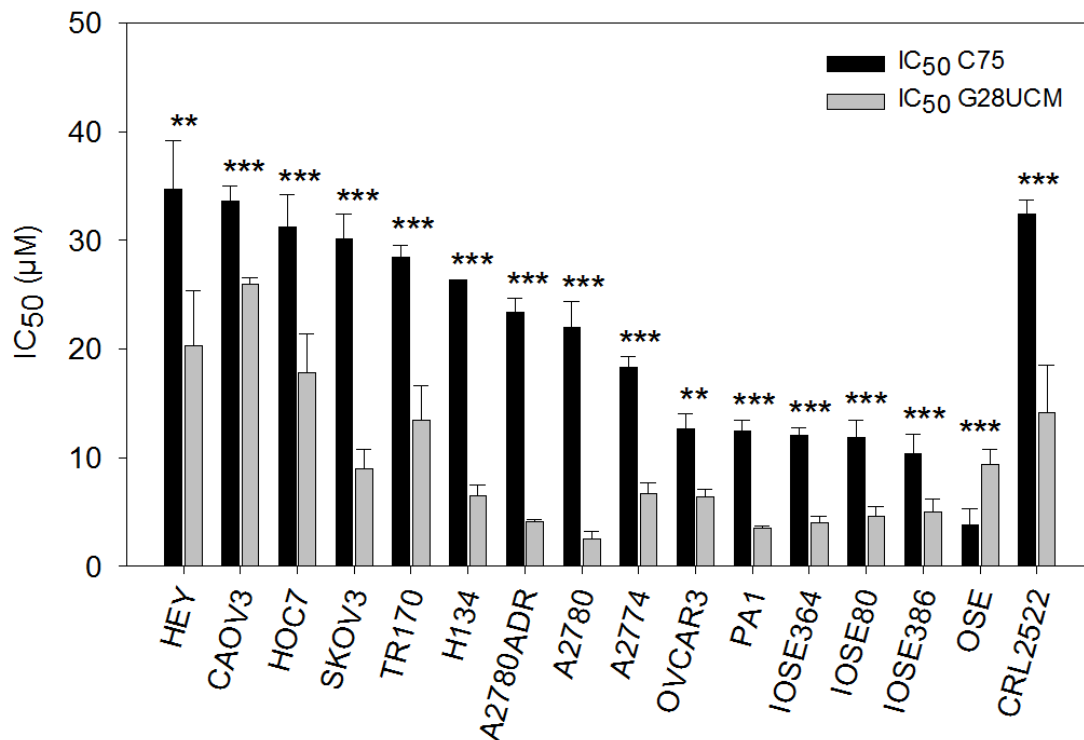


Figure 9 | IC₅₀ values for the growth inhibition by FASN-inhibitors C75 and G28UCM in 10 ovarian cancer cell lines, 3 immortalized ovarian surface epithelial cell lines (IOSE), normal ovarian surface epithelial cells (OSE) and normal foreskin fibroblasts (CRL2522). Data obtained from cell proliferation assays. 0,5x10³ – 3,0x10³ cells were seeded into wells of a 96 well plate and treated for 72h at 37°C, 5% CO₂, 5% FCS in respective media. Means ± SD; n ≥ 3; Student's t test or Mann-Whitney Rank Sum Test; C75 vs. G28UCM; ** p < 0,01; *** p < 0,001

Data obtained in cell proliferation assays and Western blots for FASN expression (Table 9A) were used to calculate the correlation coefficient between IC₅₀ values for C75 or G28UCM and FASN expression (Table 9B). Both calculations resulted in a negative correlation coefficient, indicating a reverse correlation between FASN expression and sensitivity against FASN-blockade. However, the correlation coefficient was only significant for comparison between C75-treatment and FASN expression and according to the coefficient of determination only 25% of the variances in IC₅₀ values of C75-treated cells could be explained by FASN expression. Additionally, the correlation coefficient between IC₅₀ values of both FASN – inhibitors used was calculated. The result indicates a significant, positive correlation.

A

Cell line	IC ₅₀ C75	SD	IC ₅₀ G28UCM	SD	Rel. FASN Expression
HEY	34,734	4,43	20,306	5,08	0,33
CAOV3	33,608	1,40	25,951	0,63	0,30
HOC7	31,259	2,98	17,831	3,56	0,37
SKOV3	30,151	2,24	8,969	1,77	0,32
TR170	28,409	1,15	13,476	3,16	0,40
H134	26,349	0,06	6,447	1,03	0,44
A2780ADR	23,394	1,32	4,130	0,18	0,71
A2780	21,982	2,39	2,484	0,68	0,38
A2774	18,301	0,99	6,672	1,01	0,16
OVCAR3	12,612	1,46	6,417	0,70	1,00
PA1	12,435	0,98	3,495	0,24	0,58
IOSE364	12,020	0,69	4,041	0,51	0,49
IOSE80	11,861	1,56	4,556	0,89	0,43
IOSE386	10,328	1,83	5,012	1,16	0,32
OSE	3,818	1,43	9,346	1,43	0,66
CRL2522	32,442	1,25	14,121	4,45	0,04

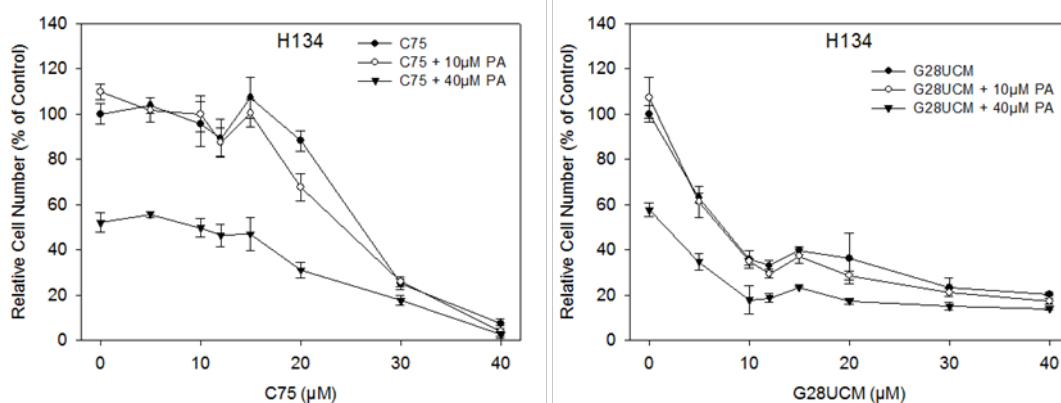
B**Correlation analysis (IC₅₀ values and FASN Expression)**

	r	r ²	t-value	p-value
IC ₅₀ C75 vs. FASN	-0,50871575	0,25879172	2,211	0,044 *
IC ₅₀ G28UCM vs. FASN	-0,35774125	0,1279788	1,433	0,174
IC ₅₀ C75 vs. IC ₅₀ G28UCM	0,69498877	0,48300939	3,617	0,003 **

Table 9 | (A) IC₅₀ values (and SD) for treatment with C75 and G28UCM derived from cell proliferation assays. Relative FASN expression levels derived from Western blot bands in Figure 6. The band from the internal positive control sample OVCAR3 has arbitrarily been set to 1,00. (B) Correlation analysis of IC₅₀ values of C75 and G28UCM and relative FASN expression level from the above cell lines as well as between IC₅₀ values of both inhibitors. SD...standard deviation; r...correlation coefficient; r²...coefficient of determination; two-tailed Student's t-test; * p<0,05, ** p<0,01

3.3 Effects of exogenously delivered palmitic acid or oleic acid on growth in cells treated with FASN-inhibitors

Blockade of the enzymatic activity of FASN by C75 or G28UCM imposes a halt in the de novo synthesis of long chain fatty acids (Zhou et al. 2003). PA acts as the basal building block for many cellular molecules such as phospholipids or triglycerides. In contrast to most normal cells, cancer cells depend on de novo synthesis of fatty acids to make up for their elevated needs of building blocks for cellular membranes. To address the question of whether or not exogenous supply of PA is sufficient to revert the cellular effects of treatment with C75 or G28UCM, cell proliferation assays were performed using H134 ovarian cancer cells and IOSE364 immortalized ovarian surface epithelial cells. Cells were treated with 10 or 40 μM PA (complexed to BSA, see Materials and Methods section) together with either C75 or G28UCM, or with C75 or G28UCM alone for 72h at standard conditions prior to measurement. The resulting growth curves (Figure 10) indicate that in both cell lines tested, exogenous PA (whether 10 or 40 μM) could not ameliorate the anti-proliferative effects of C75 or G28UCM. Furthermore, administration of 40 μM PA resulted in a more pronounced reduction of cell growth compared to treatment with FASN-inhibitors alone or in combination with 10 μM PA. Dose dependent cytotoxicity was also observed in cells treated with PA alone (data not shown).



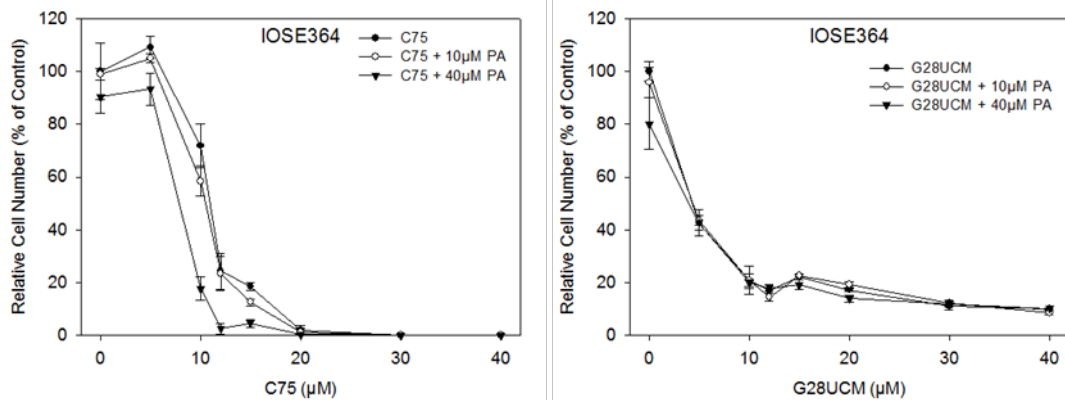


Figure 10 | Exogenous palmitic acid (PA) was not able to ameliorate anti-proliferative effects of C75 or G28UCM on H134 ovarian cancer cells and IOSE364 cells. Growth curves from cell proliferation assays after combined treatment with 0-40μM C75 or G28UCM ± 10/40μM PA complexed to BSA in a 10:1 molar ratio. 0.5×10^3 (H134) or 1.5×10^3 (IOSE364) cells were seeded into 96 well plates and treated with respective agents for 72h at 37°C, 5%CO₂, 5%FCS in respective media before measurement. Vehicle controls (0,1% DMSO, <=0,04% EtOH, 4μM BSA) without PA and FASN-inhibitors were set to 100%. Means ± SD; n=3.

To avoid these cytotoxic effects of exogenously delivered palmitic acid, oleic acid (OA, C18:1) was used to substitute for the lack of de novo fatty acid synthesis. Oleic acid, a monounsaturated (C9) fatty acid comprised of 18 carbon atoms is one of the major building blocks for phospholipids in cellular membranes. OA is derived from palmitic acid by the sequential reactions provided by the long chain fatty acid elongase Elovl-6, which elongates PA by two carbon atoms to yield stearic acid (C18:0) and subsequent desaturation at carbon 9 by the enzyme delta-9-desaturase (C18:1) (Wang et al. 2006). Again, effects of OA on cells treated with C75 or G28UCM were examined via cell proliferation assays (Figure 11). Therefore, OVCAR3 and HOC7 ovarian cancer cells were treated with respective agents for 72h at standard conditions. Like palmitic acid, oleic acid was complexed to BSA (see Materials and Methods). The experiments revealed, that in both cell lines, OA – treated cells were able to partially (OVCAR3) or even fully (HOC7) overcome the cytotoxic effects imposed by C75 or G28UCM. Treatment with OA alone did impair cell growth of OVCAR3 cells by approximately 40%, irrespectively of dose (data not shown).

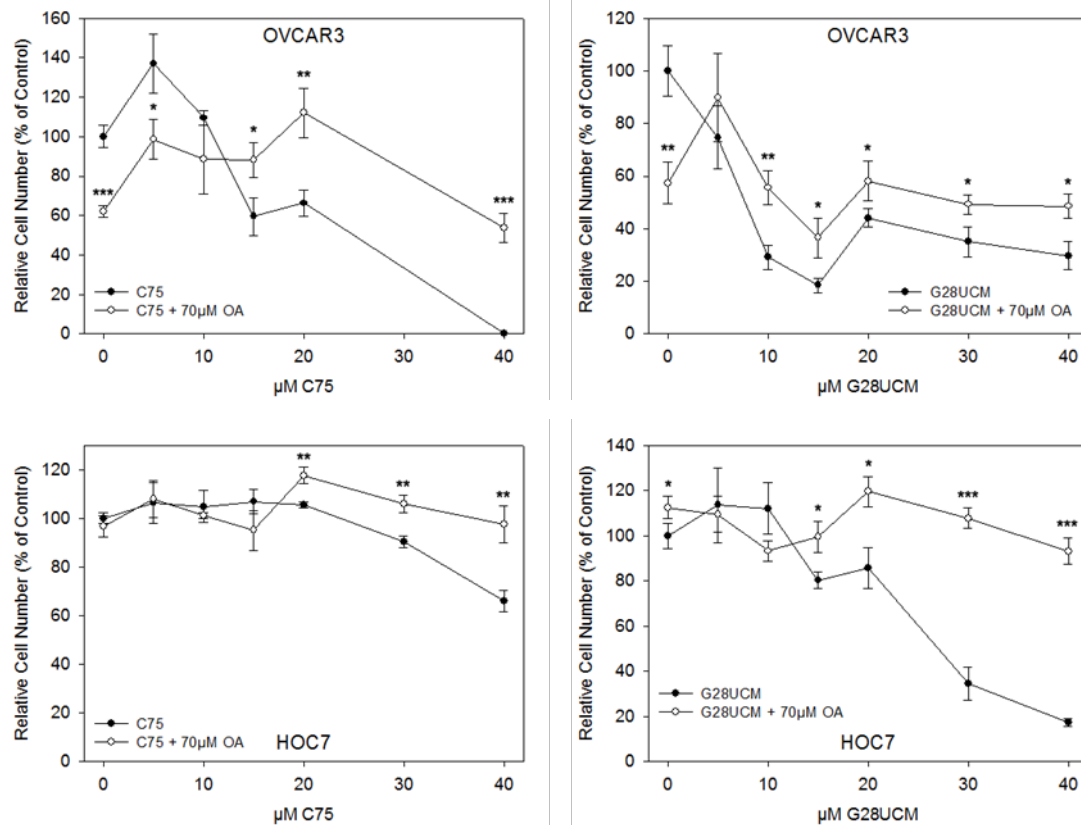


Figure 11 | Exogenous oleic acid (OA) was sufficient to restore proliferation of OVCAR3 and HOC7 ovarian cancer cells in the presence of the FASN-inhibitors C75 or G28UCM. Growth curves from cell proliferation assays after combined treatment with 0-40µM C75 or G28UCM ± 70µM OA complexed to BSA in a 2:1 molar ratio. $1,5 \times 10^3$ (HOC7) or $3,0 \times 10^3$ (OVCAR3) cells were seeded in wells of a 96 well plate and treated for 72h at standard conditions (37°C, 5%CO₂, 5%FCS). Vehicle controls (0,1% DMSO) without FASN-inhibitors and OA were set to 100%. Means ± SD; n=3; Student's t test; C75 vs. G28UCM; * p<0,05; ** p<0,01; *** p<0,001.

3.4 Effects of FASN-blockade by C75 and G28UCM on major intracellular signaling pathways

Previous studies (Tomek et al. 2011) have shown that inhibition of FASN by C75 or by siRNA-mediated silencing leads to decreased expression and activity of protein members of the phosphoinositide-3-kinase (PI3K) pathway as well as to decreased expression – but not phosphorylation – of ERK1/2. To reveal possible differential effects of FASN-inhibition between malignant and normal ovarian surface epithelial cells and between the two different FASN-inhibitors C75 and G28UCM on the expression and activity of key signaling proteins, a panel of cell lines was treated with both FASN-inhibitors and subjected to Western blot analysis. Expression and

phosphorylation status of Protein Kinase B (PKB), the downstream effector of PI3K – also known as AKT – was used to determine the activity of the PI3K pathway. Phosphorylation of AKT was monitored at amino acid residue Ser 473. Strength and activity of the mitogen-activated protein kinase (MAPK) pathway was tracked by detection of total and phosphorylated extracellular signal-regulated kinase 1/2 (ERK1/2). Phosphorylation of ERK1/2 was detected on amino acid residues Thr202 and Tyr204. Ribosomal protein S6 acts downstream of both, PI3K pathway and MAPK pathway and thereby is affected by multiple signals. S6 seems to be functionally involved in fine-tuning protein translation and in the regulation of cell growth and proliferation rate (Ruvinsky et al. 2006, Roux et al. 2007). Phosphorylation of S6 was detected on amino acid residues Ser 240/244.

SKOV3 cells were treated with 0-80µM of C75 or G28UCM for 48h prior to lysis and subjected to Western blot analysis. Results shown in Figure 12 indicate that levels of total and phosphorylated AKT remain stable upon treatment with C75 as well as G28UCM. ERK1/2 levels are also unaffected by both inhibitors. Phosphorylated ERK1/2 shows an oscillating pattern which apparently is not correlated with dose of respective inhibitor. This may be caused by an unknown time-dependent parameter of ERK1/2 regulation. S6 expression is slightly lower in C75-treated as well as G28UCM-treated cells when compared to control. Treatment with C75 and G28UCM has led to a dose dependent decrease in phosphorylation of S6. Interestingly, S6 phosphorylation does not seem to be directly affected by modulation of ERK1/2.

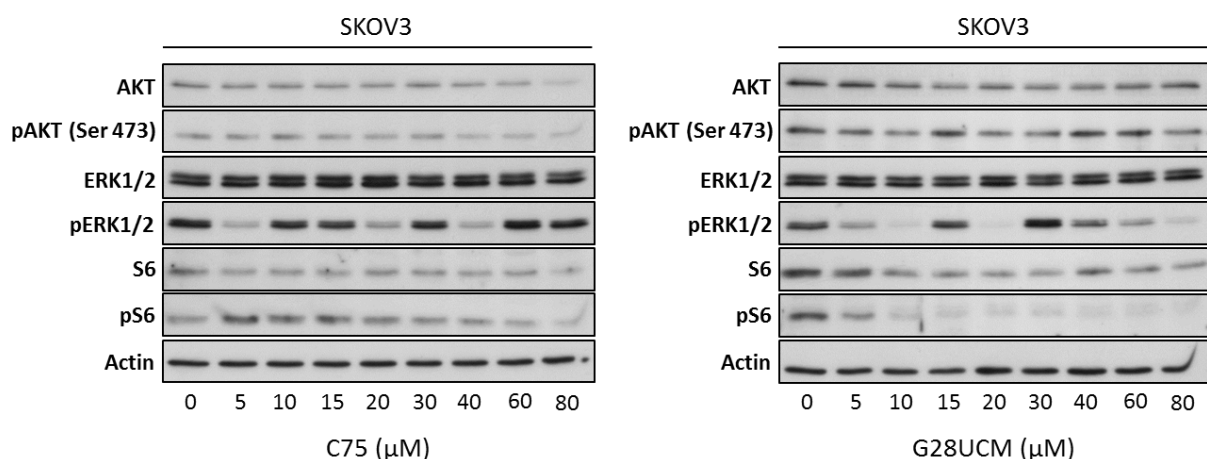


Figure 12 | Dose-dependent modulation of cell signaling proteins in SKOV3 cells after FASN-inhibition. Cells were treated with C75 or G28UCM for 48h at standard incubation conditions (37°C, 5%CO₂, 5% FCS) before harvesting. Vehicle (0,4% DMSO) treated cells were used as control. β-Actin

was used as loading control.

OVCAR3 cells, which are more sensitive to the FASN inhibitors (Table 9), were treated similar to SKOV3 cells. Figure 13 shows a dose-dependent decrease of total and phosphorylated AKT expression upon treatment with C75 and G28UCM. Expression of ERK1/2 in C75-treated cells remained stable up to a concentration of 40 μ M. Cells treated with 60 and 80 μ M C75 exhibited almost no expression of ERK1/2. In contrast, G28UCM-treated cells show a constant level of ERK1/2 expression throughout the treatment regimen. Importantly, treatment of OVCAR3 cells with C75 induced a remarkable increase of phosphorylated ERK1/2, while G28UCM-treated cells showed down-regulation of pERK1/2. Expression of S6 was mildly decreased in cells treated with 60 and 80 μ M of C75, while treatment with G28UCM had no such effect. Phosphorylation of S6 was strongly repressed in a dose-dependent manner after inhibition of FASN. β -Actin expression levels did also suffer from treatment with high doses of C75 but not in cells treated with G28UCM, thereby reflecting the greater cytotoxicity of higher doses of C75 compared to G28UCM.

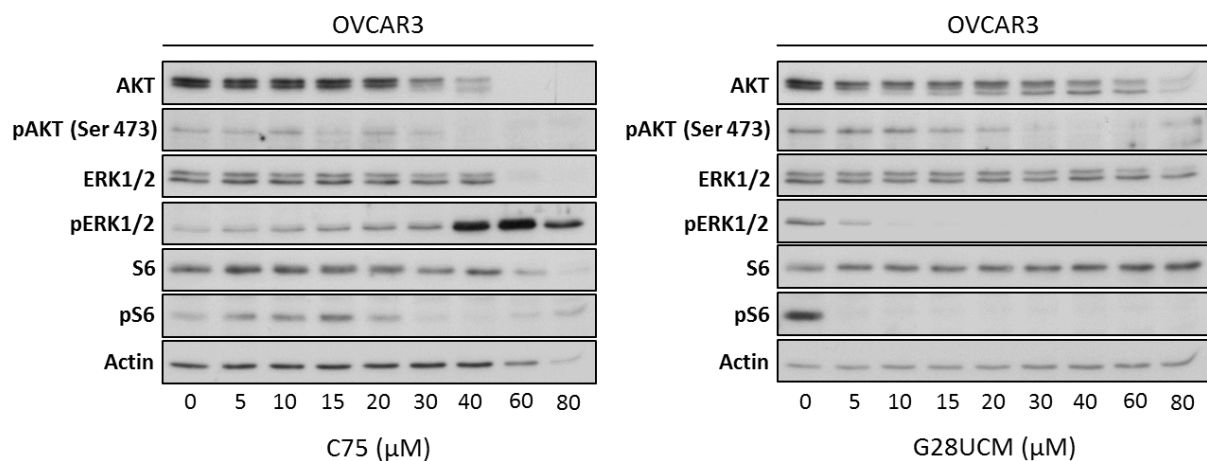


Figure 13 | Dose-dependent modulation of cell signaling proteins in OVCAR3 cells after FASN-inhibition. Cells were treated with 0-80 μ M C75 or G28UCM for 48h at standard incubation conditions (37°C, 5%CO₂, 5% FCS) before harvesting. Vehicle (0,4% DMSO) treated cells were used as control. β -Actin was used as loading control.

Similarly treated HOC7 cells, which are relatively resistant to FASN inhibitory drugs (Table 9) exhibited a slight decrease in total AKT levels only in the highest

concentrations of C75 and G28UCM, respectively (Figure 14). Phosphorylation of AKT at Serine 473 remained almost stable after treatment with either C75 or G28UCM. ERK1/2 expression levels slightly decreased upon treatment. However, phosphorylation levels were increased dose-dependently in both C75- and G28UCM-treated cells. Expression of S6 was also only mildly affected by FASN-inhibitors. Phosphorylated S6 was gradually increased upon treatment with C75, or with G28UCM. Only cells treated with the highest concentration of the respective FASN-inhibitor showed a loss of S6-phosphorylation.

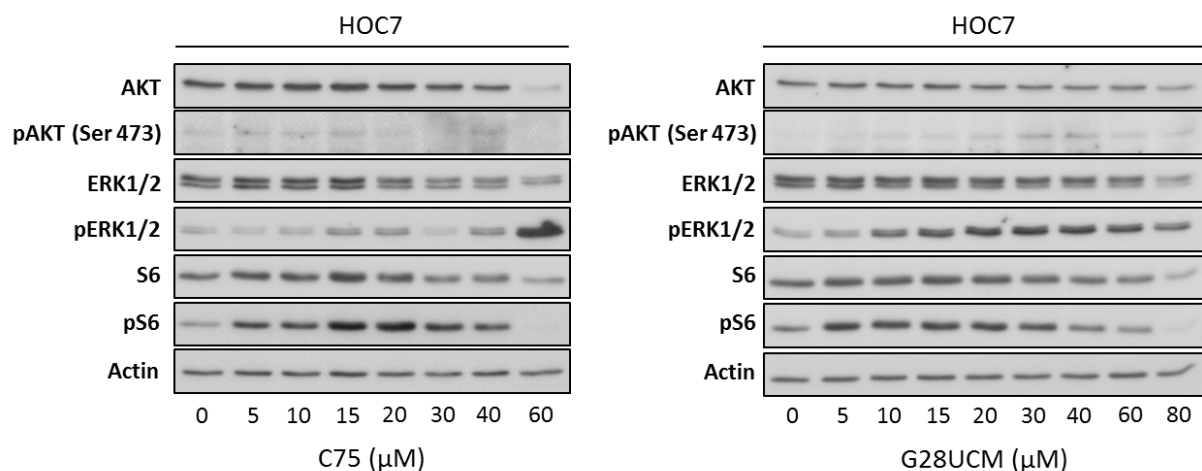


Figure 14 | Dose-dependent modulation of cell signaling proteins in HOC7 cells after FASN-inhibition. Cells were treated with C75 or G28UCM for 48h at standard incubation conditions (37°C, 5%CO₂, 5% FCS) before harvesting. Vehicle (0,4% DMSO) treated cells were used as control. β-Actin was used as loading control.

IOSE80 immortalized ovarian surface epithelial cells (Figure 15) exhibited a strong, dose-dependent inhibition of AKT expression upon treatment with FASN-inhibitors. Also phospho-AKT levels declined in cells treated with high doses of C75 or G28UCM. ERK1/2 expression was hindered almost to the same extent as AKT expression. However, phosphorylation of ERK1/2 was profoundly augmented after treatment with low doses of FASN-inhibitors but diminished in cells treated with higher doses. S6 and phospho-S6 levels were simultaneously decreasing in C75-treated IOSE80 cells. G28UCM also induced a dose-dependent decrease in S6 and phospho-S6 levels although phospho-S6 levels were reduced more rapidly. Like

OVCAR3 cells, IOSE80 cells expressed lower amounts of β -Actin when treated with 60 or 80 μ M C75.

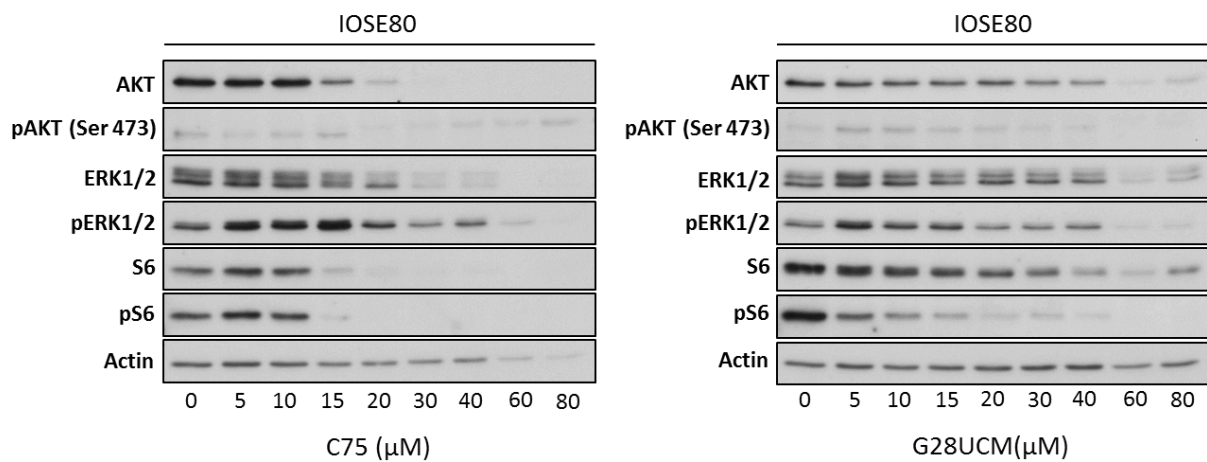


Figure 15 | Dose-dependent modulation of cell signaling proteins in IOSE80 cells after FASN-inhibition. Cells were treated with C75 or G28UCM for 48h at standard incubation conditions (37°C, 5%CO₂, 5% FCS) before harvesting. Vehicle (0,4% DMSO) treated cells were used as control. β -Actin was used as loading control.

OSE cells were very sensitive to inhibition of FASN, so the effects of blockade by C75 and G28UCM were observable already in samples received from cells treated with low doses of respective inhibitor. This is particularly evident for the expression of total AKT after treatment with C75. Both C75 and G28UCM downregulate phosphorylated AKT already at very low concentrations. Levels of ERK1/2 decrease with raising concentrations of FASN-inhibitors. C75-treated OSE cells showed a distinct increase in phosphorylated ERK1/2 at inhibitor concentrations $\leq 10\mu$ M. A comparable increase in phospho-ERK1/2 has been monitored in G28UCM-treated cells, where the increase has been seen at a dose as low as 5 μ M already. In contrast, concentrations higher than 20 μ M led to a near-total loss of ERK1/2-phosphorylation. S6 levels were decreased down to a total loss of detectability upon treatment with C75, whereas they were almost stable in G28UCM-treated samples. Phosphorylation of S6 was severely hampered by both inhibitors. Although treatment with 5 μ M C75 led to an increased phosphorylation, no phosphorylation was detectable at higher concentrations. β -Actin levels of cells treated with 40 μ M G28UCM were slightly decreased (Figure 16).

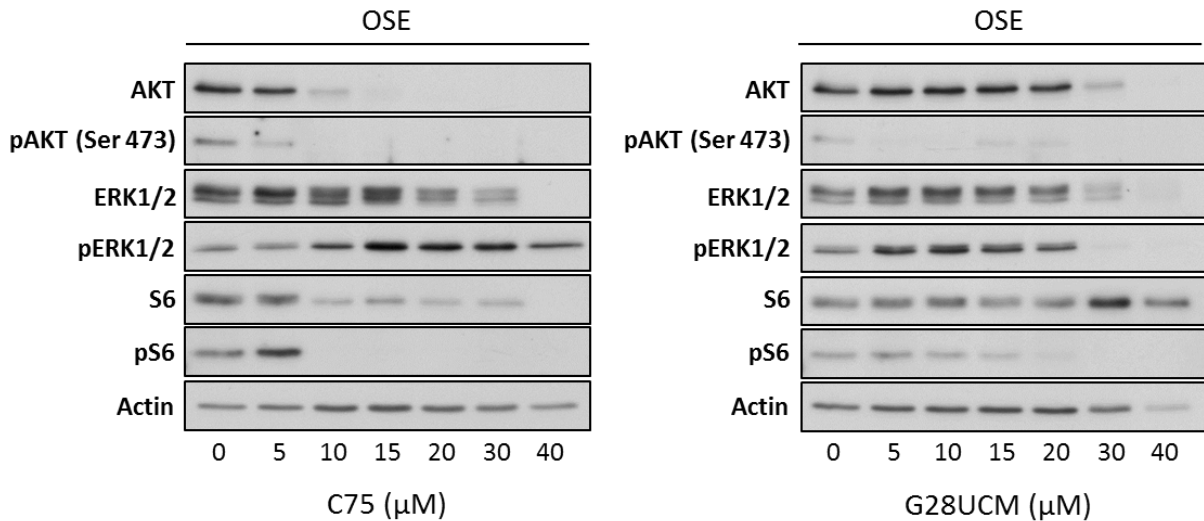


Figure 16 | Dose-dependent modulation of cell signaling proteins in OSE cells after FASN-inhibition. Cells were treated with C75 or G28UCM for 48h at standard incubation conditions (37°C, 5%CO₂, 5% FCS) before harvesting. Vehicle (0,2% DMSO) treated cells were used as control. β-Actin was used as loading control.

Above data reveal that all cell lines exhibited a dose-related decrease in AKT and phospho-AKT levels upon treatment with C75 and G28UCM for 48h, although decrease of AKT was less pronounced by G28UCM. All cell lines except SKOV3 showed a gradual decrease of ERK1/2 expression after FASN-inhibition. More interesting, all cell lines except SKOV3 and G28UCM-treated OVCAR3 exhibited a dose-dependent increase in ERK1/2 phosphorylation after treatment with C75 and G28UCM. This may be due to the loss of an inhibitory feedback loop originating from members of the PI3K-pathway (Hennessy et al. 2005, Mendoza et al. 2011). Modulation of expression of S6 – ranging from minor to total decrease - could be observed in all cell lines treated with C75. Also G28UCM led to a certain, dose-dependent decrease of S6 protein levels. However, no total loss of S6 expression was observed in the presence of G28UCM. It seems that phosphorylation of S6 at Ser240/244 is divergently regulated in malignant and non-malignant cell lines in the context of FASN-inhibition. Both inhibitors used were able to induce a dose-dependent decrease in phospho-S6 levels. However, in malignant cells lines (SKOV3, OVCAR3, HOC7), G28UCM was more effective in reducing phospho-S6 (i.e. decrease starts at lower concentrations compared to C75) than C75. The opposite is true for non-malignant cells (IOSE80, OSE), where C75 induced a more powerful reduction of phospho-S6.

3.5 Induction of apoptosis by C75 or G28UCM

As is depicted in Figure 8, blockade of FASN by C75 as well as G28UCM induces growth-inhibitory effects in malignant and non-malignant ovarian surface epithelial cells. There are several possible mechanisms that could explain this reduction of cell growth upon inhibition of FASN. One of these mechanisms is induction of apoptosis. Previous studies have shown that C75 is capable of inducing apoptosis-conferring proteins (Tomek et al. 2011, Ho et al. 2007, Menendez et al. 2004). To measure the possible extent of apoptosis elicited by C75 and G28UCM in malignant and non-malignant ovarian cell lines, two distinct approaches were conducted. One involves the detection of cleavage of the nuclear protein poly ADP-ribose polymerase 1 (PARP1). PARP1 is involved in recognizing single strand DNA breaks (SSB) and in signaling to proteins of the SSB repair machinery. Pro-caspase 3 becomes activated, if a cell experiences major damage and cleaves PARP1 (116kDa) in two fragments (89kDa, 24kDa) which are no longer functional. Therefore, presence of cleaved PARP1 is an indicator for induction and progression of apoptosis.

In a first set of experiments, ovarian cancer cell lines SKOV3, OVCAR3 and HOC7 as well as non-malignant ovarian surface epithelial cells IOSE80 and OSE were treated with different doses of either C75 or G28UCM for 48 hours at standard incubation conditions. After harvesting, protein samples were subjected to Western blot analysis and expression of whole (116kDa) and cleaved PARP1 (89kDa fragment) was investigated (Figure 17). SKOV3 cells showed stable expression of uncleaved PARP1, which was almost independent of the concentration of FASN-inhibitor used. Treatment with C75 caused a steep increase in cleavage of PARP1 at 60 and 80 μ M. In G28UCM-treated SKOV3 cells, cleavage of PARP1 could be recognized at concentrations equal to or larger than 20 μ M. OVCAR3 cells exhibited a decrease of uncleaved PARP1 expression upon treatment with high doses of C75 and G28UCM. Cleavage of PARP1 was similar to SKOV3 cells however the effects were observable at lower doses. FASN inhibitor-dependent cleavage of PARP1 could also be demonstrated in HOC7 cells. Remarkably, the rate of conversion (ratio between uncleaved and cleaved protein) from the 116kDa functional PARP1 protein to the inactive 89kDa fragment was much lower in HOC7 than in SKOV3 and OVCAR3. In contrast, C75 induced a drastic decrease in PARP1 expression in

IOSE80 cells at concentrations as low as 15 μ M. At 20 μ M, nearly all of the PARP1 protein was present in the cleaved form. Treatment with G28UCM revealed not such a sensitive decrease of PARP1, however the amount of protein was remarkably lower in high dosage samples. Induction of cleavage was observable from inhibitor concentrations of 5 μ M upwards and remained almost stable. In contrast, OSE cells were almost unresponsive to FASN-inhibition with regard to induction of PARP1 cleavage. Only cells treated with 10 μ M of C75 displayed inactivation of PARP1, whereas G28UCM could not elicit any sign of cleavage of PARP1.

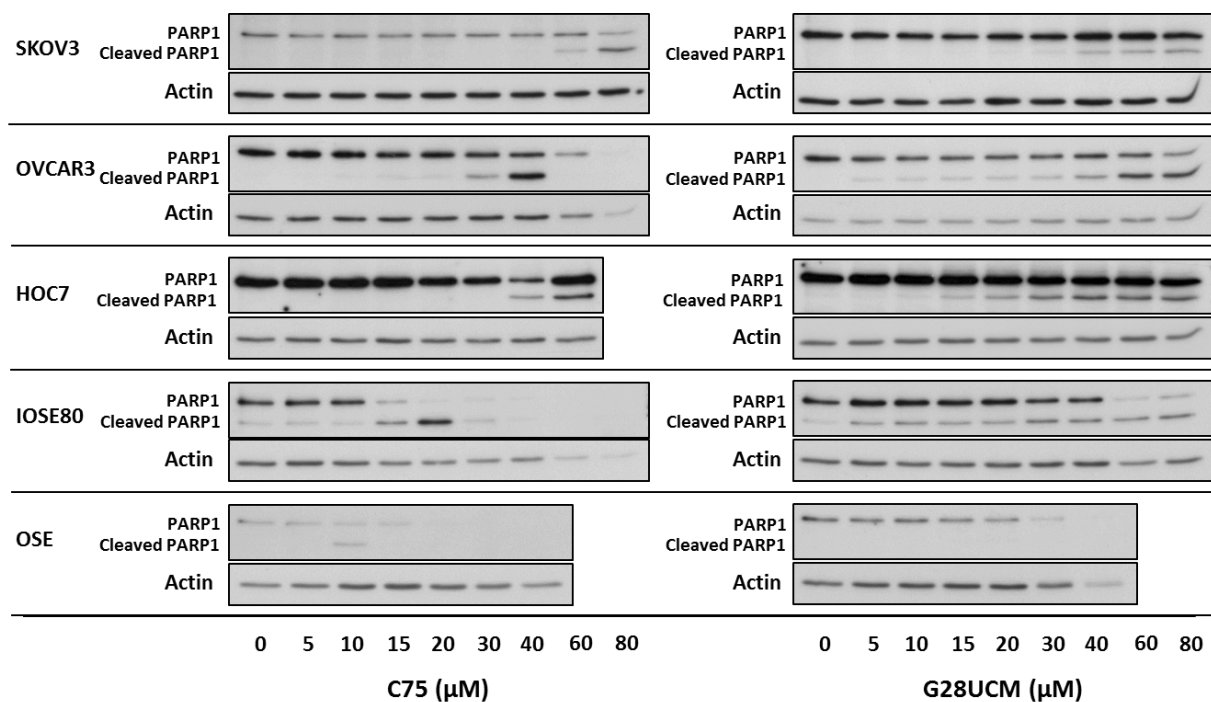


Figure 17 | Treatment with C75 or G28UCM induces dose-dependent cleavage of PARP1. SKOV3, OVCAR3, HOC7, IOSE80 and OSE cells were treated with indicated concentrations of C75, G28UCM or vehicle (0,4% DMSO, OSE 0,2% DMSO) for 48h at 37°C, 5% CO₂, 5% FCS. Proteins were separated on a 10% or 12% SDS acrylamide gel respectively. Apoptosis is indicated by cleavage of the full-length, functional, 116kDa protein into the inactive 89kDa and 24kDa (not visible) fragments. β -Actin was used as loading control.

In a second approach, the prevalence of active caspase 3 was utilized as a marker for apoptosis. Therefore, cells were treated with individual (see Figure 18) doses of C75 or G28UCM for 6, 18, 24 or 48 hours at standard conditions. These doses were selected based on data from growth assays (IC₅₀ values) and on observations of

PARP1 inactivation (Figure 17). Vehicle-treated ($\leq 0,2\%$ DMSO) cells were used as a control. Active caspase 3 was measured via flow cytometry after intracellular staining with a PE-labeled anti-active caspase 3 antibody (see Materials and Methods). The results show that induction of apoptosis increases over time. In SKOV3, IOSE80 and OSE cells, C75 was more potent to elicit apoptosis than G28UCM. HOC7 and OVCAR3 cells exhibited inverse results. The time of onset of activation of caspase 3 is located between 0 and 18 hours after treatment for both inhibitors used, with the exception of OSE cells where G28UCM could not induce apoptosis.

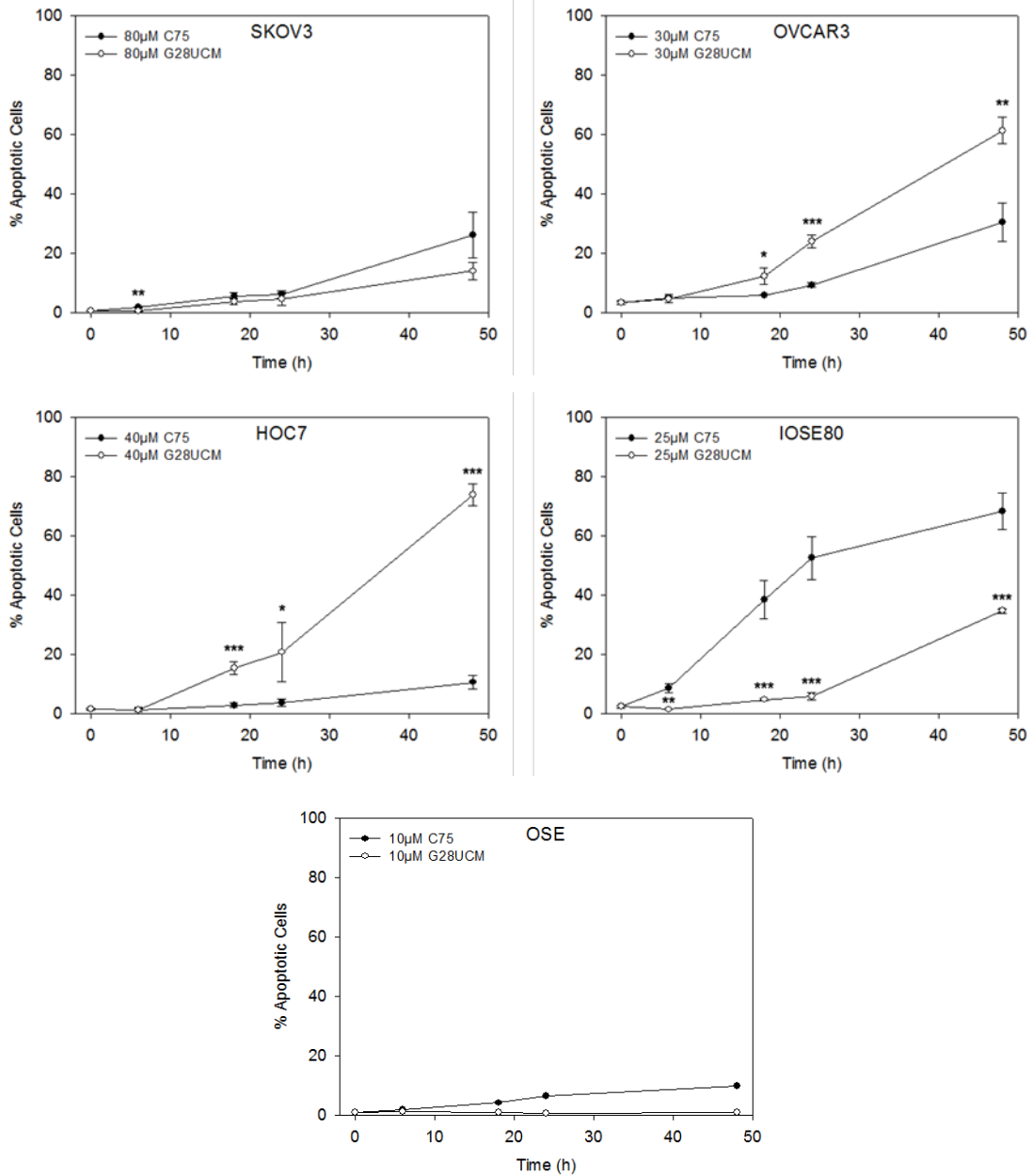
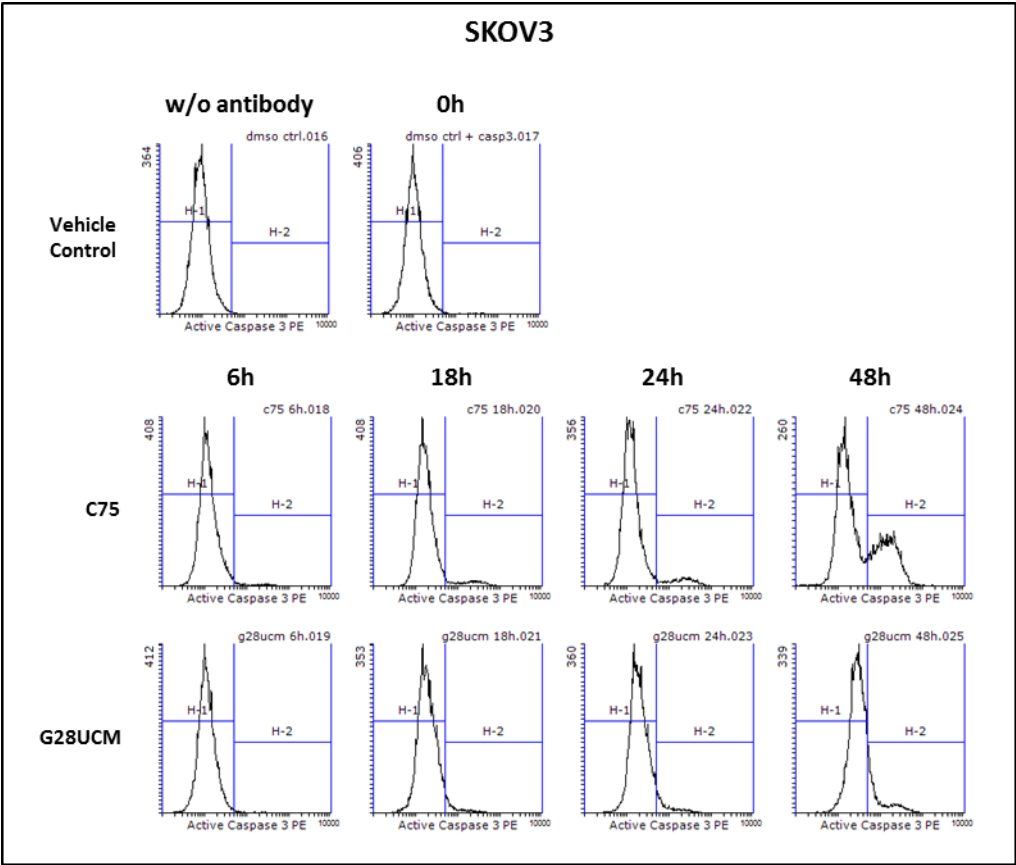


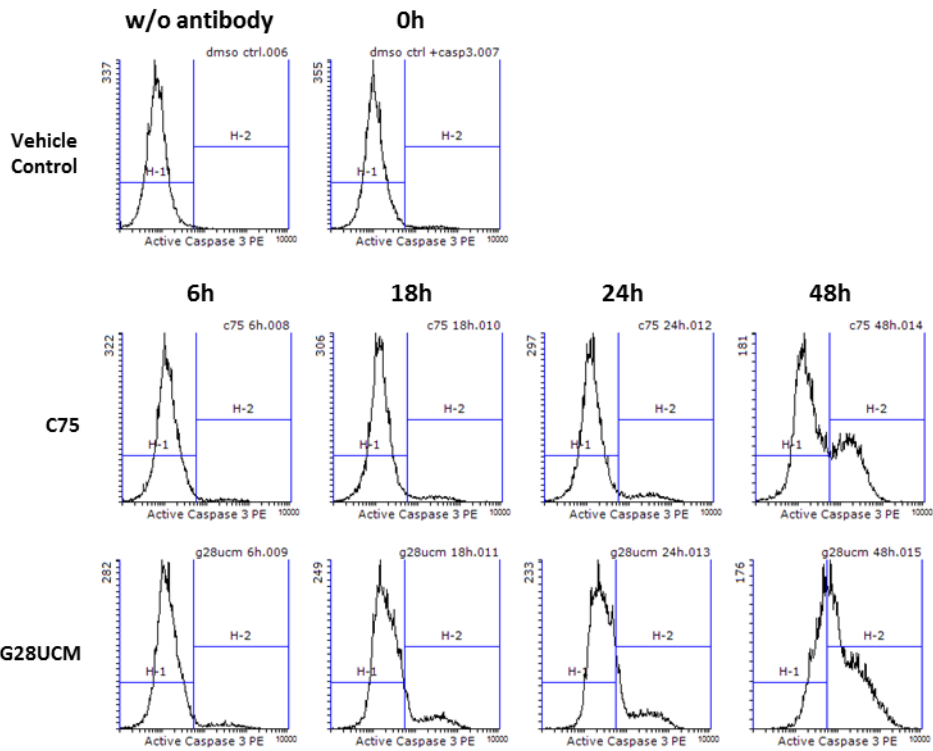
Figure 18 | Time-dependent induction of apoptosis in cells treated with C75 or G28UCM. Cells were treated with indicated concentrations of FASN-inhibitors for 6, 18, 24 and 48h at standard incubation conditions (37°C, 5% CO₂, 5% FCS). After harvesting, cells were subjected to intracellular staining

using an anti-active caspase 3 antibody. Vehicle-treated cells ($\leq 0,2\%$ DMSO) were used as a control. SKOV3, OVCAR3, HOC7, IOSE80: Means \pm SD, n=3, C75 vs. G28UCM, Student's t test; OSE: One representative experiment

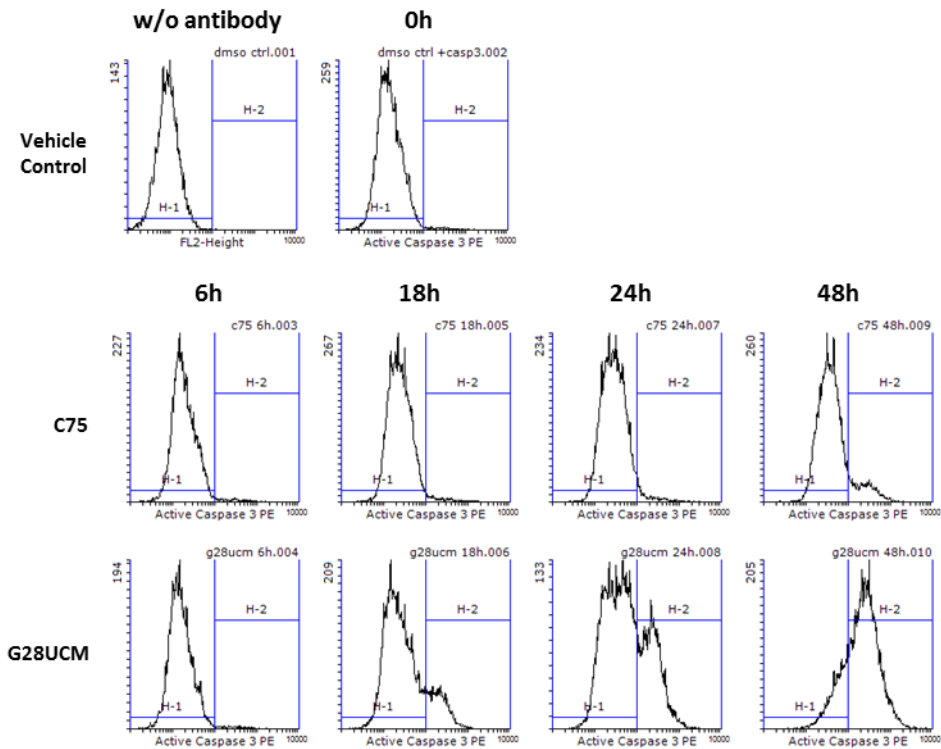
Figure 19 depicts representative histograms of data obtained from measuring active caspase 3 via flow cytometry. Regions marking viable and apoptotic cells were set according to control samples (see materials and methods).



OVCA R3



HOC7



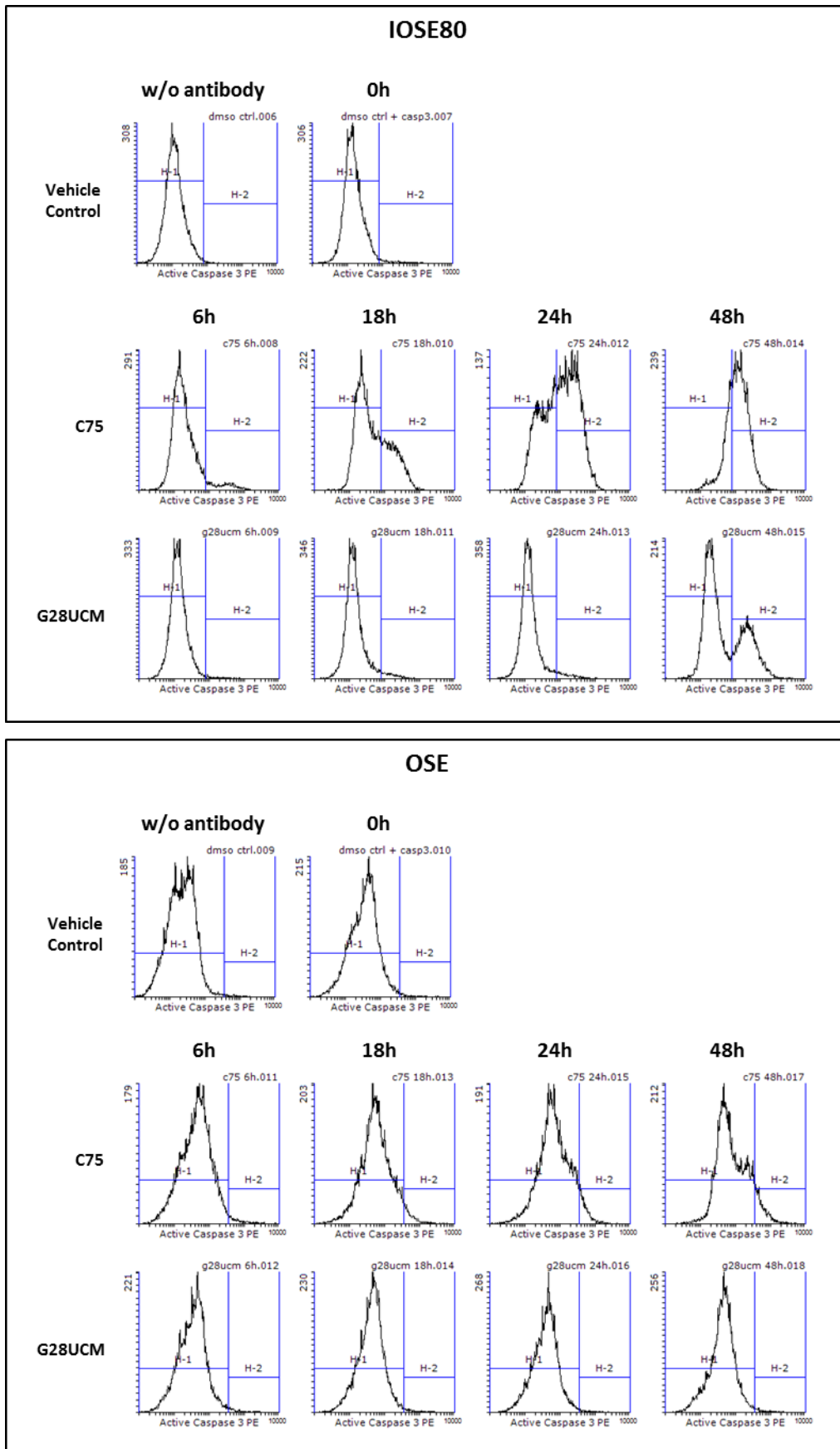


Figure 19 | Representative histograms displaying data obtained in flow cytometric measurement of active caspase 3. Regions H1 and H2 – representing viable (H1) and apoptotic (H2) cell populations

– were set according to shape of the curve in control samples (w/o antibody)(see materials and methods). w/o antibody...vehicle-treated ($\leq 0,2\%$ DMSO) cells without anti-active caspase 3 antibody; 0h...vehicle-treated ($\leq 0,2\%$ DMSO) cells with anti-active caspase 3 antibody. 6h, 18h, 24h, 48h...treatment with C75 or G28UCM for respective amount of time.

3.6 Induction of autophagy by C75 or G28UCM

In the last section, apoptosis was investigated as a process that is possibly involved in the observed growth-inhibitory effect of FASN-blockade. Another cellular mechanism that has the potential to interfere with cell growth is autophagy. Autophagic processes can be activated by many different factors, including for instance nutrient starvation or excessive misfolding of proteins. To investigate whether autophagy is inducible by C75 and G28UCM, SKOV3, OVCAR3, HOC7, IOSE80 and OSE cells were treated with different doses of these FASN-inhibitors for 48 hours at standard incubation conditions. Following harvesting of the cells, protein samples were subjected to Western blot analysis for the expression of the autophagy marker light chain 3 B (LC3B I and LC3B II). LC3B is posttranscriptionally converted into LC3B I (18kDa) via cleavage at the carboxyl terminus. During autophagy, LC3B I is further processed to become LC3B II (16kDa) via the proteins Atg7 and Atg3. Thereafter, LC3B II associates with autophagic vesicles (Wu et al. 2006).

Results of Western blots shown in Figure 20 indicate that both FASN inhibitors were able to induce a dose dependent increase in expression of LC3B I and LC3B II in all of the cell lines tested. SKOV3 cells exhibited increased expression of LC3B I and II only at high doses of C75. G28UCM induced only minor increases. In OVCAR3 cells the induction of the autophagic marker was also more pronounced by C75 than by G28UCM. In HOC7 cells, a high rate of conversion of LC3B I into LC3B II was observed after treatment with G28UCM. This was accompanied by only a moderate increase in LC3B I levels. C75-treated HOC7 cells exhibited a remarkable increase of both forms of LC3B when incubated with high doses. Immortalized and normal ovarian surface epithelial cells both showed a transient increase in LC3B I and LC3B II when treated with C75, however the levels of LC3B II were elevated even in high dosage samples, while LC3B I expression decreased to control levels. The same

holds true for IOSE80 and OSE cells when treated with G28UCM, although the peak in LC3B I expression was less pronounced than in C75-treated cells.

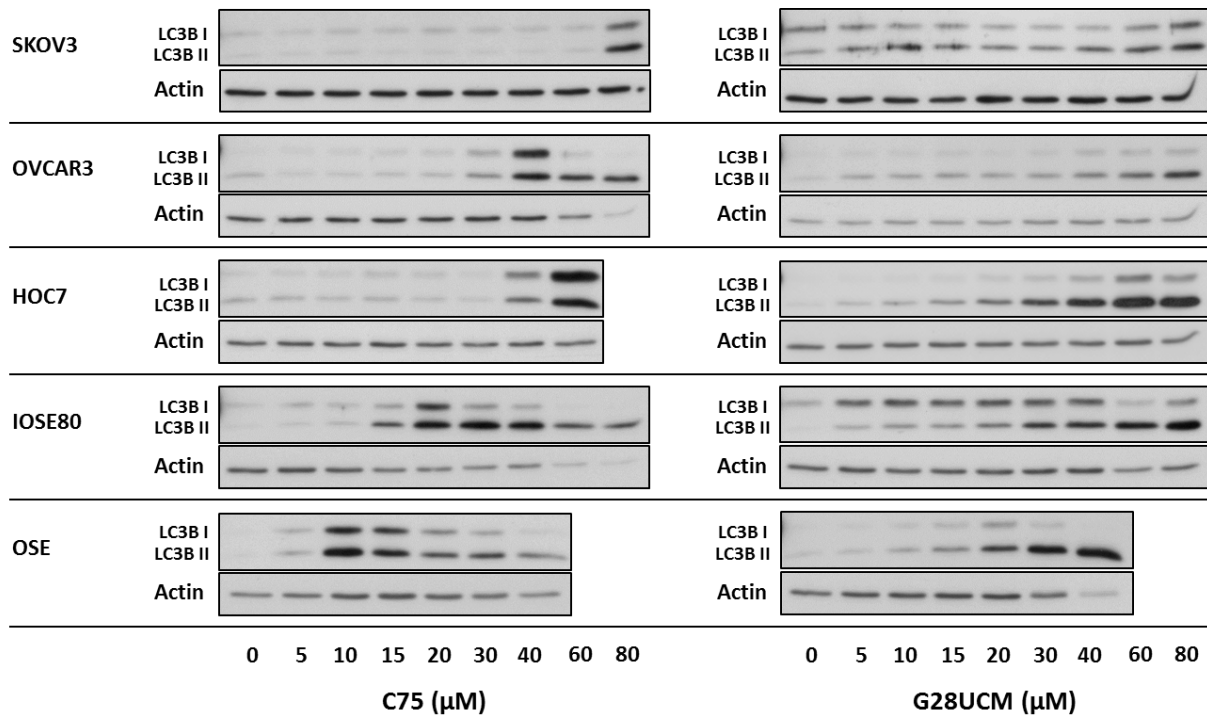


Figure 20 | Treatment with C75 or G28UCM induces a dose-dependent increase in LC3B I (18 kDa) and LC3B II (16kDa) protein levels and thereby marks intensified autophagic processes. SKOV3, OVCAR3, HOC7, IOSE80 and OSE cells were treated with indicated concentrations of C75, G28UCM or vehicle (0,4% DMSO, OSE 0,2% DMSO) for 48h at 37°C, 5% CO₂, 5% FCS. Proteins were separated on a 12% SDS polyacrylamide gel. β-Actin was used as loading control.

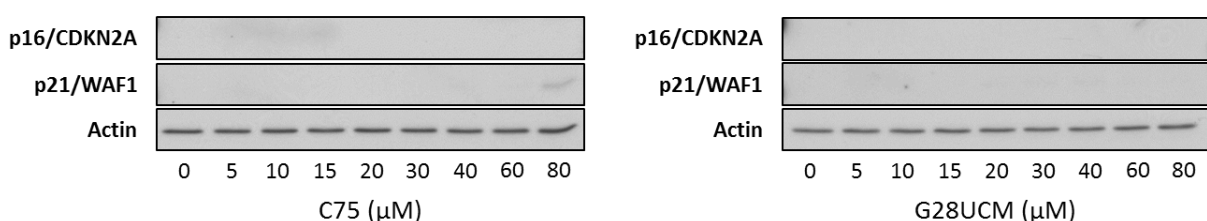
3.7 Inhibition of FASN can interfere with cell cycle distribution

In the two previous sections, apoptosis and autophagy were investigated as possible mechanisms attributable for the decrease in cell growth upon FASN-blockade by C75 and G28UCM. Cell cycle represents yet another mechanism that interferes with cell growth and proliferation. Therefore, two important regulators of cell cycle progression – p16^{Ink4A}/CDKN2A and p21/WAF1 – were investigated by Western blot analysis. p16 and p21 are inhibitors of cyclin-dependent kinases (p16 inhibits CDK4/CDK6, p21 inhibits CDK1/CDK2) and thereby are capable to block cell cycle progression at the G1 and G2 stages of the cell cycle (Peurala et al. 2013, Cmielová and Recáčová 2011). To test, whether inhibition of FASN has effects on these cell cycle regulating proteins, SKOV3, OVCAR3, HOC7, IOSE80 and OSE cells were treated with a range of different doses of C75 or G28UCM for 48 hours at standard incubation conditions.

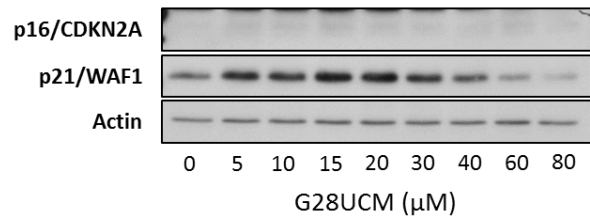
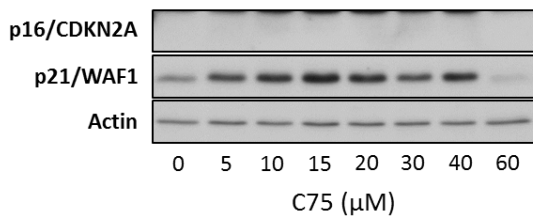
After lysis of cells, protein samples were subjected to SDS gel electrophoresis and protein levels were measured using Western blot technique (Figure 21).

SKOV 3 and HOC7 cells do not express wild type p16 due to a homozygous deletion (SKOV3) or a 16bp-deletion generating a pre-emptive stop codon (HOC7), respectively (Schuyer et al. 1996) precluding detection of p16 protein by Western blotting in these cell lines. Furthermore, in SKOV3 cells expression of p21 remained almost unresponsive to treatment with FASN-inhibitors except a minor increase in cultures treated with 80 μ M C75. In contrast, HOC7 cells revealed a distinct induction of p21-expression upon treatment with C75 or G28UCM even at the lowest doses used. These levels decreased in cells treated with high doses of FASN-inhibitors. On the other hand, OVCAR3 cells exhibited a slight decrease in p16 expression levels upon treatment with C75 or G28UCM. p21 was not induced by either C75 or G28UCM, only cells treated with 40 μ M of C75 showed p21 expression. Protein levels of p16 were slightly increased in IOSE80 cells when treated with low doses of C75 or G28UCM. p21 expression in IOSE80 cells showed a dose-dependent increase when treated with C75. In contrast, G28UCM only slightly induced p21 at the lowest concentration. When treated with higher concentrations, p21 levels resemble that of the untreated control sample. OSE cells were unresponsive to FASN inhibitors in respect to expression of p16. However, these cells exhibited a remarkable increase of p21 protein levels when treated with low doses of C75 (5 μ M) or of G28UCM (5-15 μ M).

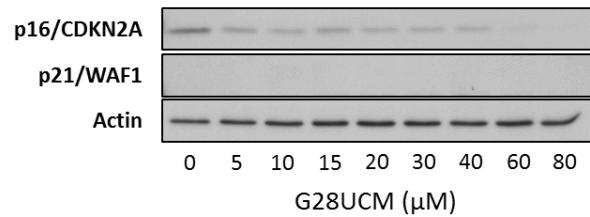
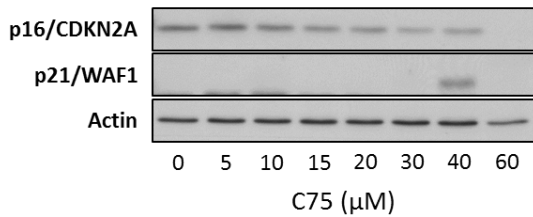
SKOV3



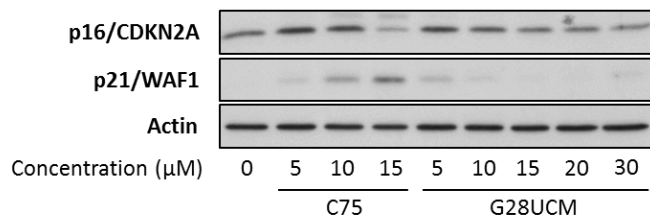
HOC7



OVCAR3



IOSE80



OSE

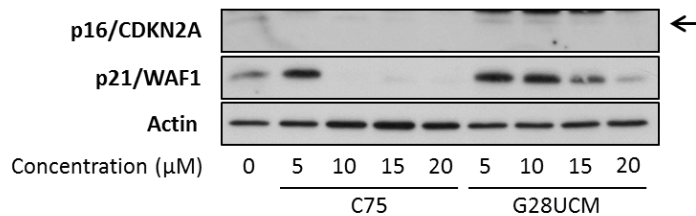


Figure 21 | Effects of C75 and G28UCM on the expression of the important cell cycle regulatory proteins p16^{Ink4A}/CDKN2A (17 kDa) and p21/WAF1 (21 kDa). SKOV3, OVCAR3, HOC7, IOSE80 and OSE cells were treated with indicated concentrations of C75 or G28UCM for 48h at 37°C, 5% CO₂, 5% FCS prior to harvesting. Vehicle (0,4% or 0,2% (OSE) DMSO) treated cells were used as control. Proteins were separated on a 12% SDS polyacrylamide gel. β-Actin was used as loading control. The arrow indicates the p16/CDKN2A protein band.

To address the question whether inhibition of de novo fatty acid synthesis by FASN causes shifts in the distribution of cell cycle stages of malignant and non-malignant ovarian surface epithelial cells, cell cycle analysis was performed by flow cytometric determination of cellular DNA content. In this set of experiments SKOV3, OVCAR3,

HOC7, IOSE80 and OSE cells were treated with individual doses of the FASN-blockers C75 or G28UCM for 6, 18, 24 or 48 hours. These doses were the same as for the measurement of active caspase 3, which were selected based on data from growth assays (IC_{50} values) and PARP1 inactivation (Figure 17). After harvesting, cellular DNA was stained using Propidium Iodide (see Materials and Methods). After acquisition on a Becton Dickinson FACScan flow cytometer, data were analysed using ModFit software (see Figure 23 for representative histograms).

Figure 22 shows stacked bar graphs of the cell cycle stage distribution after several time points of treatment with C75 and G28UCM. Control bars show the distribution of cell cycle phases in vehicle ($\leq 0,2\%$ DMSO) treated cells. Bars without shading represent C75 treated samples or vehicle control respectively. Shaded bars represent data from G28UCM-treated samples. Bars are divided into segments indicating the percentage of cells at G0/1, S and G2/M phase of the cell cycle, respectively, which accumulate to 100%. Table 10 demonstrates the exact numerical data obtained from these experiments including standard deviation and statistical significances. Treatment of SKOV3 cells with C75 and G28UCM resulted in a shift of cells at G0/G1 phase towards G2/M phase, hence a block of cell cycle at G2/M. That shift becomes more evident over time. The same holds true for C75-treated OVCAR3 cells, however to a much lesser extent. The cell cycle distribution of OVCAR3 cells remains almost stable after treatment with G28UCM. Only after 48h of treatment, a statistically significant shift towards G2/M was measureable. In HOC7 cells C75 and G28UCM elicited different effects in regard to cell cycle distribution. Whereas C75 caused a distinct time-dependent decrease at G0/1, no significant shifts could be observed in G28UCM-treated samples. The decrease at G0/1 in cells treated with C75 led to an increase of cells at S and G2/M. IOSE80 cells treated with C75 exhibited a shift towards G2/M, while treatment with G28UCM induced a shift towards S phase. Cell cycle distribution in OSE cells was mostly unaffected by C75 and G28UCM.

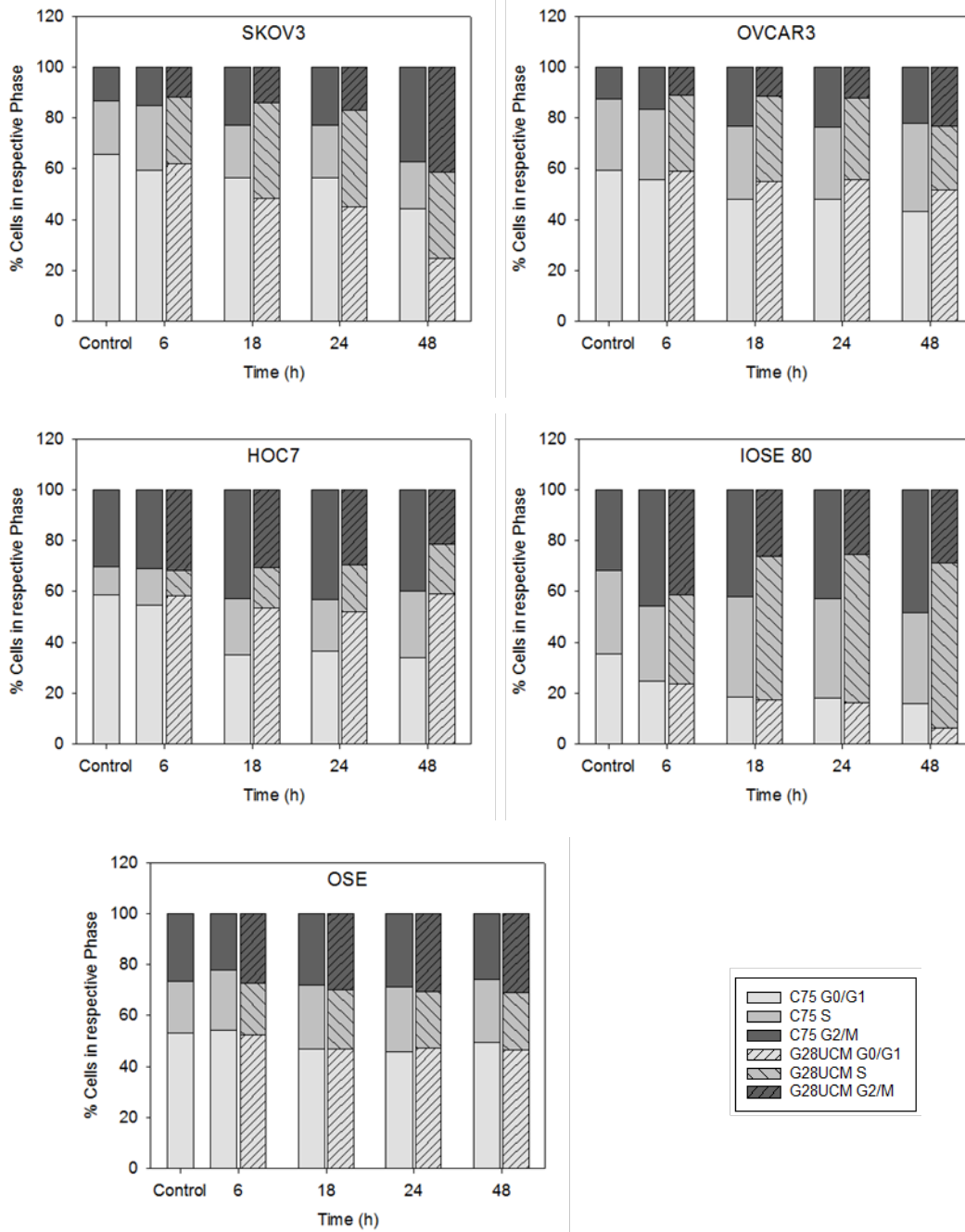


Figure 22 | Effects of FASN-inhibition by C75 and G28UCM on cell cycle distribution in malignant (SKOV3, OVCAR3, HOC7) and non-malignant (IOSE80, OSE) ovarian surface epithelial cells. Cells were treated with individual doses of C75 and G28UCM (SKOV 80 μ M, OVCAR3 30 μ M, HOC7 40 μ M, IOSE 25 μ M, OSE 10 μ M) for 6, 18, 24 or 48 hours at 37°C, 5% CO₂, 5% FCS. Stacked bar graphs show combined data obtained from flow cytometry of cells whose DNA was labelled with Propidium Iodide. Bars are divided into segments representing the percentages of cells at the various cell cycle stages. Non-shaded bars represent samples treated with C75 or vehicle (\leq 0,2% DMSO) control respectively. Shaded bars indicate samples treated with G28UCM. Each segment represents the mean of 3 independent experiments, except for OSE, where one representative experiment is shown.

Cell line	Treatment	Cell cycle phase	Mean	SD	n	p-Value vs Control	Significance
SKOV3	Control	G0/1	65,73	1,13	3		
		S	21,07	1,20	3		
		G2/M	13,20	1,25	3		
	C75 6h	G0/1	59,54	3,09	3	0,014	*
		S	25,19	2,54	3		
		G2/M	15,27	1,40	3		
	C75 18h	G0/1	56,37	1,56	3	<0,001	***
		S	20,95	1,01	3		
		G2/M	22,67	1,20	3		
	C75 24h	G0/1	56,33	1,34	3	<0,001	***
		S	20,97	0,43	3		
		G2/M	22,69	1,05	3		
	C75 48h	G0/1	44,31	2,90	3	<0,001	***
		S	18,59	0,83	3		
		G2/M	37,10	2,84	3		
	G28UCM 6h	G0/1	61,87	3,35	3		
		S	26,27	3,57	3		
		G2/M	11,85	1,54	3		
G28UCM 18h	G0/1	48,30	1,97	3	<0,001	***	
	S	37,59	2,96	3			
	G2/M	14,12	1,03	3			
G28UCM 24h	G0/1	45,11	2,27	3	<0,001	***	
	S	38,03	3,20	3			
	G2/M	16,87	1,15	3			
G28UCM 48h	G0/1	24,79	3,40	3	<0,001	***	
	S	33,74	3,68	3			
	G2/M	41,47	2,06	3			
HOC7	Control	G0/1	58,55	3,81	3		
		S	11,04	3,27	3		
		G2/M	30,41	7,02	3		
	C75 6h	G0/1	54,78	2,45	3		
		S	14,11	5,37	3		
		G2/M	31,10	7,21	3		
	C75 18h	G0/1	35,21	3,76	3	<0,001	***
		S	21,99	6,39	3		
		G2/M	42,80	3,35	3		
	C75 24h	G0/1	36,75	2,42	3	0,001	**
		S	20,10	6,09	3		
		G2/M	43,14	3,67	3		
	C75 48h	G0/1	33,91	3,48	3	<0,001	***
		S	26,22	3,50	3		
		G2/M	39,87	3,38	3		
	G28UCM 6h	G0/1	58,21	6,99	3		
		S	10,25	3,95	3		
		G2/M	31,54	10,39	3		
G28UCM 18h	G0/1	53,39	6,07	3			
	S	16,13	8,02	3			
	G2/M	30,48	3,08	3			
G28UCM 24h	G0/1	52,07	8,09	3			
	S	18,25	10,03	3			
	G2/M	29,68	4,35	3			
G28UCM 48h	G0/1	59,08	9,77	3			
	S	19,41	5,86	3			
	G2/M	21,51	7,96	3			
OVCAR3	Control	G0/1	59,53	1,78	3		
		S	27,79	1,00	3		
		G2/M	12,68	1,19	3		
	C75 6h	G0/1	55,83	0,95	3		
		S	27,66	1,59	3		
		G2/M	16,51	0,90	3	<0,001	***
	C75 18h	G0/1	48,08	0,93	3	<0,001	***
		S	28,65	0,86	3		
		G2/M	23,27	0,45	3		

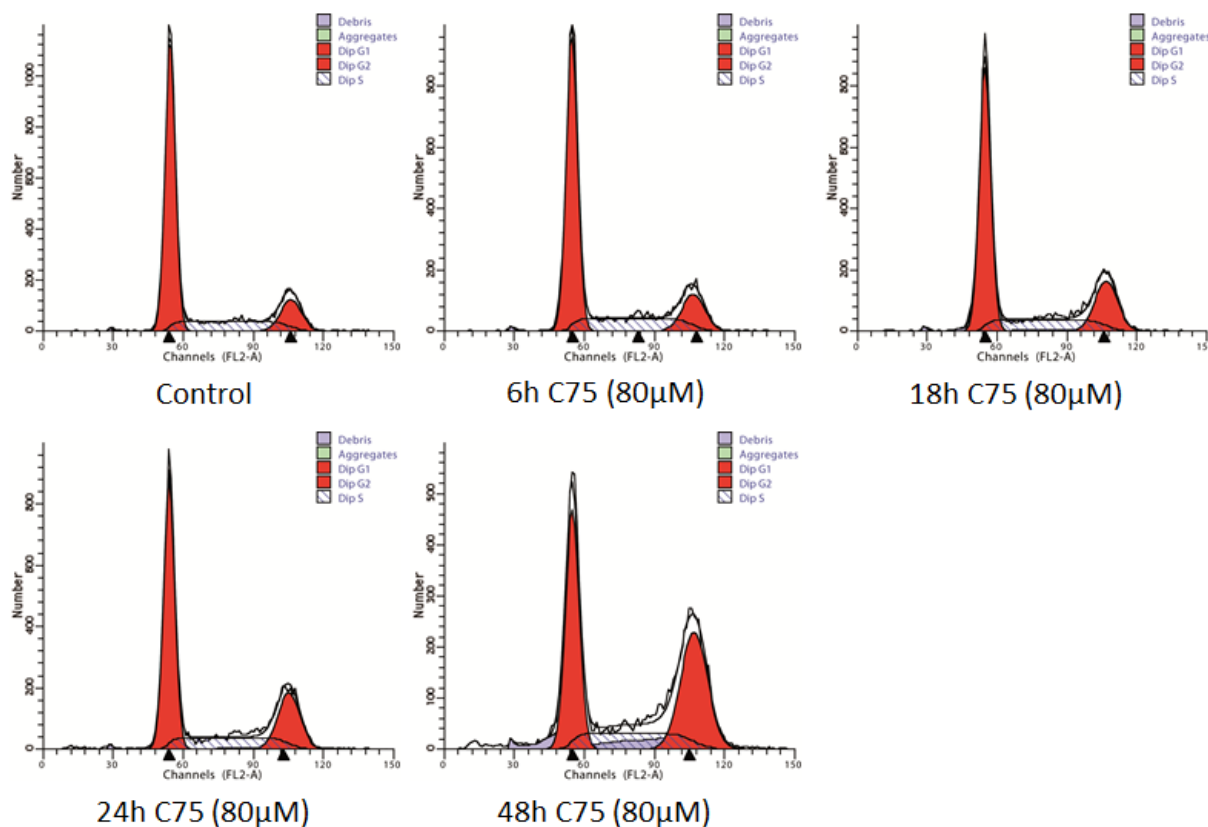
	C75 24h	G0/1	47,90	2,89	3	<0,001	***
		S	28,48	2,75	3		
		G2/M	23,62	0,29	3	<0,001	***
	C75 48h	G0/1	43,18	8,94	3	n.d.	
		S	34,63	10,00	3	n.d.	
		G2/M	22,20	1,19	3		
	G28UCM 6h	G0/1	59,26	1,57	3		
		S	29,55	1,37	3		
		G2/M	11,19	0,58	3		
	G28UCM 18h	G0/1	55,07	0,47	3		
		S	33,52	0,69	3	0,003	**
		G2/M	11,23	0,49	3		
	G28UCM 24h	G0/1	55,83	2,00	3		
		S	31,99	1,63	3	0,025	*
		G2/M	12,18	0,42	3		
	G28UCM 48h	G0/1	51,67	6,19	3	0,013	*
		S	25,11	6,58	3	n.d.	
		G2/M	23,21	0,90	3	<0,001	***
IOSE80	Control	G0/1	35,53	5,62	3		
		S	32,62	0,84	3		
		G2/M	31,85	6,39	3		
	C75 6h	G0/1	24,79	4,16	3	<0,001	***
		S	29,55	0,75	3		
		G2/M	45,66	4,90	3	0,005	**
	C75 18h	G0/1	18,51	1,87	3	<0,001	***
		S	39,45	1,08	3	<0,001	***
		G2/M	42,04	1,40	3	0,036	*
	C75 24h	G0/1	18,18	1,75	3	<0,001	***
		S	39,18	1,42	3	<0,001	***
		G2/M	42,64	3,17	3	0,029	*
	C75 48h	G0/1	16,15	2,18	3	<0,001	***
		S	35,48	0,72	3		
		G2/M	48,37	2,37	3	<0,001	***
	G28UCM 6h	G0/1	23,66	3,25	3	<0,001	***
		S	35,05	1,95	3		
		G2/M	41,29	5,20	3		
G28UCM 18h	G0/1	17,43	2,75	3	<0,001	***	
	S	56,28	0,92	3	<0,001	***	
	G2/M	26,30	3,64	3			
G28UCM 24h	G0/1	16,21	2,61	3	<0,001	***	
	S	58,49	1,27	3	<0,001	***	
	G2/M	25,30	2,70	3			
G28UCM 48h	G0/1	6,43	1,84	3	<0,001	***	
	S	64,88	2,99	3	<0,001	***	
	G2/M	28,69	4,82	3			
OSE	Control	G0/1	53,16		1	n.d.	
		S	20,30		1	n.d.	
		G2/M	26,54		1	n.d.	
	C75 6h	G0/1	54,31		1	n.d.	
		S	23,48		1	n.d.	
		G2/M	22,21		1	n.d.	
	C75 18h	G0/1	46,79		1	n.d.	
		S	25,26		1	n.d.	
		G2/M	27,95		1	n.d.	
	C75 24h	G0/1	45,72		1	n.d.	
		S	25,46		1	n.d.	
		G2/M	28,81		1	n.d.	
	C75 48h	G0/1	49,37		1	n.d.	
		S	24,85		1	n.d.	
		G2/M	25,77		1	n.d.	
	G28UCM 6h	G0/1	52,29		1	n.d.	
		S	20,57		1	n.d.	
		G2/M	27,14		1	n.d.	
G28UCM 18h	G0/1	46,80		1	n.d.		
	S	23,48		1	n.d.		
	G2/M	29,72		1	n.d.		
G28UCM 24h	G0/1	47,13		1	n.d.		
	S	22,27		1	n.d.		
	G2/M	30,60		1	n.d.		
G28UCM 48h	G0/1	46,42		1	n.d.		

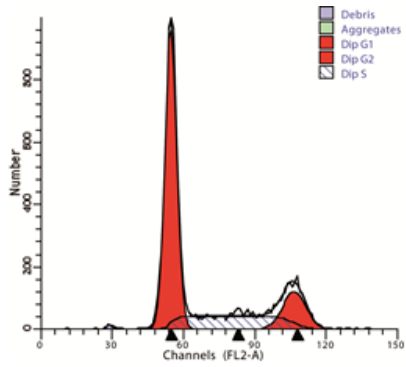
	S	22,76	1	n.d.
	G2/M	30,82	1	n.d.

Table 10 | Numerical data from cell cycle analysis of malignant (SKOV3, OVCAR3, HOC7) and non-malignant (IOSE80, OSE) ovarian surface epithelial cells. For each cell cycle phase mean values as well as standard deviations from 3 independent experiments are indicated (except for OSE). One-way ANOVA was used to calculate the significance of differences between the cell cycle stages of control and treatment samples. Only p-values below 0,05 are indicated and regarded as statistically significant. * p<0,05; ** p<0,01; *** p<0,001; n.d. not determined; Only 1 experiment was conducted with OSE cells.

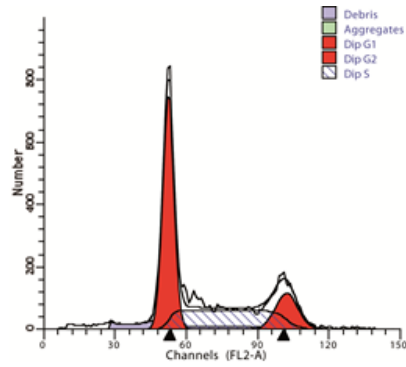
Figure 23 demonstrates representative histograms from cell cycle analysis, generated by ModFit software. A change in cell cycle progression is marked by a shift in height and/or width between the red peaks (G0/1 and G2/M) as well as the shaded area (S) in the histograms. Notice the bluish areas marking cellular debris increasing over time of treatment in most of the cell lines indicating cytotoxic effects elicited by C75 and G28UCM.

SKOV3

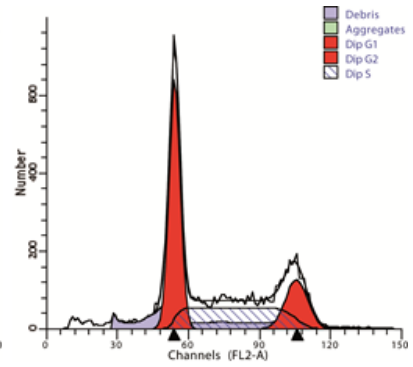




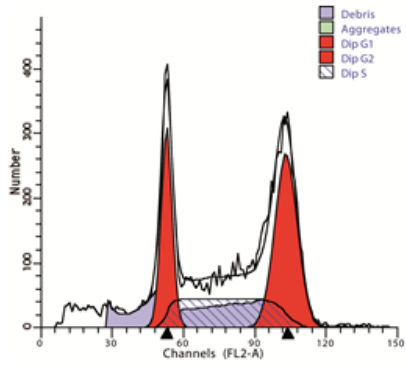
6h G28UCM (80µM)



18h G28UCM (80µM)

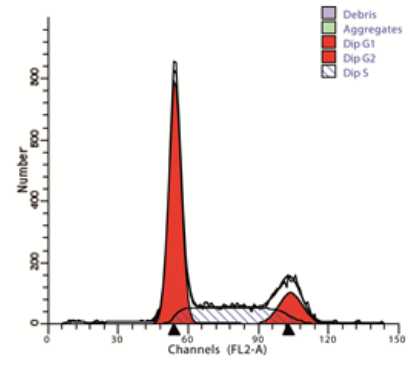


24h G28UCM (80µM)

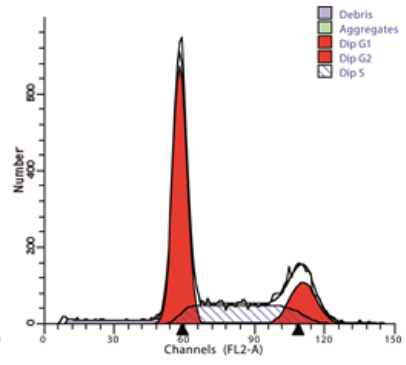


48h G28UCM (80µM)

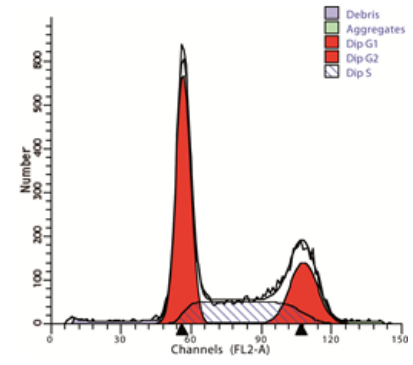
OVCAR3



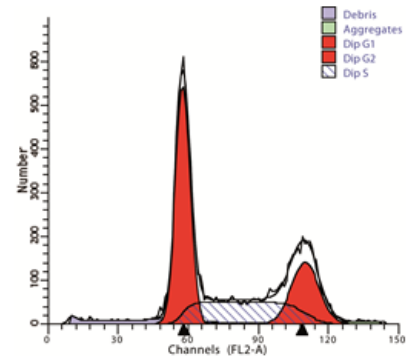
Control



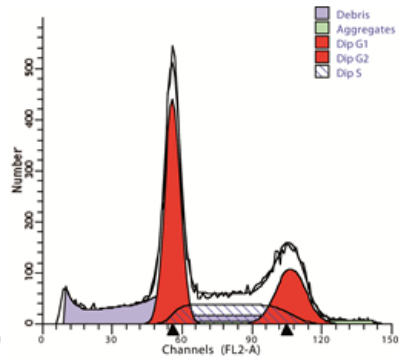
6h C75 (30µM)



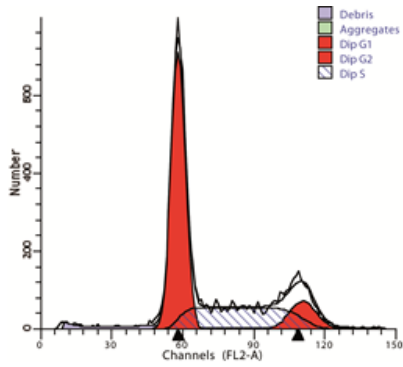
18h C75 (30µM)



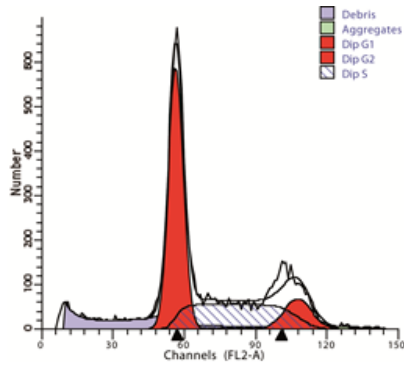
24h C75 (30µM)



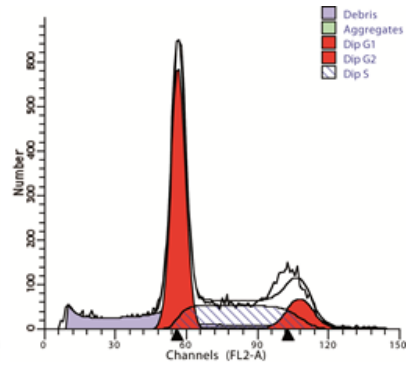
48h C75 (30µM)



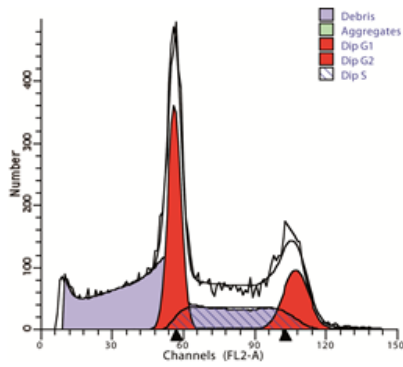
6h G28UCM (30µM)



18h G28UCM (30µM)

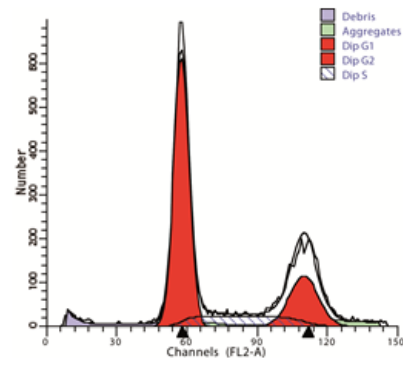


24h G28UCM (30µM)

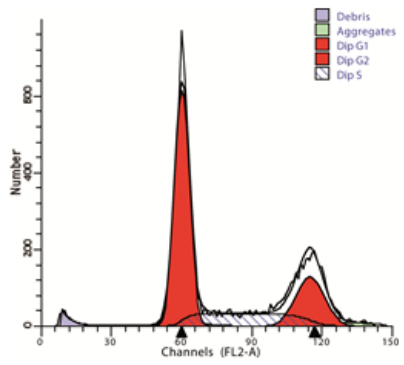


48h G28UCM (30µM)

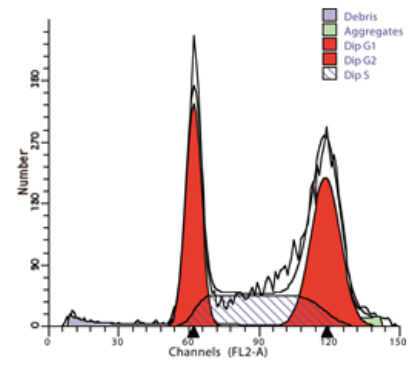
HOC7



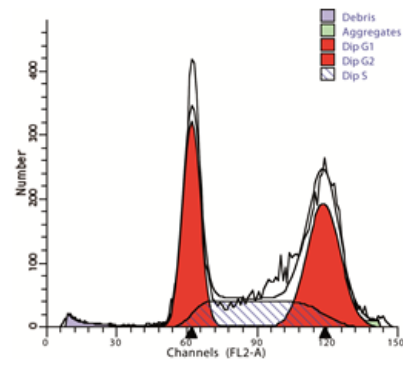
Control



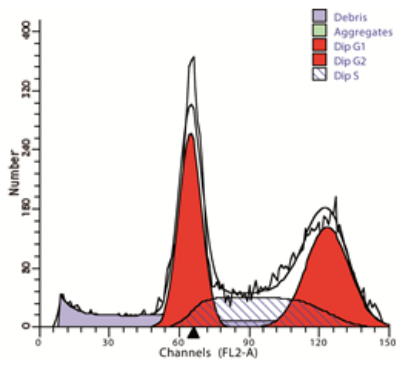
6h C75 (40µM)



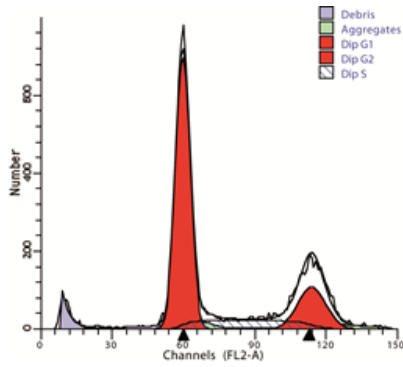
18h C75 (40µM)



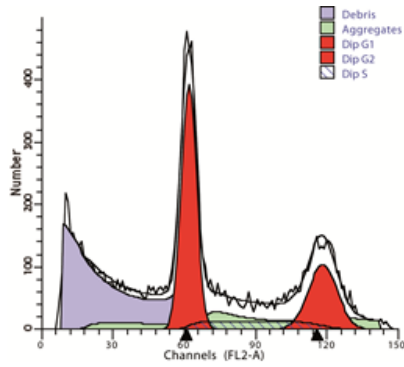
24h C75 (40µM)



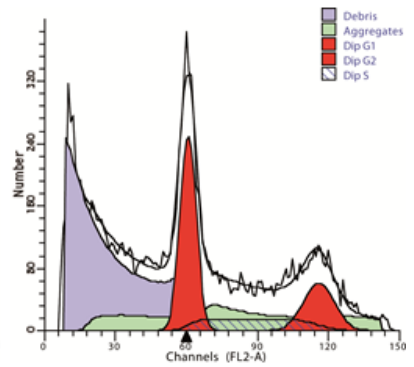
48h C75 (40µM)



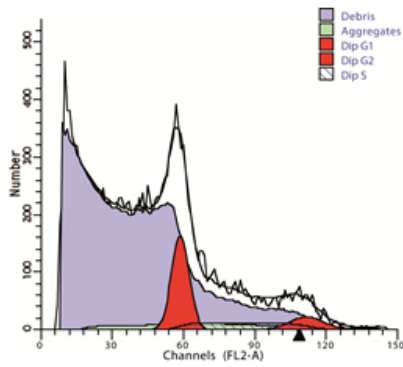
6h G28UCM (40µM)



18h G28UCM (40µM)

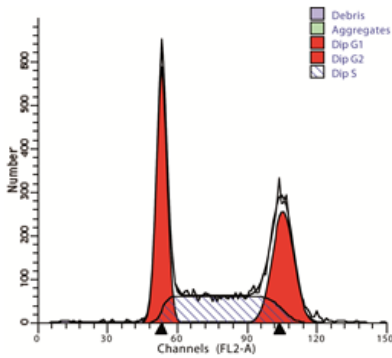


24h G28UCM (40µM)

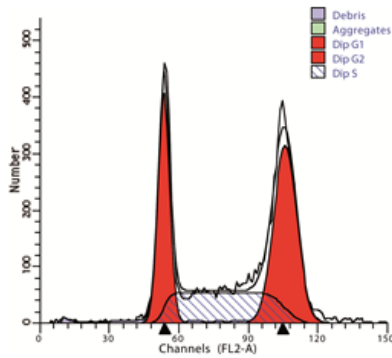


48h G28UCM (40µM)

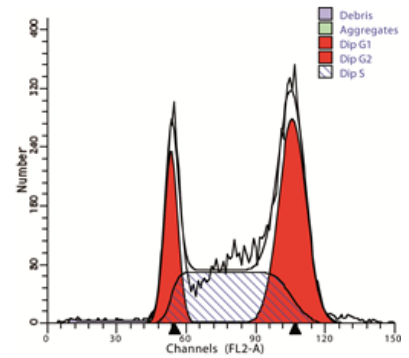
IOSE80



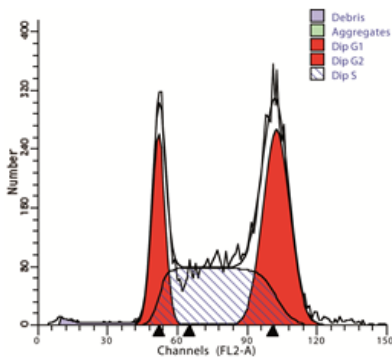
Control



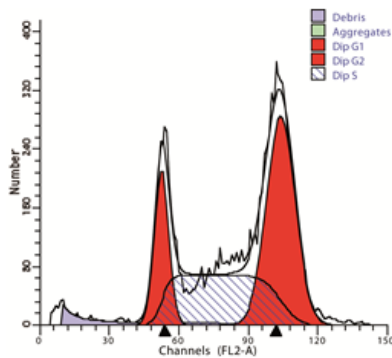
6h C75 (25µM)



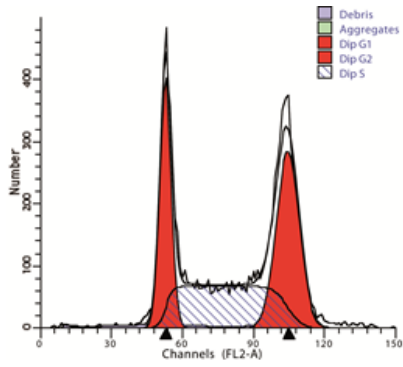
18h C75 (25µM)



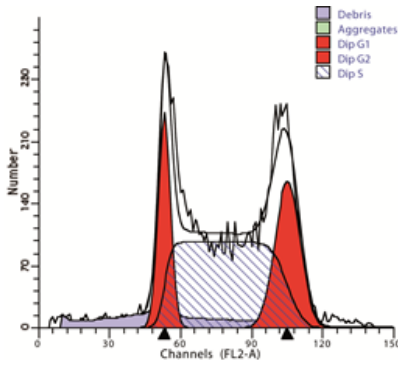
24h C75 (25µM)



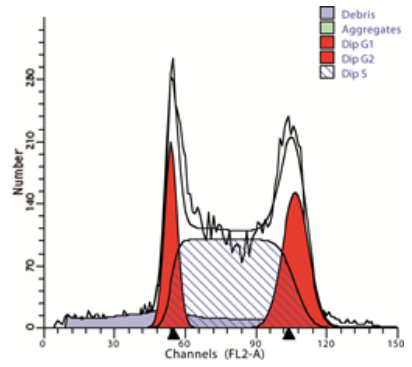
48h C75 (25µM)



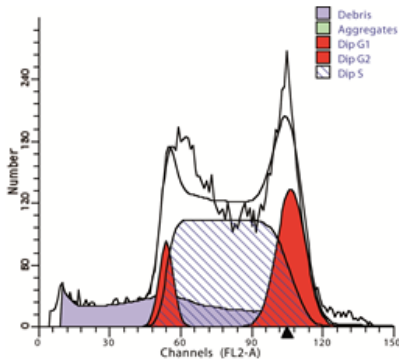
6h G28UCM (25µM)



18h G28UCM (25µM)

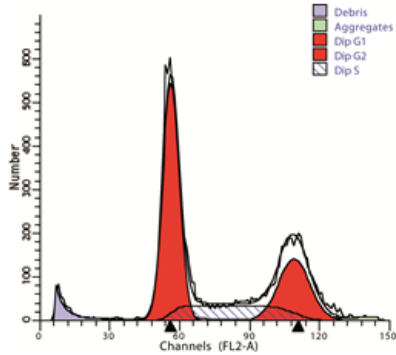


24h G28UCM (25µM)

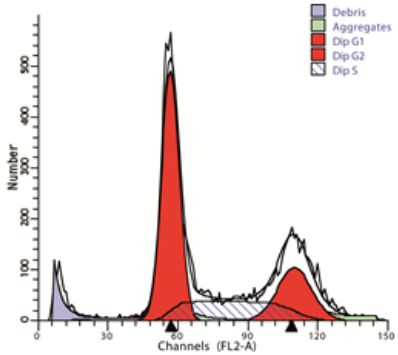


48h G28UCM (25µM)

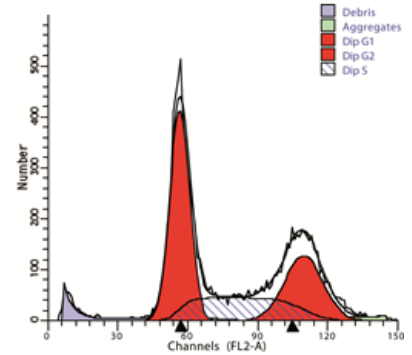
OSE



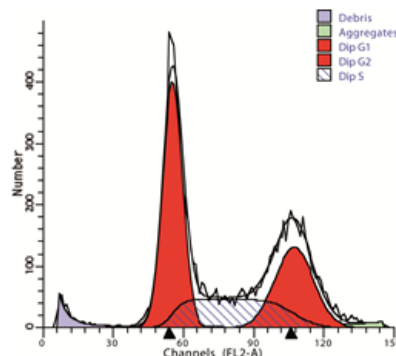
Control



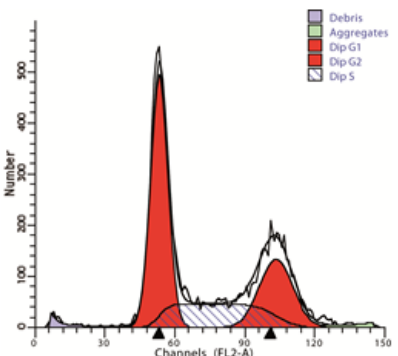
6h C75 (10µM)



18h C75 (10µM)



24h C75 (10µM)



48h C75 (10µM)

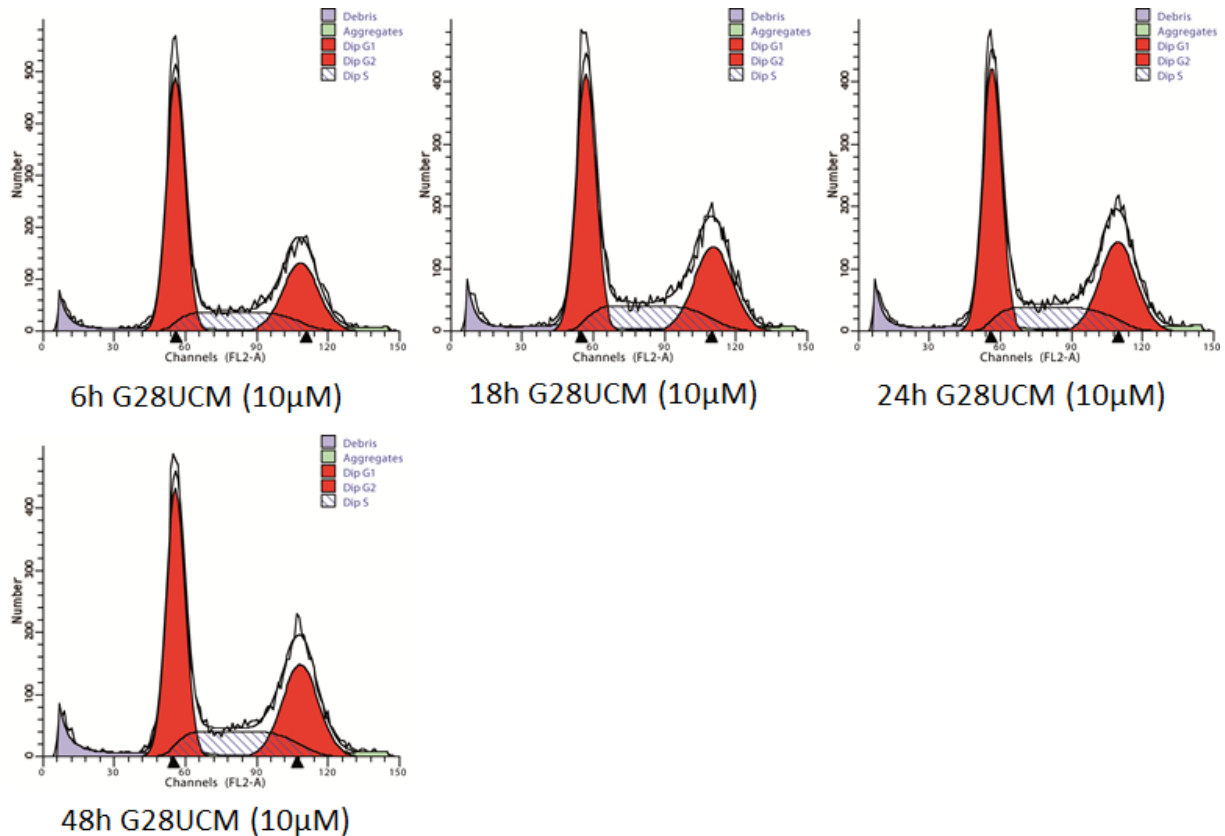


Figure 23 | Representative histograms of cell cycle data. Data were analyzed using ModFit software. Red peaks indicate G0/1 (left peak) and G2/M (right peak) stages respectively. Shaded area indicates population of cells in S-phase. Bluish areas contain cellular debris (including late apoptotic and necrotic cells as well as cell remnants). Green areas mark aggregates. Vehicle-treated ($\leq 0,2\%$ DMSO) cells were used as control.

3.8 HSP70 but not HSP90 is induced by FASN-inhibition via C75

HSP70 and HSP90 are ubiquitously expressed protein chaperones that support the correct folding of newly synthesized, as well as damaged proteins (Mayer and Bukau, 2005). HSP90 also aids in the degradation of polyubiquitinated proteins by the 26S proteasome (Lüders et al. 2000). HSP70 is also able to participate in the degradation of defective proteins through interaction with the E3 ubiquitin ligase CHIP (Qian et al. 2006). Furthermore, HSP70 can directly inhibit apoptosis by blocking pro-caspase 9 from binding to the apoptosome (Beere et al. 2000).

To investigate, whether expression of HSP70 and HSP90 is affected by the FASN inhibitors C75 and G28UCM, SKOV3, OVCAR3, HOC7, IOSE80 and OSE cells were treated with a range of doses of these inhibitors. Drug exposure was for 48h and was

followed by cell lysis and protein harvesting. Samples were separated via SDS polyacrylamide gel electrophoresis and subjected to Western blotting. The results of these experiments are presented in Figure 24-26. Interestingly, treatment with C75 led to a distinct (sometimes transient) up to 6-fold increase of HSP70 expression in all cell lines tested. In sharp contrast, none of the cell lines exhibited an increase in HSP70 protein levels upon treatment with G28UCM. Furthermore, HSP90 expression was neither increased in malignant nor in non-malignant ovarian surface epithelial cells upon treatment with C75 or G28UCM, with the exception of HOC7 cells, where treatment with C75 led to a up to 3-fold increase of HSP90 protein.

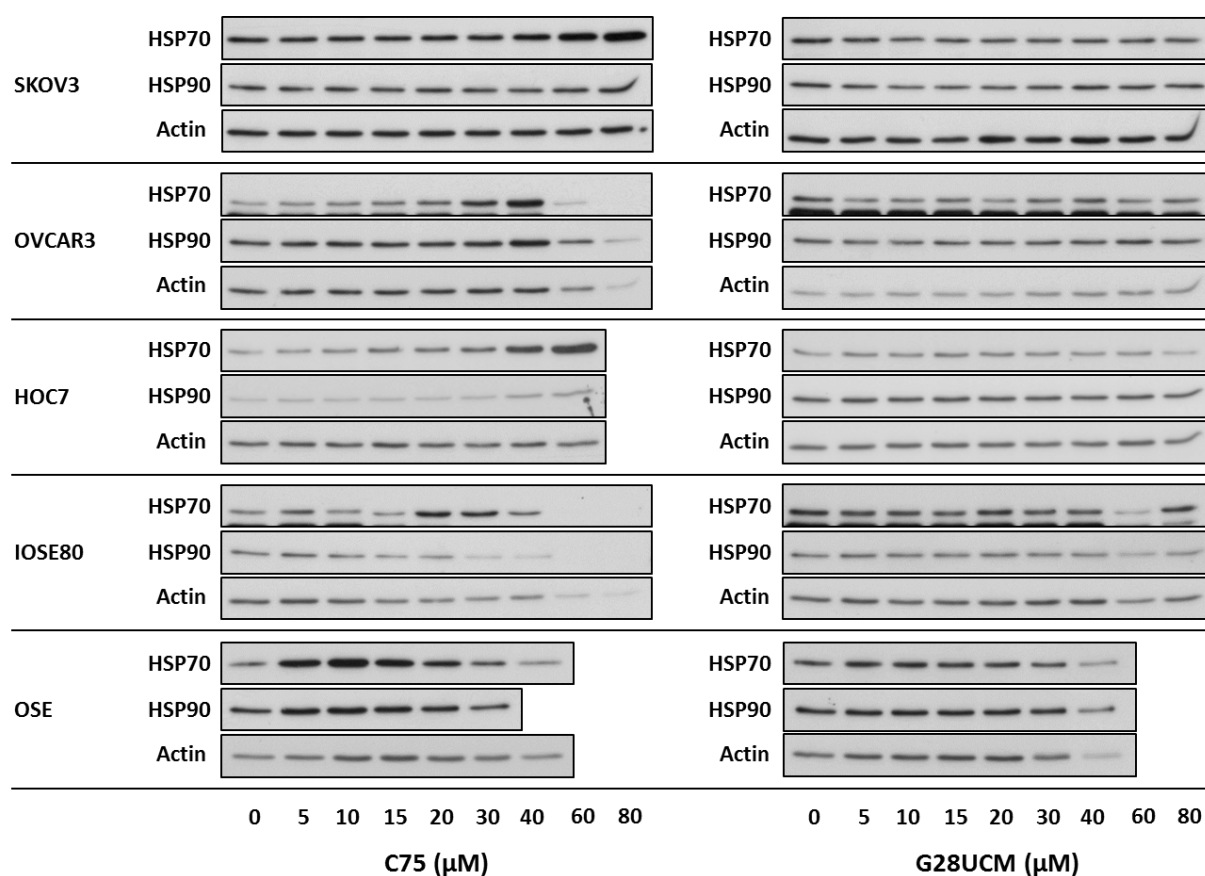


Figure 24 | Expression of the protein chaperones HSP70 and HSP90 in SKOV3, OVCAR3, HOC7, IOSE80 and OSE cells after treatment with different doses of C75 and G28UCM. Cells were treated for 48h at 37°C, 5% CO₂, 5% FCS, prior to harvesting. Protein samples were separated on a 10% or 12% SDS polyacrylamide gel and subjected to Western blot analysis. Vehicle (0,4% DMSO, OSE 0,2% DMSO) treated cells were used as control. β-Actin was used as loading control.

Figure 25 shows expression levels of HSP70 in cells treated with C75 or G28UCM plotted against concentration of inhibitor. For the calculation of the expression levels, densitometry of the protein bands from Western blots in Figure 24 was performed.

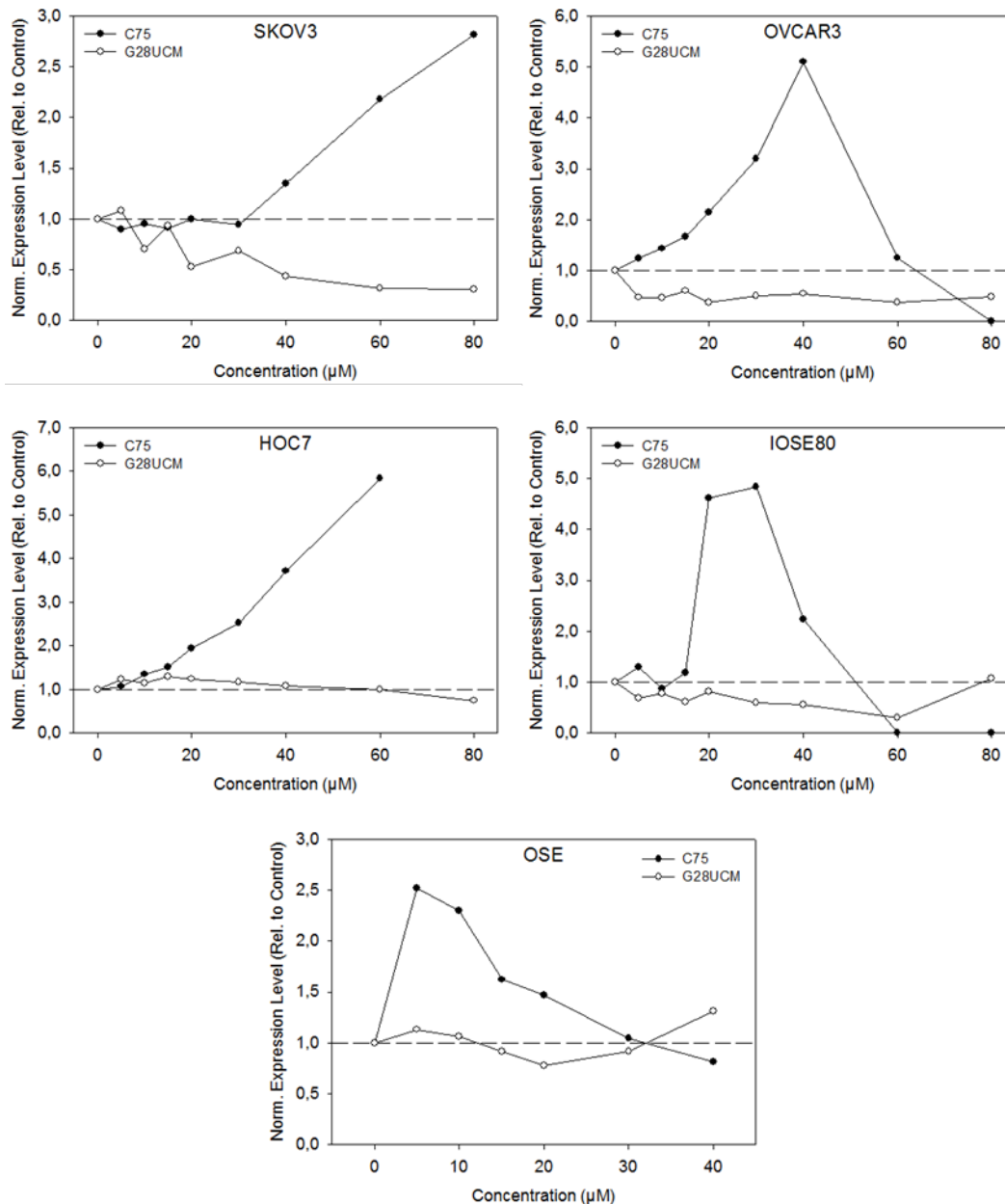


Figure 25 | Protein levels of HSP70 in indicated cell lines after treatment with various doses of C75 or G28UCM. Each protein band was related to β -Actin expression and normalized to expression in vehicle-treated control, which was arbitrarily set at 1,0 [Norm. Expression Level (Rel. to Control)]. Dashed horizontal line indicates expression level of control. Densitometry data from Western blots in Figure 24.

Figure 26 shows densitometry data of protein bands from Figure 24. Expression levels of HSP90 are plotted against concentration of FASN-inhibitor.

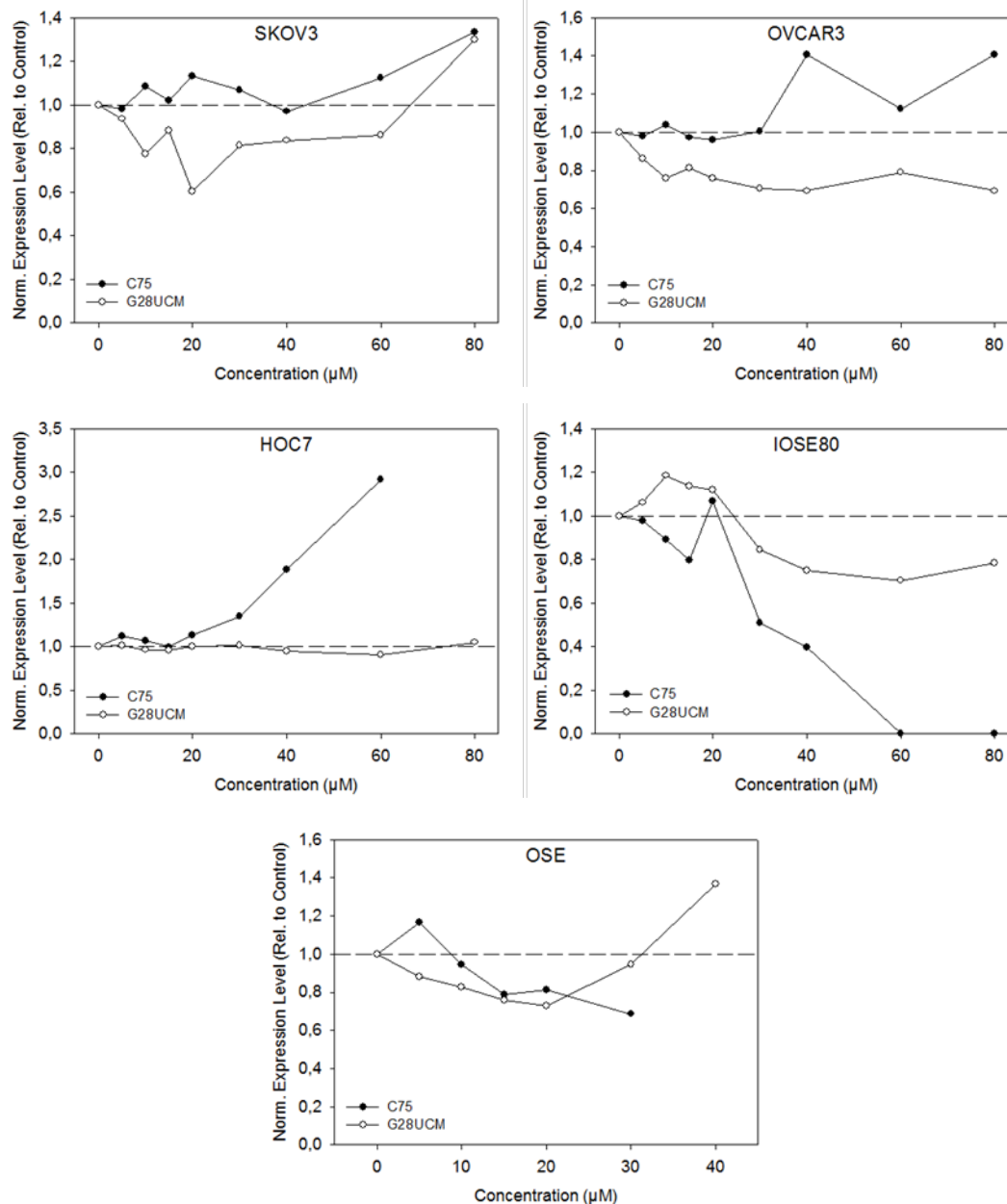


Figure 27 | Protein levels of HSP90 in indicated cell lines after treatment with various doses of C75 or G28UCM. Each protein band was related to β -Actin expression and normalized to expression in vehicle-treated control, which was arbitrarily set at 1,0 [Norm. Expression Level (Rel. to Control)]. Dashed horizontal line indicates expression level of control. Densitometry data from Western blots in Figure 24.

3.9 Protein ubiquitination occurs in C75-treated cells

In section 3.8 it was shown that C75, in contrast to G28UCM, can upregulate HSP70. As mentioned above, HSP70 is capable to support polyubiquitination of proteins. Furthermore, data presented in section 3.4 indicate that treatment with C75 and G28UCM can cause a decrease in the expression levels of key signaling proteins, yet

it is unclear if the decrease is due to reduced translation or to enhanced protein degradation. The majority of cytoplasmic proteins are degraded by the ubiquitin-proteasome pathway (Rock, 1994), where after polyubiquitination of target proteins by ubiquitin ligases, degradation of proteins is facilitated via the 26S proteasome.

To investigate the effects of FASN-blockade by C75 and G28UCM on protein ubiquitination, SKOV3, OVCAR3, HOC7, IOSE80 and OSE cells were treated with various doses of C75 or G28UCM. The amount of ubiquitination was measured by Western blot analysis and corresponding results are presented in Figure 27. In these experiments, ubiquitination was a rare event and furthermore was restricted to cells treated with C75. Heavy ubiquitination was observed in HOC7 cells (60 μ M C75) and OSE cells (10 μ M C75), whereas a slight induction was present in SKOV3 (80 μ M C75) and OVCAR3 (40 μ M C75). No increase in ubiquitination was observed in IOSE80 after treatment with C75 and none of the cell lines tested showed increased ubiquitination upon treatment with G28UCM.

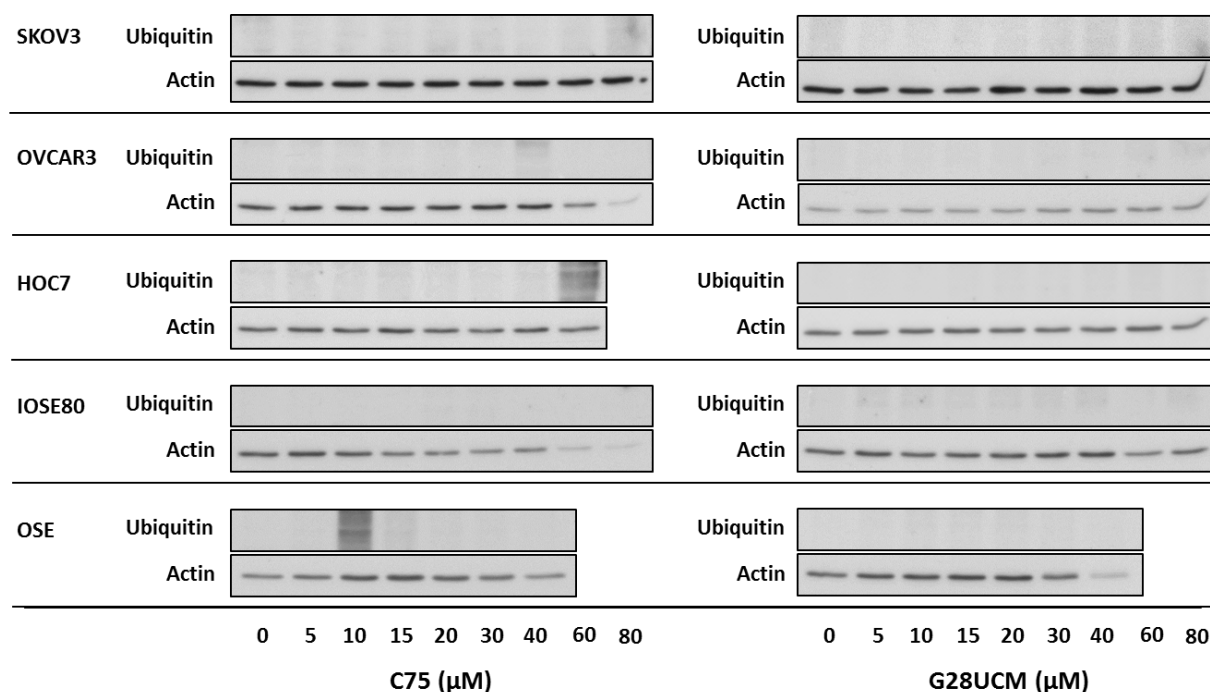


Figure 27 | Protein ubiquitination upon treatment with the FASN-inhibitors C75 and G28UCM. SKOV3, OVCAR3, HOC7, IOSE80 and OSE cells were treated with indicated concentrations of C75 or G28UCM respectively for 48h at 37°C, 5% CO₂, 5% FCS. Cells were lysed and protein samples were subjected to SDS polyacrylamide gel electrophoresis (10% SDS polyacrylamide gel), followed by Western blot analysis. Vehicle (0,4% DMSO, OSE 0,2% DMSO) treated cells were used as control. β -Actin was used as loading control.

4 Discussion

4.1 Malignant and non-malignant ovarian surface epithelial cells express FASN and are sensitive to FASN-blockade by C75 and G28UCM

As mentioned earlier, deregulated expression of fatty acid synthase (FASN) is a frequent event in carcinogenesis and in progression of tumors, including ovarian cancer. In contrast, most non-malignant tissues utilize dietary fatty acids to cover their lipid requirements and do not depend on de novo synthesis of fatty acids. Unfortunately, there is currently no data available comparing the expression of FASN in malignant and non-malignant ovarian surface epithelial cells in vitro. Therefore, we measured the protein expression of FASN in eleven ovarian cancer cell lines as well as in 3 immortalized ovarian surface epithelial cell lines, in primary non-malignant ovarian surface epithelial cells and in a non-malignant cell line of human foreskin fibroblasts. The reason behind the fact that the non-malignant ovarian surface epithelial cells (IOSE80, -364, 386, OSE) showed significant expression of FASN is not quite clear, but might be attributable to their origin from hormone-sensitive tissue (that is expressing FASN) or it might be correlated with growth rate (Kusakabe et al., 2000). Both possibilities are supported by the finding that CRL2522 human foreskin fibroblasts – which do not origin from a hormone-sensitive tissue and are slower growing cells – do not express high protein levels of FASN.

As mentioned above, previous studies have shown that C75 is able to reduce cancer cell growth in a variety of tumors including colon, breast, lung, liver and ovarian cancer in vitro and of breast and lung cancer in vivo (Pizer et al. 2000, Li et al. 2001, Gao et al. 2006, Grunt et al. 2009, Relat et al. 2012). Similar effects on breast cancer cell growth in vitro and in vivo have been shown for the novel compound G28UCM (Oliveras et al. 2010). In this study, for the first time we compared the anti-proliferative properties of C75 and G28UCM in malignant and non-malignant cells of ovarian origin. Clearly, G28UCM elicits growth inhibitory effects on malignant and non-malignant ovarian surface epithelial cells at significantly lower doses than C75, with the important exception of normal ovarian surface epithelial cells where it is less toxic to cells than C75. Being less toxic to normal cells than to tumor cells is a very fundamental prerequisite of any potentially therapeutic substance in order to be considered for further preclinical or even clinical studies. Furthermore, lower IC₅₀ values and the rapid decline of growth curves in Figure 8 potentially reflect a higher

target specificity of G28UCM in comparison to C75. Graphs depicted in Figure 8 also point out that the overall cytotoxicity of G28UCM is lower compared to C75, as only C75 was able to abolish cell growth completely. Regarding the amount of cytotoxicity elicited by modulation of CPT1 or other – yet unknown – unspecific targets of C75, additional experiments have to be realized. Interestingly, the correlation analysis of IC_{50} values and protein expression of FASN reveals only moderate negative correlations, hence only a small proportion of the variances in IC_{50} values can be attributed to the variation of FASN protein levels. This is indicative of the presence of other, cell line dependent cellular mechanisms that interfere with the uptake, processing and binding of these FASN-inhibitors or with effects in cellular signaling and metabolism caused by C75 and G28UCM. In other words, sensitivity of malignant and non-malignant ovarian surface epithelial cells against FASN-inhibitors is not merely a question of the amount of cytosolic FASN protein.

4.2 Oleic acid but not palmitic acid can ameliorate growth-inhibitory/cytocidal effects of FASN blockade

Endogenous production of fatty acids seems to be an important property for many malignant cells in order to maintain the elevated need for lipid precursors that are used as substrates for phospholipids in membranes or as signaling cofactors (Kuhajda 2006, Mashima et al. 2009). Inhibition of FASN ultimately reduces the production of new fatty acids - mostly in the form of palmitic acid, which represents the primary end product of the FASN enzymatic action - and has been shown to reduce cell growth (Zhou et al. 2003, Zecchin et al. 2011). Cells were treated with FASN-inhibitors in combination with either exogenous palmitic acid or exogenous oleic acid in order to address the question whether the availability of primary or slightly processed secondary end products of FASN synthetic action are crucial for growth activity of the cells. Unfortunately, the intrinsic cytotoxic effect of exogenously supplied palmitic acid did not allow for a definitive answer of this question. The reason why exogenously provided palmitic acid is toxic to cells is not quite clear, however previous reports from others showed that lipotoxicity of PA is associated with the insufficient capability of cells to incorporate PA into triglycerides that correlates with reduced activity of stearoyl-CoA desaturase (SCD1) (Listenberger et al. 2003). SCD1 desaturates stearic acid and is the rate-limiting enzyme in the production of oleic acid (Enoch et al. 1976). SCD1 is regulated by sterol regulatory

element binding protein 1 (SREBP1), which in turn is regulated by mTORC1 signaling (Porstmann et al. 2008). Inhibition of FASN leads to reduced activation of mTORC1 (Knowles et al. 2008, Tomek et al. 2011). This constellation provides a hypothetical explanation why the monounsaturated fatty acid OA but not the saturated fatty acid PA can revert the anti-proliferative effects elicited by FASN-inhibition, because blockade of FASN ultimately leads to decreased activity of SCD1. Thus, exogenously provided PA is not sufficiently enough converted into OA, depriving the cell from acylglycerides and phospholipids. The use of OA to supplement for the halt in de novo fatty acid synthesis could bypass the need for elongation and desaturation of PA and thereby the cells were able to overcome the anti-proliferative effects of FASN-inhibition. Amelioration of cellular growth arrest through OA was comparable between cells treated with either C75 or G28UCM. Although the possible differences in target specificity between C75 and G28UCM could not be revealed by this experiment, this shows that both inhibitors target FASN. The fact that substitution with OA was not sufficient to fully reverse the growth-inhibitory effects of FASN-blockade in OVACAR3 cells indicates the existence of additional mechanisms by which FASN-inhibition interferes with proliferation.

4.3 C75 and G28UCM decrease signaling through MAPK and PI3K/Akt pathways in malignant and non-malignant ovarian surface epithelial cells

PI3K/Akt and MAPK are important signaling pathways, which regulate major cellular tasks like growth, proliferation and survival. It is known that PI3K/Akt activity and – at least partially – MAPK signalling positively regulates the expression of FASN via SREBP1c (Swinnen et al. 2000, Yang et al. 2002, Van de Sande et al. 2002). On the other hand, as mentioned above, inhibition of FASN was shown to reduce signaling via the PI3K/Akt pathway and was able to reduce expression of ERK1/2 (Tomek et al. 2011, Puig T et al. 2008). Our experiments reveal similar effects on the expression and phosphorylation of Akt and on the expression of ERK1/2 in cells treated with C75 or G28UCM, whereby C75 caused a more rapid decline in expression of these proteins. As expected, down-regulation of expression of Akt and ERK1/2 seems to positively correlate with sensitivity against FASN-inhibitors. Of note, down-regulation of the PI3K/Akt and MAPK pathways occurs in malignant as well as in non-malignant cells, indicating that the same mechanistic background is responsible irrespective of malignant transformation. Conceivable causes include the loss of important

secondary messenger molecules (e.g. PIP₂) or unfavourable changes in cellular membrane composition elicited by blockade of de novo fatty acid synthesis, as well as changes in protein translation or degradation initiated by FASN-inhibition (Tomek et al. 2011). However, the exact reason for shutdown of signaling remains unclear and has to be subjected to further research. Additional evidence for implications of FASN-inhibition by C75 or G28UCM on cellular signaling could be drawn from the assessment of phosphorylation of ribosomal protein S6 at Ser 240 and Ser 244. S6 is comprised in the 40S ribosomal subunit and hence it is linked to protein translation and regulation of cell size (Ruvinsky et al. 2005). Phosphorylation and activity of S6 are driven by different kinases, most important p70-S6 Kinase 1 (S6K1) and p70-S6 Kinase 2 (S6K2) that are regulated by the PI3K/Akt/mTORC1 pathway (Fingar and Blenis 2004, Richardson et al. 2004). In addition, phosphorylation of S6 also occurs by p90 ribosomal S6 kinase (RSK) that is regulated by the MAPK pathway (Pende et al. 2004). However, S6K1/2 but not RSK is involved in phosphorylation of S6 at Ser 240 and Ser 244, since RSK only phosphorylates S6 at Ser 235 and Ser 236 (Roux et al. 2007) and thus is not monitored in the above experiments. Therefore, the observed reduction in phosphorylation of S6 (Figure 12-16) is likely due to abrogated signaling via the PI3K/Akt/mTORC1 pathway. Interestingly, among the malignant cell lines tested, SKOV3 and OVCAR3 which both harbour an amplification of PIK3CA – the gene coding for the p110 α catalytic subunit of phosphatidylinositol 3-kinase (PI3K) – showed a rapid decline in S6 – phosphorylation when treated with G28UCM (Shayesteh et al. 1999). In contrast, HOC7 cells that have a known KRAS mutation are less prone to a decrease of pS6 upon FASN-inhibition (Yang et al. 2013). This gives rise to the hypothetical idea that cells with hyperactive PI3K/Akt signaling are more susceptible to lose S6 phosphorylation at Ser 240 and Ser 244 after treatment with C75 and especially G28UCM than cells showing wild type PI3K/Akt signaling but elevated MAPK signaling. In this regard it would be of interest to investigate phosphorylation of S6 at Ser 235 and Ser 236. Non-malignant cell lines that are lacking mutations in both of these signaling pathways show intermediate loss of S6-phosphorylation upon FASN-blockade. Aside from this observation it is noteworthy that while G28UCM is the more active substance in inhibiting S6 phosphorylation in most of the malignant cell lines tested, decline of S6 phosphorylation in non-malignant cell lines is more pronounced by C75. Also, the greater reduction of expression/enhanced degradation of total signaling proteins by C75 in comparison to

G28UCM in some of the tested cells (in particular the non-malignant cells) indicates that C75 is more cytotoxic than G28UCM. These observations are of importance in respect to possible future clinical applications of G28UCM, since a compound that does not/only weakly interfere(s) with signaling in cells of normal tissues likely causes less severe side-effects.

4.4 Mechanisms implicated in the anti-proliferative effects of C75 and G28UCM include apoptosis, autophagy, protein degradation and cell cycle arrest

Apoptosis as a response to inhibition of FASN was shown by previous reports (Pizer et al. 1996, Tomek et al. 2011). Several possible mechanisms were proposed regarding the activation of apoptosis elicited by FASN-blockade, including the accumulation of malonyl-CoA, or an induction of ceramide production, followed by upregulation of pro-apoptotic proteins (Thupari et al. 2001, Bandyopadhyay et al. 2006). However, the processes leading to apoptosis by FASN-inhibition are still not fully understood. Above experiments reveal that C75 and G28UCM are both able to activate the apoptotic biomarker protein caspase 3, which in turn cleaves and inactivates poly ADP-ribose polymerase 1 (PARP1) ultimately leading to overt apoptosis. Comparing the effectiveness of both inhibitors in induction of apoptosis, no clear answer could be derived from the experiments. Furthermore, induction of cell death occurred in all three malignant cell lines used as well as in immortalized ovarian surface epithelial cells in a dose- and time-dependent manner. In contrast, normal ovarian surface epithelial cells showed almost no activation of the two apoptotic markers. However, as can be derived from proliferation assays shown in Figure 8, cell growth is severely reduced in OSE cells treated with FASN-inhibitors. Assumingly, the stress response to FASN-inhibition is differentially regulated in malignant and immortalized ovarian surface epithelial cells compared to normal OSE cells. A possible mechanism explaining the high amount of apoptosis observed in malignant and immortalized ovarian surface epithelial cells in contrast to normal OSEs involves the regulation of the cell cycle. Malignant cells often harbour mutations in cell cycle regulating proteins (for instance p53) which interfere with the cells ability to stop cell cycle progression upon the encounter of cellular and/or extracellular stresses. Transfection of OSE cells with SV40 T/t antigen (as present in IOSE80) also modulates cell cycle control (Bryan and Reddel 1994). Therefore, it can

be hypothesized that malignant and immortalized ovarian surface epithelial cells are not able to stop cell cycle progression after inhibition of FASN, leading to cell death, while normal OSE cells can halt their cell cycle to avoid apoptosis.

A previous study by Tomek et al (2011) has shown that protein degradation is altered by inhibition or siRNA mediated knockdown of FASN involving increased autophagy and protein ubiquitination. Furthermore, a genome-wide study revealed changes in transcription of genes regulating protein degradation after knockdown of FASN (Knowles and Smith, 2007). Here, autophagy was tracked by monitoring cleavage of LC3B I into LC3B II. All cell lines tested exhibited dose-dependent increases in expression of both, LC3B I and LC3B II (Figure 20), signifying a clear increase in autophagic processes after treatment with FASN-inhibitors. Regarding effectiveness, C75 was able to elicit increased expression of both protein variants at slightly lower doses than G28UCM.

Interestingly, protein ubiquitination - another mechanism involved in protein degradation - was only activated, when cells were treated with C75. Activation of ubiquitination was not observed using G28UCM. This finding indicates, that protein ubiquitination is not necessarily a common phenomenon in cells treated with inhibitors of FASN. The high level of cytotoxicity - potentially caused by unspecific modulation/binding of C75 to CPT1 and other, unknown binding partners - could possibly evoke the differential effects of the FASN-inhibitors on protein ubiquitination. Possible differential impacts of C75 and G28UCM on protein folding should also be considered as potential triggers of protein ubiquitination.

In order to be able to proliferate, cells have to progress through the distinct phases of the cell cycle. Normal cells have means by which they can impose a halt in a certain stage in order to recover from environmental or intracellular stresses. In contrast, malignant cells often have aberrant cell cycle checkpoints, e.g. by loss of the tumor suppressor p53 or inhibitors of cyclin dependent kinases (CDKs) and thus are able to continually proliferate, ignoring stress signals. Previous reports showed that blockade of FASN can lead to a cell cycle arrest at G1 phase in hepatoma and colorectal carcinoma cells as well as to an arrest in G2/M phase in melanoma and renal cancer cells, accompanied by an increase in the CDK inhibitor p21/WAF (Huang et al. 2009, Chuang et al. 2011, Ho et al. 2007, Horiguchi et al. 2008). The experiments conducted in this study revealed, that inhibition of FASN by C75 and G28UCM dose-

independently induces up-regulation of the CDK inhibitor p21/WAF, while p16/CDKN2A was not influenced by FASN-blockade. Furthermore, C75 and G28UCM were able to elicit cell cycle arrest in S and G2/M phases of the cell cycle in a time dependent manner. By contrast, the number of cells in G1 phase decreased upon treatment with C75 or G28UCM. Interestingly, pharmacologic inhibition of FASN in OSE cells did not cause major changes in cell cycle distribution, despite a remarkable, dose-dependent induction of p21/WAF. As mentioned in chapter 4.4 the reason for this observation may lie in differential cell cycle regulation of malignant/immortalized and normal ovarian surface epithelial cells. While malignant/immortalized cells experienced a halt in cell cycle progression followed by apoptosis, these effects were almost absent in normal OSE cells despite a quite severe reduction of proliferation as evidenced by proliferation assays in these cells (Figure 8). A possible explanation for this phenomenon (reduced proliferation without presence of apoptosis and cell cycle arrest) would be that normal OSE cells are able to decelerate their cell cycle progression without causing changes in the ratio of the distinct phases. Experiments measuring the cell doubling time should be performed to investigate this idea.

The sub-G1 peaks (Figure 23) - indicating apoptotic cells and debris - emerging concomitantly with the shift in cell cycle distribution after treatment with C75 or G28UCM closely resemble the results measured in the analysis of apoptosis by active caspase-3. Altogether, regarding the effects of C75 and G28UCM on the cell cycle, no significant differences were observed between both FASN-inhibitors.

4.5 HSP70 is upregulated by C75 and may ameliorate cytotoxic effects of FASN-inhibition

Here, for the first time we investigated the implications of FASN-inhibition by C75 and G28UCM in malignant and non-malignant ovarian surface epithelial cells on the expression of the important protein chaperones HSP70 and HSP90. We found that HSP70 is strikingly induced by inhibition of FASN using C75 but remains rather unaffected by treatment with G28UCM. Because HSP70 among other functions can prevent apoptosis, this finding provides a hypothetical explanation why G28UCM has stronger anti-proliferative effects in malignant and immortal ovarian surface epithelial cells than C75, especially when low doses are used. HSP70 can be associated with endoplasmic reticulum stress, which in turn was shown to be elicited by FASN-inhibition (Little et al. 2007, Gupta et al. 2010). Therefore, induction of endoplasmic

reticulum stress by FASN-inhibition would explain an increase in HSP70 expression. Another explanation involves the capacity of HSP70 to aid in protein ubiquitination and degradation (Lüders et al. 2000). This is backed by the fact, that protein ubiquitination was only monitored in cells treated with C75 but not in G28UCM-treated cells. Altogether, these findings are in favour of the hypothesis that G28UCM has higher target specificity and is less cytotoxic to cells than C75 and thereby causes fewer side effects.

4.6 Conclusion

The results presented above show, that the novel FASN-inhibitor G28UCM is a potent inhibitor of cell growth in malignant and non-malignant ovarian surface epithelial cells. The mechanisms conferring the anti-proliferative state evoked by G28UCM include shortage in palmitic acid production, apoptosis, autophagy, and cell cycle arrest, which are equally present in cells treated with C75. The major improvement of G28UCM over C75 is that it has higher target specificity (G28UCM does not interfere with CPT1) and lower cytotoxicity as could be seen in proliferation assays, and by the fact that C75 but not G28UCM induces protein ubiquitination and expression of HSP70. Unfortunately, not only malignant but also normal ovarian surface epithelial cells experience the aforementioned anti-proliferative effects, giving rise to the idea that oncogenic signaling is not a prerequisite for FASN-inhibitors in order to reduce cell growth. More likely, sensitivity to FASN-inhibition depends on the individual growth rate of a cell and the associated demand for lipid molecules.

5 References

- Abramson HN. The Lipogenesis Pathway as a Cancer Target. *Journal of Medicinal Chemistry* 2011;54(16):5615-5638
- Ahmed AA, Etemadmoghadam D, Temple J, Lynch AG, Riad M, Sharma R, Stewart C, Fereday S, Caldas C, deFazio A, Bowtell D, Brenton JD. Driver mutations in TP53 are ubiquitous in high grade serous carcinoma of the ovary. *The Journal of Pathology* 2010;221(1):49-56
- Audeh MW, Carmichael J, Penson RT, Friedlander M, Powell B, Bell-McGuinn KM, Scott C, Weitzel JN, Oaknin A, Loman N, Lu K, Schmutzler RK, Matulonis U, Wickens M, Tutt A. Oral poly(ADP-ribose) polymerase inhibitor olaparib in patients with BRCA1 or BRCA2 mutations and recurrent ovarian cancer: a proof-of-concept trial. *Lancet* 2010;376(9737):245-251
- Auersperg N. Ovarian surface epithelium as a source of ovarian cancers: Unwarranted speculation or evidence-based hypothesis? *Gynecologic Oncology* 2013;<http://dx.doi.org/10.1016/j.ygyno.2013.03.021>
- Auersperg N, Wong AS, Choi KC, Kang SK, Leung PC. Ovarian surface epithelium: biology, endocrinology, and pathology. *Endocrine Reviews* 2001;22(2):255-288
- Bandyopadhyay S, Zhan R, Wang Y, Pai SK, Hirota S, Hosobe S, Takano Y, Saito K, Furuta E, Iizumi M, Mohinta S, Watabe M, Chalfant C, Watabe K. Mechanism of Apoptosis Induced by the Inhibition of Fatty Acid Synthase in Breast Cancer Cells. *Cancer Research* 2006;66(11):5934-5940
- Beere HM, Wolf BB, Cain K, Mosser DD, Mahboubi A, Kuwana T, Taylor P, Morimoto RI, Cohen GM, Green DR. Heat-shock protein 70 inhibits apoptosis by preventing recruitment of procaspase-9 to the Apaf-1 apoptosome. *Nature Cell Biology* 2000;2(8):469-475
- Bell DA, Scully RE. Early De Novo Ovarian Carcinoma. *Cancer* 1994;73(7):1859-1864
- Bryan TM, Reddel RR. SV40-induced immortalization of human cells. *Critical Reviews in Oncogenesis* 1994;5(4):331-357

- Chen Y, Zhang L, Hao Q. Olaparib: a promising PARP inhibitor in ovarian cancer therapy. *Archives of Gynecology and Obstetrics* 2013;DOI 10.1007/s00404-013-2856-2
- Chuan HY, Chang YF, Hwang JJ. Antitumor effect of orlistat, a fatty acid synthase inhibitor, is via activation of caspase-3 on human colorectal carcinoma-bearing animal. *Biomedicine and Pharmacotherapy* 2011;65(4):286-292
- Cmielová J, Recáková M. p21 Cip1/Waf1 Protein and its Function Based on a Subcellular Localization. *Journal of Cellular Biochemistry* 2011;112(12):3502-3506
- Costello LC, Franklin RB. 'Why do tumor cells glycolyse?': from glycolysis through citrate to lipogenesis. *Molecular and Cellular Biochemistry* 2005;280(1-2):1-8
- Daniilidis A, Karagiannis V. Epithelial Ovarian Cancer: Risk factors, screening and the role of prophylactic oophorectomy. *Hippokratia* 2007;11(2):63-66
- David CJ, Chen M, Assanah M, Canoll P, Manley JL. HnRNP proteins controlled by c-Myc deregulate pyruvate kinase mRNA splicing in cancer. *Nature* 2010;463(7279):364-368
- Drew Y, Mulligan EA, Vong WT, Thomas HD, Kahn S, Kyle S, Mukhopadhyay A, Los G, Hostomsky Z, Plummer ER, Edmondson RJ, Curtin NJ. Therapeutic potential of poly(ADP-ribose) polymerase inhibitor AG014699 in human cancers with mutated or methylated BRCA1 or BRCA2. *Journal of the National Cancer Institute* 2011;103(4):334-346
- Elstrom RL, Bauer DE, Buzzai M, Karnauskas R, Harris MH, Plas DR, Zhuang H, Cinalli RM, Alavi A, Rudin CM, Thompson CB. Akt stimulates aerobic glycolysis in cancer cells. *Cancer Research* 2004;64(11):3892-3899
- Enoch HG, Catalá A, Strittmatter P. Mechanism of Rat Liver Microsomal Stearyl-CoA Desaturase. *The Journal of Biological Chemistry* 1976;251(16):5095-5103
- Farrell C, Lyman M, Freitag K, Fahey C, Piver MS, Rodabaugh KJ. The role of hereditary nonpolyposis colorectal cancer in the management of familial ovarian cancer. *Genetics in Medicine* 2006;8(10):653-657

- Fingar DC, Blenis J. Target of rapamycin (TOR): an integrator of nutrient and growth factor signals and coordinator of cell growth and cell cycle progression. *Oncogene* 2004;23:3151-3171
- Flavin R, Peluso S, Nguyen PL, Loda M. Fatty acid synthase as a potential therapeutic target in cancer. *Future Oncology* 2010;6(4):551-562
- Ford D, Easton DF, Stratton M, Narod S, Goldgar D, Devilee P, Bishop DT, Weber B, Lenoir G, Chang-Claude J, Sobol H, Teare MD, Struewing J, Arason A, Scherneck S, Peto J, Rebbeck TR, Tonin P, Neuhausen S, Barkardottir R, Eyfjord J, Lynch H, Ponder BA, Gayther SA, Zelada-Hedman M. Genetic heterogeneity and penetrance analysis of the BRCA1 and BRCA2 genes in breast cancer families. *The American Journal of Human Genetics* 1998;62(3):676-689
- Fujimoto J, Sakaguchi H, Hirose R, Ichigo S, Tamaya T. Biologic implications of the expression of vascular endothelial growth factor subtypes in ovarian carcinoma. *Cancer* 1998;83(12):2528-2533
- Gao Y, Lin LP, Zhu CH, Chen Y, Hou YT, Ding J. Growth Arrest Induced by C75, a Fatty Acid Synthase Inhibitor, was Partially Modulated by p38 MAPK but Not by p53 in Human Hepatocellular Carcinoma. *Cancer Biology and Therapy* 2006;5(8):978-985
- Garzetti GG, Ciavattini A, Goteri G, De Nictolis M, Stramazotti D, Lucarini G, Biagini G. Ki67 Antigen Immunostaining (MIB 1 Monoclonal Antibody) in Serous Ovarian Tumors: Index of Proliferative Activity with Prognostic Significance. *Gynecologic Oncology* 1995;56(2):169-174
- Gilks CB, Prat J. Ovarian carcinoma pathology and genetics: recent advances. *Human Pathology* 2009;40:1213-1223
- Gordon AN, Finkler N, Edwards RP, Garcia AA, Crozier M, Irwin DH, Barrett E. Efficacy and safety of erlotinib HCl, an epidermal growth factor receptor (HER1/EGFR) tyrosine kinase inhibitor, in patients with advanced ovarian carcinoma: results from a phase II multicenter study. *International Journal of Gynecological Cancer* 2005;15(5):785-792

- Graner E, Tang D, Rossi S, Baron A, Migita T, Weinstein LJ, Lechpammer M, Huesken D, Zimmermann J, Signoretti S, Loda M. The isopeptidase USP2a regulates the stability of fatty acid synthase in prostate cancer. *Cancer Cell* 2004;5(3):253-261
- Gross TP, Schlesselman JJ. The estimated effect of oral contraceptive use on the cumulative risk of epithelial ovarian cancer. *Obstetrics and Gynecology* 1994;83(3):419-424
- Grunt TW, Wagner R, Grusch M, Berger W, Singer CF, Marian B, Zielinski CC, Lupu R. Interaction between fatty acid synthase- and ErbB-systems in ovarian cancer cells. *Biopchem. Biophys. Res. Commun.* 2009 385(3):454-9
- Gupta S, Deepti A, Deegan S, Lisbona F, Hetz C, Samali A. HSP72 Protects Cells from ER Stress-induced Apoptosis via Enhancement of IRE α -XBP1 Signaling through a Physical Interaction. *PLOS Biology* 2010;8(7):e1000410
- Hanker LC, Loibl S, Burchardi N, Pfisterer J, Meier W, Pujade-Lauraine E, Ray-Coquard I, Sehouli J, Harter P, du Bois A. The impact of second to sixth line therapy on survival of relapsed ovarian cancer after primary taxane/platinum-based therapy. *Annals of Oncology* 2012;23(10):2605-2612
- Hankinson SE, Colditz GA, Hunter DJ, Willett WC, Stampfer MJ, Rosner B, Hennekens CH, Speizer FE. A Prospective Study of Reproductive Factors and Risk of Epithelial Ovarian Cancer. *Cancer* 1995;76(2):284-290
- Hennessy BT, Smith DL, Ram PT, Lu Y, Mills GB. Exploiting the PI3K/Akt pathway for cancer drug discovery. *Nature Reviews Drug Discovery* 2005;4(12):988-1004
- Ho TS, Ho YP, Wong WY, Chiu L, Wong YS, Ooi V. Fatty acid synthase inhibitors cerulenin and C75 retard growth and induce caspase-dependent apoptosis in human melanoma A-375 cells. *Biomedicine and Pharmacotherapy* 2007;61(9):578-587
- Holschneider CH, Berek JS. Ovarian Cancer: Epidemiology, Biology and Prognostic Factors. *Seminars in Surgical Oncology* 2000;19(1):3-10

- Horiguchi A, Asano T, Ito K, Sumitomo M, Hayakawa M. Pharmacologic inhibitor of fatty acid synthase suppresses growth and invasiveness of renal cancer cells. *The Journal of Urology* 2008;180(2):729-736
- Huang CH, Tsai SJ, Wang YJ, Pan MH, Kao JY, Way TD. EGCG inhibits protein synthesis, lipogenesis and cell cycle progression through activation of AMPK in p53 positive and negative human hepatoma cells. *Molecular Nutrition and Food Research* 2009;53(9):1156-1165
- Itamochi H, Kigawa J. Clinical trials and future potential of targeted therapy for ovarian cancer. *International Journal of Clinical Oncology* 2012;17(5):430-440
- Jemal A, Bray F, Center MM, Ferlay J, Ward E, Forman D. Global Cancer Statistics. *CA Cancer Journal for Clinicians* 2011;61:69-90
- Jones NP, Schulze A. Targeting cancer metabolism – aiming at a tumor’s sweet spot. *Drug Discovery Today* 2012;17(5-6):232-241
- Knowles LM, Smith JW. Genome-wide changes accompanying knockdown of fatty acid synthase in breast cancer. *BioMed Central* 2007;8:168
- Knowles LM, Yang C, Osterman A, Smith JW. Inhibition of Fatty-acid Synthase Induces Caspase-8-mediated Tumor Cell Apoptosis by Up-regulating DDIT4. *The Journal of Biological Chemistry* 2008;283(46):31378-31384
- Kotsopoulos J, Terry KL, Poole EM, Rosner B, Murphy MA, Hecht JL, Crum CP, Missmer SA, Cramer DW, Tworoger SS. Ovarian cancer risk factors by tumor dominance, a surrogate for cell of origin. *International Journal of Cancer* 2013; doi: 10.1002/ijc.28064
- Kuhajda FP. Fatt Acid Synthase and Cancer: New Application of an Old Pathway. *Cancer Research* 2006;66(12):5977-5980
- Kurman RJ, Shih IM. Molecular pathogenesis and extraovarian origin of epithelial ovarian cancer – shifting the paradigm. *Human Pathology* 2011;42:918-931
- Kusakabe T, Maeda M, Hoshi N, Sugino T, Watanabe K, Fukuda T, T Suzuki. Fatty Acid Synthase is expressed mainly in adult hormone-sensitive cells or cells with

- high lipid metabolism and in proliferating fetal cells. *J Histochem Cytochem* 2000
48:613
- Landen CN, Birrer JM, Sood AK. Early Events in the Pathogenesis of Epithelial Ovarian Cancer. *Journal of Clinical Oncology* 2008;26(6):995-1005
- Lee JY, Sohn KH, Rhee SH, Hwang D. Saturated fatty acids, but not unsaturated fatty acids, induce the expression of cyclooxygenase-2 mediated through Toll-like receptor 4. *Journal of Biological Chemistry* 2001;276(20):16683-16689
- Lee Y, Miron A, Drapkin R, Nucci MR, Medeiros F, Saleemuddin A, Garber J, Birch C, Mou H, Gordon RW, Cramer DW, McKeon FD, Crum CP. A candidate precursor to serous carcinoma that originates in the distal fallopian tube. *Journal of Pathology* 2007;211(1):26-35
- Little JL, Wheeler FB, Fels DR, Koumenis C, Kridel SJ. Inhibition of Fatty Acid Synthase Induces Endoplasmic Reticulum Stress in Tumor Cells. *Cancer Research* 2007;67(3):1262-1269
- Li JN, Gorospe M, Chrest FJ, Kumaravel TS, Evans MK, Han WF, Pizer ES. Pharmacological Inhibition of Fatty Acid Synthase Activity Produces Both Cytostatic and Cytotoxic Effects Modulated by p53. *Cancer Research* 2001;61:1493-1499
- Li L, Wang L, Zhang W, Tang B, Zhang J, Song H, Yao D, Tang Y, Chen X, Yang Z, Wang G, Li X, Zhao J, Ding H, Reed E, Li QQ. Correlation of serum VEGF levels with clinical stage, therapy efficacy, tumor metastasis and patient survival in ovarian cancer. *Anticancer Research* 2004;24(3b):1973-1979
- Listenberger LL, Han X, Lewis SE, Cases S, Farese RV, Ory DS, Schaffer JE. Triglyceride accumulation protects against fatty acid-induced lipotoxicity. *PNAS* 2003;100(6):3077-3082
- Loftus TM, Jaworsky DE, Frehywot GL, Townsend CA, Ronnett GV, Lane MD, Kuhajda FP. Reduced food intake and body weight in mice treated with fatty acid synthase inhibitors. *Science* 2000;288(5475):2379-2381

- Lowe KA, Chia VM, Taylor A, O'Malley C, Kelsh M, Mohamed M, Mowat FS, Goff B. An international assessment of ovarian cancer incidence and mortality. *Gynecologic Oncology* 2013;<http://dx.doi.org/10.1016/j.ygyno.2013.03.026>
- Lüders J, Demand J, Höhfeld J. The Ubiquitin-related BAG-1 Provides a Link between the Molecular Chaperones Hsc70/Hsp70 and the Proteasome. *The Journal of Biological Chemistry* 2000;275(7):4613-4617
- Lunt SY, Vander Heiden MG. Aerobic Glycolysis: Meeting the Metabolic Requirements of Cell Proliferation. *Annual Reviews of Cell and Developmental Biology* 2011;27:441-464
- Lupo R, Menendez JA. Pharmacological inhibitors of Fatty Acid Synthase (FASN)--catalyzed endogenous fatty acid biogenesis: a new family of anti-cancer agents? *Current Pharmaceutical Biotechnology* 2006;7(6):483-493
- Lynch HT, Casey MJ, Shaw TG, Lynch JF. Hereditary Factors in Gynecologic Cancer. *The Oncologist* 1998;3:319-338
- Majewski N, Nogueira V, Bhaskar P, Coy PE, Skeen JE, Gottlob K, Chandel NS, Thompson CB, Robey RB, Hay N. Hexokinase-mitochondria interaction mediated by Akt is required to inhibit apoptosis in the presence or absence of Bax and Bak. *Molecular Cell* 2004;16(5):819-830
- Makhija S, Amler LC, Glenn D, Ueland FR, Gold MA, Dizon DS, Paton V, Lin CY, Januario T, Ng K, Strauss A, Kelsey S, Sliwkowski MX, Matulonis U. Clinical activity of gemcitabine plus pertuzumab in platinum-resistant ovarian cancer, fallopian tube cancer, or primary peritoneal cancer. *Journal of Clinical Oncology* 2010;28(7):1215-1223
- Mashima T, Seimiya H, Tsuruo T. De novo fatty-acid synthesis and related pathways as targets for cancer therapy. *British Journal of Cancer* 2009;100:1369-1372
- Mayer MP, Bukau B. HSP70 chaperones: Cellular functions and molecular mechanism. *Cellular and Molecular Life Sciences* 2005;62:670-684
- Mendoza MC, Er EE, Blenis J. The RAS-Erk and PI3K-mTOR pathways: cross-talk and compensation. *Trends in Biochemical Sciences* 2011;36(6):320-328

- Menendez JA, Lupu R. Fatty acid synthase and the lipogenic phenotype in cancer pathogenesis. *Nature Reviews Cancer* 2007;7(10):763-777
- Menendez JA, Oza BP, Atlas E, Verma VA, Mehmi I, Lupu R. Inhibition of tumor-associated fatty acid synthase activity antagonizes estradiol- and tamoxifen-induced agonist transactivation of estrogen receptor (ER) in human endometrial adenocarcinoma cells. *Oncogene* 2004;23:4945-4958
- Ness RB, Cramer DW, Goodman MT, Kruger Kjaer S, Mallin K, Mosgaard GJ, Purdie DM, Risch HA, Vergona R, Wu AH. Infertility, Fertility Drugs, and Ovarian Cancer: A Pooled Analysis of Case-Control Studies. *American Journal of Epidemiology* 2002;155(3):217-224
- Obata K, Morland SJ, Watson RH, Hitchcock A, Chenevix-Trench G, Thomas EJ, Campbell IG. Frequent PTEN/MMAC Mutations in Endometrioid but not Serous or Mucinous Epithelial Ovarian Tumors. *Cancer Research* 1998;58:2095-2097
- Oliveras G, Blancafort A, Urruticoechea A, Campuzano O, Gómez-Cabello D, Brugada R, López-Rodríguez ML, Colomer R, Puig T. Novel anti-fatty acid synthase compounds with anti-cancer activity in HER2+ breast cancer. *Annals of the New York Academy of Sciences* 2010;1210:86-92
- Pende M, Um SH, Mieulet V, Sticker M, Goss VL, Mestan J, Mueller M, Fumagalli S, Kozma SC, Thomas G. S6K1^{-/-} / S6K2^{-/-} Mice Exhibit Perinatal Lethality and Rapamycin-Sensitive 5'-Terminal Oligopyrimidine mRNA Translation and Reveal a Mitogen-Activated Protein Kinase-Dependent S6 Kinase Pathway. *Molecular and Cellular Biology* 2004;24(8):3112-3124
- Peurala E, Koivunen P, Haapasaari KM, Bloigu R, Jukkola-Vuorinen A. The prognostic significance and value of cyclin D1, CDK4 and p16 in human breast cancer. *Breast Cancer Research* 2013;15(1):R5
- Pizer ES, Jackisch C, Wood FD, Pasternack GR, Davidson NE, Kuhajda FP. Inhibition of Fatty Acid Synthesis Induces Programmed Cell Death in Human Breast Cancer Cells. *Cancer Research* 1996;56(6):2745-2747
- Pizer ES, Thupari J, Han WF, Pinn ML, Chrest FJ, Frehywot GL, Townsend CA, Kuhajda FP. Malonyl-Coenzyme-A is a Potential Mediator of Cytotoxicity Induced

- by Fatty-Acid-Synthase Inhibition in Human Breast Cancer Cells and Xenografts. *Cancer Research* 2000;60:213-218
- Porstmann T, Griffiths B, Chung YL, Delpuech O, Griffiths JR, Downward J, Schulze A. PKB/Akt induces transcription of enzymes involved in cholesterol and fatty acid biosynthesis via activation of SREBP. *Oncogene* 2005;24(43):6465-6481
- Porstmann T, Santos CR, Griffiths B, Cully M, Wu M, Leever S, Griffiths JR, Chung YL, Schulze A. SREBP activity is regulated by mTORC1 and contributes to Akt-dependent cell growth. *Cell Metabolism* 2008;8(3):224-236
- Prat J. Ovarian carcinomas: five distinct diseases with different origins, genetic alterations and clinicopathological features. *Virchows Archiv* 2012;460:237-249
- Puig T, Relat J, Marrero PF, Haro D, Brunet J, Colomer R. Green Tea Catechin Inhibits Fatty Acid Synthase without Stimulating Carnitine Palmitoyltransferase-1 or Inducing Weight Loss in Experimental Animals. *Anticancer Research* 2008;28:3671-3676
- Puig T, Turrado C, Benhamú B, Aguilar H, Relat J, Ortega-Gutiérrez S, Casals G, Marrero PF, Urruticoechea A, Haro D, López-Rodríguez ML, Colomer R. Novel Inhibitors of Fatty Acid Synthase with Anticancer Activity. *Clinical Cancer Research* 2009;15(24):7608-7615
- Puig T, Aguilar H, Cufí S, Oliveras G, Turrado C, Ortega-Gutiérrez S, Benhamú B, López-Rodríguez ML, Urruticoechea A, Colomer R. A novel inhibitor of fatty acid synthase shows activity against Her2+ breast cancer xenografts and is active in anti-Her2 drug-resistant cell lines. *Breast Cancer Res.* 2011 13(6):R131
- Qian SB, McDonough H, Boellmann F, Cyr DM, Patterson C. CHIP-mediated stress recovery by sequential ubiquitination of substrates and Hsp70. *Nature* 2006;440(7083):551-555
- Relat J, Blancafort A, Oliveras G, Cufí S, Haro D, Marrero PF, Puig T. Different fatty acid metabolism effects of (-)-epigallocatechin-3-gallate and C75 in adenocarcinoma lung cancer. *BioMed Central Cancer* 2012;12:280
- Richardson CJ, Schalm SS, Blenis J. PI3-kinase and TOR: PIKTORing cell growth. *Seminars in Cell and Developmental Biology* 2004;15(2):147-159

- Robey RB, Hay N. Is Akt the "Warburg kinase"?-Akt-energy metabolism interactions and oncogenesis. *Seminars in Cancer Biology* 2009;19(1):25-31
- Rock KL, Gramm C, Rothstein L, Clark K, Stein R, Dick L, Hwang D, Goldberg AL. Inhibitors of the proteasome block the degradation of most cell proteins and the generation of peptides presented on MHC class I molecules. *Cell* 1994 78(5):761-771
- Ross JS, Yang F, Kallakury BV, Sheehan CE, Ambros RA, Muraca PJ. HER-2/neu oncogene amplification by fluorescence in situ hybridization in epithelial tumors of the ovary. *American Journal of Clinical Pathology* 1999;111(3):311-316
- Roux PP, Shahbazian D, Vu H, Holz MK, Cohen MS, Taunton J, Sonenberg N, Blenis J. RAS/ERK Signaling Promotes Site-specific Ribosomal Protein S6 Phosphorylation via RSK and Stimulates Cap-dependent Translation. *The Journal of Biological Chemistry* 2007;282(19):14056-14064
- Ruvinsky I, Sharon N, Lerer T, Cohen H, Stolovich-Rain M, Nir T, Dor Y, Zisman P, Meyuhas O. Ribosomal protein S6 phosphorylation is a determinant of cell size and glucose homeostasis. *Genes Dev.* 2005 19: 2199-2211
- Schulze A, Harris AL. How cancer metabolism is tuned for proliferation and vulnerable to disruption. *Nature* 2012;491(7424):364-373
- Schuyer M, van Staveren IL, Klijn JG, vd Burg ME, Stoter G, Henzen-Logmans SC, Foekens JA, Berns EM. Sporadic CDKN2 (MTS1/p16ink4) gene alterations in human ovarian tumours. *Br J Cancer* 1996 October; 74(7):1069-1073
- Senturk E, Cohen S, Dottino PR, Martignetti JA. A critical re-appraisal of BRCA1 methylation studies in ovarian cancer. *Gynecologic Oncology* 2010;119(2):376-383
- Shayesteh L, Lu Y, Kuo WL, Baldocchi R, Godfrey T, Collins C, Pinkel D, Powell B, Mills GB, Gray JW. PIK3CA is implicated as an oncogene in ovarian cancer. *Nature Genetics* 1999;21(1):99-102
- Shih IM, Kurman RJ. Ovarian Tumorigenesis: A Proposed Model Based on Morphological and Molecular Genetic Analysis. *American Journal of Pathology* 2004;164:1511-1518

- Singer G, Kurman RJ, Chang HW, Cho SKR, Shih IM. Diverse Tumorigenic Pathways in Ovarian Serous Carcinoma. *American Journal of Pathology* 2002;160(4):1223-1228
- Smith Sehdev AS, Kurman RJ, Kuhn E, Shih I. Serous Tubal Intraepithelial Carcinoma upregulates markers associated with high-grade serous carcinomas including Rsf-1 (HBXAP), cyclin E and fatty acid synthase. *Mod Pathol.* 2010 June 23(6):844-855
- Swinnen JV, Esquenet M, Goossens K, Heyns W, Verhoeven G. Androgens stimulate fatty acid synthase in the human prostate cancer cell line LNCaP. *Cancer Research* 1997;57(6):1086-1090
- Swinnen JV, Heemers H, Deboel L, Fougelle F, Heyns W, Verhoeven G. Stimulation of tumor-associated fatty acid synthase expression by growth factor activation of the sterol regulatory element-binding protein pathway. *Oncogene* 2000;19:5173-5181
- Soga T. Cancer metabolism: Key players in metabolic reprogramming. *Cancer Science* 2013;104(3):275-281
- Thupari JN, Landree LE, Ronnett GV, Kuhajda FP. C75 increases peripheral energy utilization and fatty acid oxidation in diet-induced obesity. *PNAS* 2002;99(14):9498-9502
- Thupari JN, Pinn ML, Kuhajda FP. Fatty Acid Synthase Inhibition in Human Breast Cancer Cells Leads to Malonyl-CoA-Induced Inhibition of Fatty Acid Oxidation and Cytotoxicity. *Biochemical and Biophysical Research Communications* 2001;285(2):217-223
- Tomek K, Wagner R, Varga F, Singer CF, Karlic H, Grunt TW. Blockade of Fatty Acid Synthase Induces Ubiquitination and Degradation of Phosphoinositide-3-Kinase Signaling Proteins in Ovarian Cancer. *Mol Cancer Res* 2011;9:1767-1779
- Van de Sande T, De Shrijver, Heyns W, Verhoeven G, Swinnen JV. Role of Phosphatidylinositol 3-Kinase/PTEN/Akt Kinase Pathway in the Overexpression of Fatty Acid Synthase in LNCaP Prostate Cancer Cells. *Cancer Research* 2002;62:642-646

- Vander Heiden MG, Cantley LC, Thompson CB. Understanding the Warburg Effect: The Metabolic Requirements of Cell Proliferation. *Science* 2009;324(5930):1029-1033
- Vang R, Shih IE, Kurman RJ. Fallopian tube precursors of ovarian low- and high-grade serous neoplasms. *Histopathology* 2013;62(1):44-58
- Wagle S, Bui A, Ballard PL, Shuman H, Gonzales J, Gonzales LW. Hormonal regulation and cellular localization of fatty acid synthase in human fetal lung. *The American Journal of Physiology* 1999;277(2 Pt 1):L381-390
- Walker GR, Schlesselman JJ, Ness RB. Family history of cancer, oral contraceptive use, and ovarian cancer risk. *American Journal of Obstetrics and Gynecology* 2002;186(1):8-14
- Wang Y, Botolin D, Xu J, Christian B, Mitchell E, Jayaprakasam B, Nair M, Peters JM, Busik J, Olson LK, Jump DB. Regulation of hepatic fatty acid elongase and desaturase expression in diabetes and obesity. *J. Lipid Res.* 2006 Oct;47(10):2353
- Warburg O, Wind F, Negelein E. The metabolism of tumors in the body. *The Journal of General Physiology* 1927;8(6):519-530
- Whittemore AS, Gong G, Itnyre J. Prevalence and Contribution of BRCA1 Mutations in Breast Cancer and Ovarian Cancer: Results from three U.S. Population-Based Case-Control Studies of Ovarian Cancer. *The American Journal of Human Genetics* 1997;60:496-504
- Wu J, Dang Y, Su W, Liu C, Ma H, Shan Y, Pei Y, Wan B, Guo J, Yu L. Molecular cloning and characterization of rat LC3A and LC3B--two novel markers of autophagosome. *Biochem. Biophys. Res. Comm.* 2006 Jan 6;339(1):437-42
- Yang G, Mercado-Uribe I, Multani AS, Sen S, Shih IM, Wong KK, Gershenson DM, Liu J. RAS promotes tumorigenesis through genomic instability induced by imbalanced expression of Aurora-A and BRCA2 in midbody during cytokinesis. *International Journal of Cancer* 2013;doi: 10.1002/ijc.28032

Yang Y, Han WF, Morin PJ, Chrest FJ, Pizer ES. Activation of Fatty Acid Synthesis during Neoplastic Transformation: Role of Mitogen-Activated Protein Kinase and Phosphatidylinositol 3-Kinase. *Experimental Cell Research* 2002;279:80-90

Zecchin KG, Rossato FA, Raposo HF, Melo DR, Alberici LC, Oliveira HCF, Castilho RF, Coletta RD, Vercesi AE, Graner E. Inhibition of fatty acid synthase in melanoma cells activates the intrinsic pathway of apoptosis. *Laboratory Investigation* 2011;91:232-240

Zhou W, Simpson PJ, McFadden JM, Townsend CA, Medghalchi SM, Vadlamudi A, Pinn ML, Ronnett GV, Kuhajda FP. Fatty Acid Synthase Inhibition Triggers Apoptosis during S Phase in Human Cancer Cells. *Cancer Research* 2003;63:7330-7337

Curriculum vitae

Daniel Veigel

Date of birth: May 2nd, 1985

Education

- 2005-2013 Studies of molecular biology and genetics at the University of Vienna
- 1999-2004 HTLBUVA St. Pölten (electronic data processing & operational organization)
- 1995-1999 First – fourth form of secondary modern school (HS Etsdorf)
- 1994-1995 Fourth form of elementary school (VS Etsdorf)
- 1991-1994 First – third form of elementary school (VS Mauerbach)

Laboratory experience

- 2010 Three weeks project collaboration at the laboratory of Univ.-Prof. Dr. Renée Schröder (University of Vienna)
- 2011-2013 Diploma thesis at the Medical University of Vienna, Department of Medicine I, Division of Oncology, laboratory of Univ.-Prof. Dr. Thomas W. Grunt. External supervision by Univ.-Prof. Dr. Thomas Decker (University of Vienna)